

Inter- and intra-annual variations of carbon fluxes in boreal peatlands

Inauguraldissertation

zur

Erlangung des akademischen Grades eines

doctor rerum naturalium (Dr. rer. nat.)

an der Mathematisch-Naturwissenschaftlichen Fakultät

der

Ernst-Moritz-Arndt-Universität Greifswald

vorgelegt von

Michal Gažovič

geboren am 28. 01. 1983

in Poprad (Slowakei)

Greifswald

Dekan: Prof. Dr. K. Fesser
1. Gutachter: Prof. M. Wilmking, PhD
2. Gutachter: Prof. Dr. S. Glatzel
Tag der Promotion: 12. 10. 2011

Abstract

Northern peatlands are ecosystems with unique hydrological properties, storing about 400-500 Gt of carbon. As the production rate of organic material is higher than its decomposition, which is slowed down in the wet and cold environment, peatlands store a great amount of carbon. Carbon assimilated from the atmosphere during photosynthesis by plants is partly lost due to autotrophic and heterotrophic respiration as carbon dioxide (CO₂), as methane (CH₄) or/and as dissolved organic carbon. The proportion of each carbon component is strongly controlled by environmental conditions as temperature, radiation, precipitation and subsequent water table changes and active role of vegetation.

With predicted changes in the global climate, changes in the influence of environmental parameters on peatland ecology are expected. Thus thorough research is essential for a better understanding of mechanisms which influence carbon cycling in peatlands.

In this thesis, various components of the carbon cycle were studied at two boreal peatland sites (Ust Pojega in Komi Republic in Russian Federation and Salmisuo in Eastern Finland) using the micrometeorological eddy covariance method. The focus was placed on the temporal changes of the controlling parameters, ranging from a few days during short snow thawing through the rest of the year. At the Salmisuo site, two measurement seasons allowed to address possible inter-annual variation.

We observed that diurnal variations in methane emissions which are typically controlled by vegetation during the growing season, might appear during snow melt as a result of the influence of physical factors rather than biological factors. The diurnal pattern in methane emissions was caused by the interaction of the freeze-thaw cycle and near surface turbulence. During the night time, when surface temperatures fell below zero and caused formation of the ice layer, methane emissions were only around 0.8 mg m⁻² h⁻¹, however after the increase in temperature and melting of the ice layer they reached peak values of around 3 mg m⁻² h⁻¹. The near surface turbulence had a significant influence on methane emissions, however only after the thawing of the ice layer. The effect of changing environmental parameters over the year was further

elaborated on a carbon dioxide time series from the Ust Pojeg site. The generally accepted effects of temperature on ecosystem respiration during the night are not stable throughout the year and can change rapidly during the growing season. Using moving window regression analysis I could show that the strength of the exponential relationship between ecosystem respiration and temperature is changing during the year. This was in correspondence with recent publications elaborating on sub-seasonal changes of the controlling parameters. In general, measurements from the Ust Pojeg site represent estimates of annual CO₂ and CH₄ fluxes with an annual carbon balance of -94.5 g C m⁻² and a new contribution to the quantification of trace gases emissions from a Russian boreal peatland.

The inter-annual comparison of net ecosystem exchange (NEE) measurements with previously published data on CH₄ and DOC flux from the Salmisuo site showed that the NEE of CO₂ is the most important component of the carbon balance at this site. However, primary production was not responsible for the inter-annual changes in NEE. Rather, the effects of water table position during the year had a strong influence on ecosystem respiration, which was probably due to the influence on soil respiration, and higher NEE was observed during the year with smaller primary production, but higher water table levels. The effects of higher precipitation and higher water table during the wet year were shown to increase CH₄ flux and the export of DOC, but their effects could not compensate for changes in ecosystem respiration. In the presented thesis intra- and inter- annual changes in carbon flux components and their controls, in our case attributed mostly to hydrological conditions in combination with other environmental parameters as temperature and the role of peatland vegetation, are discussed.

Zusammenfassung

Nördliche Moore sind Ökosysteme mit einzigartigen hydrologischen Eigenschaften, die zirka 400-500 Gt Kohlenstoff speichern. Da die Produktion von organischem Material höher als die durch die nasse Umgebung inhibierte Zersetzung ist, repräsentieren Moore meistens eine netto Kohlenstoffsénke. Der durch die Photosynthese assimilierte atmosphärische Kohlenstoff geht teilweise durch autotrophe und heterotrophe Respiration als Kohlenstoffdioxid, als Methan oder/und als gelöster organischer Kohlenstoff wieder verloren. Die Anteile von jeder Kohlenstoffkomponente werden durch Umweltparameter wie Temperatur, Strahlung, Niederschlag und daraus folgende Grundwasserniveauänderungen sowie durch die aktive Rolle der Pflanzen stark beeinflusst.

Mit prognostizierten globalen Klimaänderungen sind auch Veränderungen im Einfluss von Klimaparametern auf die Moorökologie zu erwarten. Daher ist eine sorgfältige Forschung, die zum Verstehen der die den Kohlenstoffkreislauf in Mooren beeinflussenden Mechanismen beiträgt, von hoher Priorität.

In dieser Dissertation wurden verschiedene Komponenten des Kohlenstoffkreislaufes auf zwei borealen Moorestandorten, Ust Pojeg in Komi Republik in der Russischen Föderation und Salmisuo in Ostfinnland, mit Hilfe der mikrometeorologischen „eddy covariance“ Methode untersucht. Der Fokus wurde auf die zeitlichen Änderungen der Kontrollparameter gelegt, die sich sowohl innerhalb weniger Tage während der kurzen Schneeschmelze als auch über den Rest des Jahres verändern. Zweijährige Messungen vom Standort Salmisuo erlaubten es, sich mit möglichen Mechanismen interannueller Variabilität zu befassen.

In der Arbeit wurde gezeigt, dass Tagesschwankungen in den Methanemissionen – die in der Vegetationsperiode typischer Weise als von Pflanzen kontrolliert beobachtet werden – während der Schneeschmelze eher als ein Resultat des Einflusses der physikalischen Parameter als der biologischen Parameter gesehen werden können. Es wurde gezeigt, dass die Tagesschwankungen der Methanemissionen durch die Interaktion von dem Gefrier-Tau-Zyklus mit bodennaher Turbulenz entstanden. In der Nacht, wenn die Oberflächentemperatur unter Null fiel und sich eine Eisschicht formte,

waren die Methanemissionen nur zirka $0.8 \text{ mg m}^{-2} \text{ h}^{-1}$, obgleich die Emissionen nach Anstieg der Temperatur, wenn die Eisschicht geschmolzen war, Spitzenwerte von zirka $3 \text{ mg m}^{-2} \text{ h}^{-1}$ erreichten. Bodennahe Turbulenz hatte signifikanten Einfluss auf die Methanemissionen, jedoch nur nachdem die Eisschicht geschmolzen war.

Der Effekt wechselnder Kontrollparameter während des Jahres wurde näher an Kohlenstoffdioxidflüssen vom Standort Ust Pojeg untersucht. Wir fanden heraus, dass generell akzeptierte Temperatureffekte auf die Ökosystemrespiration während der Nacht nicht stabil über das Jahr sind und sich in der Vegetationsperiode schnell ändern können. Mittels der „moving window“ Regression konnte gezeigt werden, dass die Stärke der exponentiellen Beziehung zwischen Ökosystemrespiration und Temperatur sich über das Jahr ändert. Dieses Ergebnis war in Übereinstimmung mit aktuellen Veröffentlichungen, die sich mit subsaisonalen Änderungen von Kontrollparametern beschäftigen.

Generell gelten die Messungen von Ust Pojeg als Abschätzungen der Kohlenstoffdioxid- und Methanflüsse sowie als neuer Beitrag zur Quantifizierung von Spurengasen aus der borealen Moorregion Russlands mit einer jährlichen Kohlenstoffbilanz von -94.5 g C m^{-2} .

Der interannuelle Vergleich der „eddy covariance“ Kohlenstoffdioxidmessungen mit früher veröffentlichten Daten von Methan- und gelöster organischer Kohlenstoffflüsse vom Standort Salmisuo hat gezeigt, dass der Kohlenstoffdioxidaustausch die wichtigste Komponente der Kohlenstoffbilanz auf diesem Standort ist. Jedoch war nicht die Primärproduktion für die interannuellen Schwankungen der NEE verantwortlich. Die Auswirkungen der Lage des Grundwasserniveaus über das Jahr hatten – wahrscheinlich durch den Einfluss auf die Bodenrespiration – einen starken Einfluss auf die Ökosystemrespiration. Eine höhere NEE wurde in dem Jahr mit geringerer Primärproduktion, aber höheren Wasserständen beobachtet. Die Folgen von höherem Niederschlag und höherem Wasserstand während des nassen Jahres waren ein erhöhter Methanfluss und erhöhter Export von gelöstem organischen Kohlenstoff, aber ihre Auswirkungen konnten nicht die Veränderungen in der Ökosystemrespiration kompensieren.

Contents

Abstract	i
Zusammenfassung	iii
1 Introduction	9
1.1 Present understanding	9
1.1.1 CO ₂ fluxes	10
1.1.2 CH ₄ fluxes	11
1.1.3 DOC fluxes	12
1.1.4 Changes in peatland ecology in a changing environment.....	12
1.1.5 Temporal and spatial variations in C fluxes from the peatlands.....	14
1.2 Objectives of this dissertation.....	16
1.3 The author's contribution to the single publications.....	16
2 Diurnal dynamics of CH₄ from a boreal peatland during snowmelt	19
2.1 Introduction.....	21
2.2 Site and methods.....	22
2.3 Results.....	23
2.3.1 Temperature characteristics and snow-melt dynamic.....	23
2.3.2 CH ₄ flux	23
2.4 Discussion.....	24
2.5 Conclusions.....	26
3 Temperature and plant phenology control the seasonal variability of CO₂ and CH₄ fluxes from a boreal peatland in North-West Russia	33
3.1 Introduction.....	34
3.2 Methods.....	35
3.2.1 Study site.....	35
3.2.2 Experimental setup.....	36
3.2.3 Raw data processing and flux calculation.....	38
3.2.4 Gap-filling models	39
3.2.4.1 CO ₂ flux model	39
3.2.4.2 CH ₄ flux model	41
3.2.5 Footprint modelling	41
3.2.6 Estimating the annual C balance.....	42
3.3 Results.....	43
3.3.1 Weather characteristics	43
3.3.2 CO ₂ flux	46
3.3.3 Moving window analysis of CO ₂ fluxes.....	46

3.3.4 CH ₄ flux.....	49
3.3.5 Footprint analysis	50
3.3.6 Annual carbon balance and uncertainty estimates.....	51
3.4 Discussion.....	52
3.4.1 Annual carbon balance	52
3.4.2 Seasonal development of photosynthesis and ecosystem respiration.....	53
3.4.3 Effects of abiotic and biotic factors on CH ₄ fluxes	54
3.4.4 Winter Fluxes: an important constituent of annual C budget.....	55
3.5 Conclusions	56

4 Hydrology driven ecosystem respiration determines the carbon balance of a boreal peatland 57

4.1 Introduction	58
4.2 Methods	60
4.2.1 Study area	60
4.2.2 Net ecosystem exchange measurements.....	61
4.2.3 Gap-filling and flux-partitioning	62
4.2.4 Regression analysis of relationships between environmental parameters and CO ₂ fluxes	62
4.2.5 Discharge and DOC concentrations measurements.....	62
4.2.6 CH ₄ flux measurements.....	63
4.3 Results	64
4.3.1 Hydro-meteorological variables	64
4.3.2 Carbon balance components: Comparison between dry and wet year	64
4.3.2.1 Monthly NEE.....	64
4.3.2.2 Regulation of photosynthesis and respiration.....	65
4.3.2.3 NEE partitioning.....	67
4.3.2.4 Monthly DOC export.....	67
4.3.2.5 Monthly CH ₄ emissions.....	67
4.3.2.6 Annual C balance	68
4.4 Discussion.....	68
4.5 Conclusions	72

5 Boreal peatland net ecosystem CO₂ exchange – an integrative comparison between measured fluxes and LPJ-GUESS model output..... 75

5.1 Introduction	76
5.2 Methods	78
5.2.1 Study site	78
5.2.2 Experimental setup and flux calculations.....	78
5.2.2.1 Chamber measurements – plot scale	78
5.2.2.2 Eddy covariance flux measurements – ecosystem scale	79
5.2.2.3 Ancillary measurements	80
5.2.3 Empirical time series modeling.....	81
5.2.3.1 Chamber measurements – plot scale	81
5.2.3.2 Eddy covariance flux measurements – ecosystem scale	82
5.2.4 Determination of the microform coverage and remote sensing	82

5.2.5 Footprint modeling.....	85
5.2.6 Upscaling of CO ₂ fluxes from plot scale to ecosystem scale.....	86
5.2.7 LPJ-GUESS model	87
5.2.7.1 LPJ-GUESS model and changes made to the model for this study	87
5.2.7.2 Modeling protocol.....	90
5.2.8 Uncertainty analysis.....	91
5.2.9 Evaluation of the model performance.....	92
5.3 Results.....	92
5.3.1 Variability of NEE fluxes at plot and ecosystem scales	92
5.3.2 Microform distribution at the intensive study site	94
5.3.3 Footprint analysis.....	95
5.3.4 Comparison of CO ₂ fluxes observed from chamber and eddy covariance measurements.....	95
5.3.5 Evaluation of LPJ-GUESS model output	99
5.4. Discussion.....	103
5.4.1 Mismatch between NEE fluxes upscaled from chamber and observed from eddy covariance measurements.....	103
5.4.2 Biases in land cover classification and upscaling	105
5.4.3 Sources of uncertainty in the model simulations	107
5.4.4 Comparison to other peatland studies and forest flux estimates.....	108
5.5 Summary and conclusions	108
6 General discussion and conclusions	111
Bibliography	117

Chapter 1

Introduction

1.1 Present understanding

Peatlands are unique ecosystems with partially decomposed peat layer of more than 30 cm. Depending on trophic status and water source they can be classified into bogs and fens. Ombrotrophic bogs receive nutrients solely from precipitation and minerogenic fens are influenced by more alkaline and nutrient rich ground water (and rain water). The nutrient deficient environment of bogs favours the establishment of ericaceous shrubs and *Sphagnum* moss, while fens are dominated by sedges, herbs and bryophytes (Lai, 2009).

The largest areas of peatlands are located in sub-arctic and boreal regions storing between 400-500 Gt of carbon (C) (Gorham, 1991; Davidson and Janssens, 2006). For comparison, today's C content of the Earth's atmosphere is ~730 Gt and C stored in vegetation amounts to ~650 Gt (Zimov et al., 2006). The rates of organic material production in northern peatlands are typically limited by short growing seasons and its decomposition is strongly limited by usually wet and cold subsurface conditions (Gorham, 1991).

Gross primary production (GPP) and ecosystem respiration (ER) were previously identified as the two strongest C balance components in peatlands, both being of equal importance (Houghton et al., 1998, Davidson et al., 2006). However, under certain conditions other non-CO₂ fluxes might become important as well. Worrall et al. (2009) identified uptake by primary producers as the single biggest component of the C budget, followed by ER and lateral export of dissolved organic carbon (DOC). Deeper in the peat profile with low oxygen concentrations, anaerobic reduction of organic material favors methanogenesis and peatlands act as a net source of methane (CH₄) to the atmosphere (Gorham, 1991).

All components responsible for the C balance do not exist as separate entities but are strongly connected to each other and are constantly modified by changing environmental conditions. One important factor modifying the plant phenology is photoperiod length (Badeck et al., 2004). Annual changes in solar radiation initiate changes in temperatures. As a main driver of many developmental processes in biology (Badeck et al., 2004), temperature has a direct influence on the phenological development of plants and thus determines green leaf development and connected surface biophysical parameters e.g. albedo and CO₂ flux (Menzel, 2002). In the following I will briefly describe each of the main C balance components, temporal and spatial variations in carbon fluxes from the peatlands and then I will proceed to the individual chapters.

1.1.1 CO₂ fluxes

The acquisition of C from the atmosphere is done through photosynthetic CO₂ assimilation by plants. As energy from photosynthetically active radiation is used for CO₂ fixation, the amount of energy fixed from the atmosphere through photosynthesis is termed GPP. Not all C assimilated in photosynthesis is stored in the ecosystem and part of it is returned to the atmosphere as CO₂ through autotrophic (plants) and heterotrophic (organisms other than plants) respiration. These processes are referred to as ecosystem respiration (ER). Adding the opposing CO₂ fluxes GPP and ER gives the net ecosystem exchange (NEE) of CO₂ (Lund, 2009).

The ER is typically related to temperature effects (Lafleur et al., 2005; Sottocornola and Kiely, 2010) as the highest ER rates appear in the time of the highest temperatures in the annual course. A large proportion of ecosystem respiration is soil derived and approximately 10% of the atmosphere's C passes through the soil each year (Raich and Tufekcioglu, 2000). Soil respiration is widely considered to be controlled by soil temperatures (Lloyd, 1994), however the temperature is not the single most important parameter influencing soil respiration. When temperature is not strongly limiting the site productivity, water availability is more important than temperature (Reichstein et al., 2003).

The leaf area index (LAI) influencing the carbon assimilation potential correlates with soil respiration rates and higher plant activity (photosynthesis) may enhance soil

respiration (Houghton et al., 1998, Reichstein et al., 2003; Davidson et al., 2006) as a large portion of soil respiration originates from recently assimilated C via root respiration. Root derived CO₂ is the dominant component in the total CO₂ efflux from planted soil and is very sensitive to changes in photosynthesis and thus, photosynthesis strongly controls the total soil CO₂ flux (Kuzyakov and Cheng, 2001).

1.1.2 CH₄ fluxes

The CH₄ emissions in the peatland are mainly controlled by soil temperature and water table (WT) position (Bubier et al., 1993; Thomas et al., 1996; Bellisario et al., 1999), increasing with increasing temperatures in the seasonal course (Williams and Crawford, 1984; Christensen et al., 2003). WT depth is one of the key factors controlling CH₄ emissions from peatlands (Lai, 2009). The relationship between WT position and CH₄ emissions is very complex and might not seem clear in a day to day pattern, but when seasonal averages are examined, higher CH₄ emissions are usually associated with higher WT levels (Moore and Roulet, 1993; Funk et al., 1994; Bellisario et al., 1999). Vascular plants with their aerenchyma might act as CH₄ transport mediators (Lai, 2009). For example, Morrissey and Livingstone (1992) found that in the arctic coastal plains plant mediated transport and release of CH₄ was on average 92% of the observed net emission rates.

Besides the mechanical influence of plants acting as CH₄ transport mediators, CH₄ emissions are related to GPP by stimulation of methanogenesis through increased substrate supply to the soil (Whitting and Chanton, 1993, Christensen et al., 2003). When anaerobic conditions are developed, organic substrate availability is a major control factor of methane production (Segers, 1998). However, the increase of CH₄ emissions with increasing primary production might be not always valid, as a negative correlation between plant productivity and CH₄ production can be a species related phenomenon showing exceptions to the widely-held view of increasing CH₄ emissions with increase in plant production (Sutton-Grier and Megonigal, 2011).

When WT decreases conditions for methanogenesis are not favorable due to oxidation of the peat layer, depending on the depth to which the WT decreases (Lai, 2009). In this case, microbes oxidizing the organic substrate might benefit. However, a low WT level is not the only reason for low CH₄ emissions. Despite a large CH₄ stock present in

the ecosystem, CH₄ emissions might be very low and approach zero, even with high WT levels. The main reason for such a phenomenon is the oxygenation of the rooting zone by oxygen loss from the roots (Fritz et al., 2010).

1.1.3 DOC fluxes

Lateral export of DOC from peatlands is typically influenced by the precipitation pattern during the year and in turn by fluctuations of WT and water discharge with usually highest DOC export during the spring thaw (Jager et al., 2009; Dyson et al., 2011). The highest DOC concentrations in the soil water appear during the summer months and thus increased frequency of precipitation events during summer might increase annual DOC flux (Jager et al., 2009; Worrall et al., 2009). It might well be expected that highest DOC concentrations, similar to the highest rates of CH₄ production during summer months are related to the highest rates of GPP and its contribution to soil C substrates. With low water discharge from the peatland (e.g. drought due to warming), retention of DOC rather than its export is expected. This DOC might be either stored in the peat column or exported to the atmosphere by microbial respiration as CO₂. Exponential increase in gaseous emissions of CO₂ and CH₄ was observed with increased DOC retention (Pastor et al., 2003). The schematic diagram depicting general ideas about main C components in the peatland ecosystems is on Fig. 1.1.

1.1.4 Changes in peatland ecology in a changing environment

In the past 100 years, the Earth's climate has warmed by approximately 0.6°C. From what was mentioned in the previous paragraph it is clear that the fine C balance of boreal peatland is highly dependent on regional climate properties through multiple links between its components and complex loops (e.g substrate) affecting all parts of the C cycle independently of the origin of the climate variability. For ecological communities, regional changes showing high level of spatial variability are more relevant than global approximations (Walther et al., 2002). Ecological responses of plants to recent climate

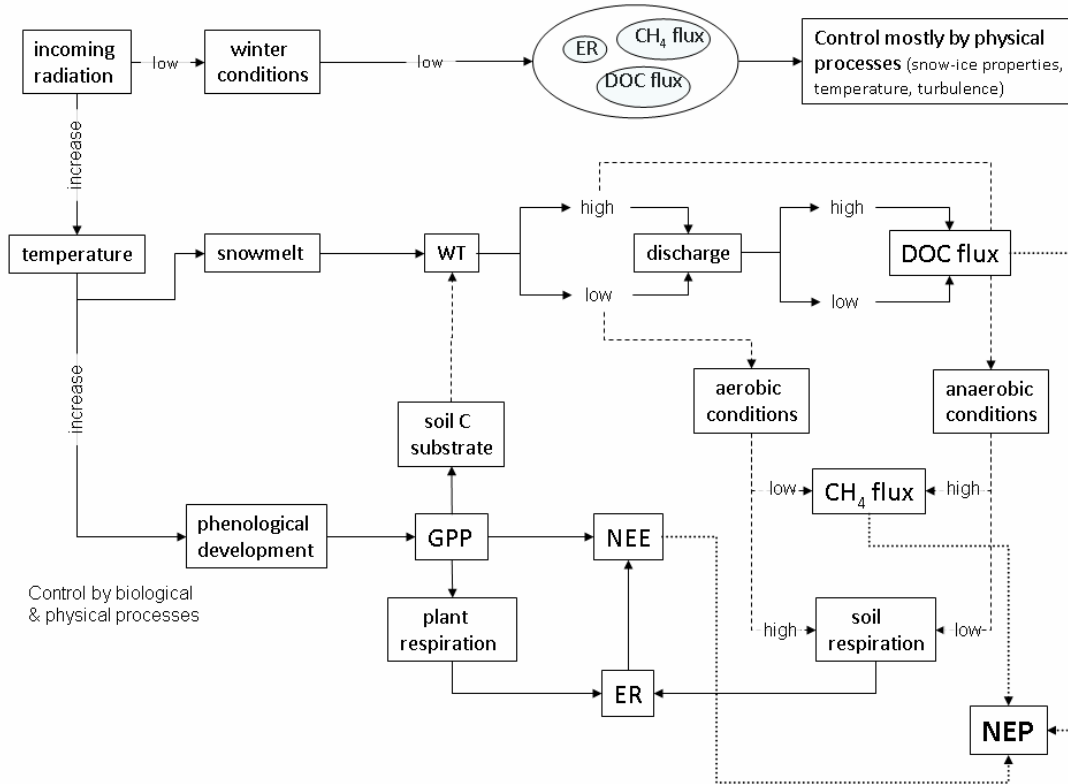


Figure 1.1 Schematic flow chart of the three main carbon balance components in the peatland ecosystems: net ecosystem exchange (NEE), methane (CH₄) and dissolved organic carbon (DOC) in the relation to environmental characteristics as radiation, temperature and water table (WT).

change can be of various natures but documented effects report mostly changes in the phenology and subsequent changes in the length of the growing season. As a consequence of changes in diurnal temperature ranges, frost-free periods in most mid- and high- latitudes are lengthening (Walther et al., 2002). From the beginning to the end of the 20th century, freeze-free periods in the US prolonged by about two weeks were consistent with the timing of increases in mean annual temperature, with clear spatial (east-west) differences (Kunkel et al., 2004). However, the directions pointing towards earlier or later onset of spring activities are heterogeneous (Walther et al., 2002, Badeck et al., 2004). For example, annual net ecosystem exchange (NEE) from an Atlantic blanket bog studied for 5 years showed higher CO₂ uptake in the years with an earlier onset of the growing season (Sottocornola and Kiely, 2010). Rocha and Goulden (2008) reported higher CO₂ uptake during longer growing seasons brought by

warm spring temperatures, however their simulations indicated that air temperature alone cannot explain the start of the growing season.

Even predicted longer growing seasons do not have to lead to higher uptake of CO₂ by ecosystems, as apparently higher plant activity may enhance respiration and thus shift the ecosystems to being a source rather than a sink (Houghton et al., 1998, Davidson et al., 2006). On the other hand, the shortening of the growing season might occur due to earlier senescence, which was attributed to indirect control of WT on GPP and ER causing dry conditions in the peatland (Sonnentag et al., 2010) and thus might decrease the C uptake. Such changes in the phenology will inevitably lead to changes in the ecosystem production and the C balance and will have an effect on all C cycle components (e.g. NEE, CH₄, DOC) above and below ground.

1.1.5 Temporal and spatial variations in C fluxes from the peatlands

The control of C flux by environmental parameters in the annual course leads to high temporal variation in strength of the various C flux components. In case of CO₂ and CH₄ it is typically represented by an annual pattern with lowest fluxes during the winter months and the highest fluxes during the growing season following the seasonal signal of radiation and temperature. Although recent studies from a tundra environment showed that under certain conditions CH₄ emissions during autumn/winter transition might exceed the emissions from the growing season (Mastepanov et al., 2008). On the other hand, dynamic conditions during spring thaw and after the thaw might result in high CH₄ emissions amounting to 24% and up to 77% of the annual CH₄ flux (Comas et al., 2008), thus the emissions during and after the thaw period might also exceed those from the growing season. Nevertheless, it might well be expected that temporal variations appear due to changes in controlling parameters throughout the year of both biological and physical nature. Temporal variability does not occur only in the seasonal course. Inter-annual variability in C flux components is of utmost interest as it gives additional information on ecological processes which might not be covered during a single year measurement and might better answer the questions of possible effects of changing ecological response to climate change (Sottocornola and Kiely, 2010).

Besides temporal variations, strong spatial differences in C fluxes on different scales can be observed. Peatlands are heterogeneous ecosystems with heterogeneous surface

forming microforms as hummocks, lawns and hollows, which function fundamentally different and all scales of peatland topography are important to properly estimate total CH₄ and CO₂ exchange (Waddington and Roulet, 1996). Spatial differences are observed also on the regional scales and strong differences were observed between tundra and boreal regions e.g. in CO₂ (Friborg et al, 2003; Kutzbach et al., 2007) and CH₄ emissions (Hargreaves et al., 2001; Huttunen et al., 2003; Rinne et al., 2007; Wille et al., 2008).

Although boreal and subarctic peatlands are located almost wholly in the Russian Federation, Canada, the USA and Fennoscandia (Gorham, 1991), there exists a bias toward “western” measurement sites, with little knowledge about vast peatland areas in the Russian Federation.

To properly understand the C cycle of northern peatlands, a careful study of its components has to be conducted. Plenty of methods used for determination of gaseous C fluxes from the peatland (e.g. chamber method, eddy covariance) have been previously described and reviewed (e.g. Alm et al., 2007). In recent years with progress in instrumentation technology, the eddy covariance method became particularly popular, as it allows noninvasive measurements of ecosystem scale trace gas fluxes (e.g. Moncrieff et al., 1997; Baldocchi, 2003; Reichstein et al., 2005; Lasslop et al., 2010). In-depth analysis of measured NEE over peatlands requires partitioning of NEE into its components GPP and ER which are not measured directly. For this purpose, empirical models describing the correlation between environmental parameters and the C flux components are typically used, however, new methods are being developed which take other influences e.g. the effect of vapor pressure deficit (VPD) on NEE partitioning into consideration (Lasslop et al., 2010).

1.2 Objectives of this dissertation

The presented dissertation aims for new contributions to C cycle studies in boreal ecosystems. In the first publication (chapter 2), changes in the CH₄ emissions during the short but dynamic winter/spring transition period at the boreal peatland site in Ust Pojeg in the Russian Federation are presented. The chapter highlights the influence of physical factors and their effects on CH₄ emission and further emphasizes the changes in the parameters controlling CH₄ emission over time.

The second publication (chapter 3) focuses on the quantification of the annual NEE and CH₄ fluxes from the Ust Pojeg site and establishes the connections to environmental parameters influencing the emissions. As a new contribution to the knowledge about annual CO₂ and CH₄ emissions from Russian boreal region, it offers a good comparison of trace gas emission strength, compares them to the other sites in the boreal region and elaborates on the influence of changing controlling parameters responsible for temporal variability over the course of a year.

The third publication (chapter 4) deals with the inter-annual variations of the C cycle components CO₂, CH₄ and DOC in contrasting environmental conditions during one dry and one wet year at a boreal peatland site Salmisuo located in Eastern Finland. It elaborates on the importance of the effects of particular environmental parameters, which could lead to high inter-annual differences in C balance due to peculiar characteristics of partitioning of the C flux components.

Last, the fourth publication (chapter 5) compares chamber and eddy covariance measurements from the Ust-Pojeg site with the output of the dynamic global vegetation model LPJ.

1.3 The author's contribution to the single publications

Chapter 2 (publication 1) I was conducting the eddy covariance field measurements in Komi Republic, which were part of the original research proposal of Prof. Martin Wilking, Ph.D. I was responsible for the data analysis, literature reviews and writing of the manuscript. Christian Wille helped with MATLAB[®] and EdiRe[®] programs. Dr.

Lars Kutzbach was supervising the modeling part. All coauthors were supervising and commenting the writing of the manuscript.

Chapter 3 (publication 2) I was conducting the field measurements, data analysis, literature reviews and I wrote the manuscript. The footprint modeling was done by Inke Forbrich. The idea of using a moving response function came from Prof. Martin Wilmking, Ph.D. Dr. Lars Kutzbach and Christian Wille were helping with MATLAB[®] scripts and data analysis. All coauthors were contributing during writing of the manuscript. Leaf area indices were calculated by Julia Schneider.

Chapter 4 (publication 3) Data collection was done by members of the working group lead by M. Wilmking, Ph.D. Methane data were collected, analyzed and prepared by Inke Forbrich. Daniel Jager sampled dissolved organic carbon export and discharge in the field and prepared the data for publication. Dr. Lars Kutzbach and Christian Wille were helping during data analysis and the field work. I analyzed the carbon dioxide data and wrote the entire manuscript after discussions with M. Wilmking. All coauthors were contributing to the manuscript during the writing process.

Chapter 5 (publication 4) The original idea was developed and the manuscript was written by Julia Schneider. I was responsible for the eddy covariance parts of the manuscript. I was helping to conduct the field sampling.

Chapter 2

Diurnal dynamics of CH₄ from a boreal peatland during snowmelt*

* This article was published as: M. Gažovič, P. Schreiber, L. Kutzbach, C. Wille and M. Wilmking (2010), Diurnal dynamics of CH₄ from a boreal peatland during snowmelt, *Tellus B*, 62, 133-139.

Diurnal dynamics of CH₄ from a boreal peatland during snowmelt

By MICHAL GAŽOVIČ^{1*}, LARS KUTZBACH^{1,2}, PETER SCHREIBER^{1,2}, CHRISTIAN WILLE^{1,2} and MARTIN WILMKING¹, ¹Institute for Botany and Landscape Ecology, Ernst Moritz Arndt University Greifswald, Grimmer Straße 88, 17487 Greifswald, Germany; ²Institute of Soil Science, KlimaCampus, University of Hamburg, Allende-Platz 2, 20146 Hamburg, Germany

(Manuscript received 18 November 2009; in final form 12 March 2010)

ABSTRACT

Peatlands are one of the major natural sources of methane (CH₄), but the quantification of efflux is uncertain especially during winter, fall and the highly dynamic spring thaw period. Here, we report pronounced diurnal variations in CH₄ fluxes (F_{CH_4}), measured using the eddy-covariance technique during the snow-thawing period at a boreal peatland in north-western Russia. Following the background winter emission of $\sim 0.5 \text{ mg m}^{-2} \text{ h}^{-1}$, strong diurnal variability in CH₄ fluxes from 21 April to 3 May was apparently controlled by changes in surface temperature (T_{sur}) and near-surface turbulence as indicated by the friction velocity (u^*). CH₄ fluxes were $\sim 0.8 \text{ mg m}^{-2} \text{ h}^{-1}$ during night and $\sim 3 \text{ mg m}^{-2} \text{ h}^{-1}$ during peak efflux. Primarily, the freeze-thaw cycle of an ice layer observed at the wet peatland microforms due to surface temperatures oscillating between $>0^\circ\text{C}$ during the days and $<0^\circ\text{C}$ during the nights appeared to strongly influence diurnal variability. Once the ice layer was melted, increases in wind speed seemed to enhance CH₄ efflux, possibly by increased mixing of the water surface. Apparently, a combination of physical factors is influencing the gas transport processes of CH₄ efflux during the highly dynamic spring thaw period.

1. Introduction

Wetlands are a major natural source of methane (CH₄) to the atmosphere (Denman et al., 2007). The majority of natural wetlands are situated in the boreal region (Fischlin et al., 2007). Generally, most of the CH₄ is released during the short growing season; however, recent literature from cold tundra region reported greater autumnal emissions than was observed during the growing season (Mastepanov, 2008). CH₄ efflux is mainly controlled by soil temperature, water table (WT) position (Bubier et al., 1993; Thomas et al., 1996; Bellisario et al., 1999; Christensen et al., 2003) and organic acid concentrations (Christensen et al., 2003). In water-logged environments, near-surface turbulence appears to play an important role for CH₄ emissions (Hargreaves et al., 2001; Sachs et al., 2008; Wille et al., 2008). Temporal fluctuations in CH₄ flux (F_{CH_4}) during the growing season are driven by several factors, for example, temperature effects on decomposition of soil organic matter and subsequent CH₄ production, plant photosynthesis and carbon translocation to roots and plant-mediated transport of CH₄

(Mikkilä et al., 1995; Thomas et al., 1996). Short-term correlation of surface temperature and diurnal variation in CH₄ flux found in some microsites during the growing season indicates that control mechanisms of CH₄ emission are changing over the growing season (Kettunen, 2002). Due to diverse peatland microtopography, CH₄ efflux can show high-spatial variability (Bubier et al., 1993; Becker et al., 2008).

Despite the dominant role of the vegetation season for the CH₄ balance, non-zero CH₄ fluxes during the cold seasons can contribute significantly to the annual CH₄ emissions, with estimates ranging from 3.5 to 21% (Dise, 1992; Panikov and Dedysh, 2000). From the long cold season, the short thawing period at the end of winter and the period right after the snowmelt are of high interest. During the snowmelt period, CH₄ fluxes can dynamically change over short times, amounting to 11% of the annual CH₄ budget (Hargreaves et al., 2001), while spring emissions after snowmelt can amount to 24% or even 77% (Comas et al., 2008). Thus, in some cases, the spring emissions after the snowmelt can even exceed the emission during the vegetation period. High temporal variability in CH₄ fluxes during the spring might also include diurnal variations possibly caused by freezing and refreezing of the surface water as hypothesized by Tokida et al., (2007). During the snow-thawing period 2008, we have observed pronounced diurnal variations in CH₄ fluxes from

*Corresponding author.

e-mail: gazovic@uni-greifswald.de

DOI: 10.1111/j.1600-0889.2010.00455.x

a boreal peatland in Komi Republic, Russia, lasting for several days. In this paper, our objective was to further elaborate the above-mentioned hypothesis, and to try to explain the process of diurnal variations in CH_4 fluxes during this particular period.

2. Site and methods

The study site is located in the 25 km² mire complex 'Ust Pojæg' (61°56'N, 56°13'E) near the village of Sludka, approximately 60 km north-west of Syktyvkar, the capital of Komi Republic, Russia (Fig. 1). The climate is boreal continental and humid with maximum precipitation in summer. The measurement system was set up in the south-western part of the peatland accessible via a 1300-m-long boardwalk, passing different ecosystem types from swampy birch-pine forest to open peatland. The eddy-covariance tower was placed at the border between a minerogenic part of the peatland in the south-west and an ombrogenic part in the north-east with the transition zone in-between. The minerogenic depression, close to the eddy-covariance system was somewhat lower in elevation resulting in higher WT during parts of the study period, compared to the other parts of the peatland (Fig. 2). The dominant moss vegetation cover is *Sphagnum angustifolium* in the ombrogenic bog part and *S. jensenii* and *S. fuscum* in the minerogenic fen part. *Carex limosa* and *Scheuchzeria palustris* dominate in hollows; *Andromeda polifolia*, *Chamaedaphne calyculata*, *Betula nana* and *Pinus sylvestris* dominate on hummocks. Vegetation on lawns is a mixture of hummock and hollow vegetation with *Vaccinium oxycoccus*. The occurrence of *Menyanthes trifoliata* and *Utricularia intermedia*

indicates greater nutrient supply in the minerogenic part of the mire. *Carex rostrata* dominates in the transition zone between bog and fen. The average depth of the peat is ~2 m.

Fluctuations of wind speed components were measured 3 m above the surface using a three-dimensional sonic anemometer (Solent R3, Gill Instruments Ltd., Lymington, UK). The air from the sample intake was drawn by a vacuum pump through a 12-m long, 8-mm inner diameter tube and a fast CH_4 analyser RMT-200 (Los Gatos Research Inc., Mountain View, California, USA) where the fluctuations of CH_4 concentrations were measured. Before entering the RMT-200, the sample air was dried using a gas dryer (Perma Pure Inc., New Jersey, USA). Data were logged at 20 Hz, and the eddy-covariance fluxes were calculated over 30-min intervals. The time lag between wind and CH_4 concentration measurements was determined and removed for every averaging period. Turbulent fluxes were calculated using the EdiRe software (Robert Clement, University of Edinburgh, Edinburgh, UK; version 1.4.3. 1184). Flux losses due to the limited frequency response of the eddy-covariance system were corrected in the flux-calculation process. The fluxes were corrected for the frequency attenuation due to tube attenuation, sensor path separation and spectral response of the instruments (Moore, 1986; Moncrieff et al., 1997). On average, 11% were added to the calculated CH_4 flux. Data obtained during conditions that violated basic assumptions of the eddy-covariance theory were rejected using filters evaluating integral turbulence characteristics and stationarity (Foken and Wichura, 1996). By these procedures, 13% of the data were removed. No data gap filling was applied.



Fig. 1. Aerial picture of the study site (Quickbird; 8 July 2008) in the Komi Republic, Russia. The white cross represents the position of the eddy-tower accessible via boardwalk (white line). The circle shows an approximate fetch of 300 m in radius. The wide dark stripe in the fetch is the border between the minerogenic and ombrogenic part (minerogenic depression). Dark areas in the upper ombrogenic part are clouds.

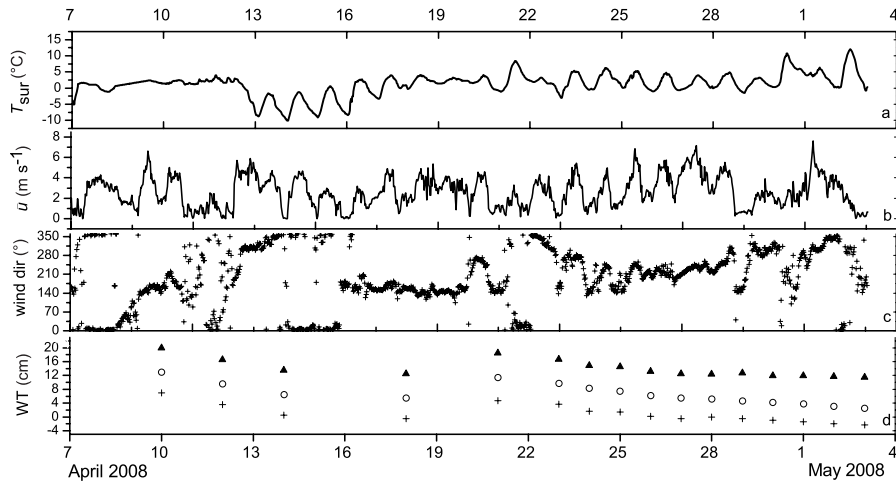


Fig. 2. Meteorological and environmental conditions on Ust Pojæg peatland in the early spring period 2008: (a) surface temperature, (b) mean wind speed, (c) wind direction, (d) water table; (▲) minerogenic depression, (○) ombrogenic part and (+) transition zone. In a, b and c 30-min averages, in d daily averages are displayed.

Supporting meteorological measurements of air temperature, wind components, barometric pressure, relative humidity and net radiation were logged at a climate station installed at the eddy-covariance site. The surface radiative temperature T_{sur} (°C) was calculated from outgoing long-wave radiation, using the Stefan-Boltzman law and an emissivity of 0.98.

Linear and exponential functions were fitted to the data with different environmental factors as explanatory parameters. The best model performance was obtained when CH₄ flux was modelled as a linear function of surface temperature ($r^2_{\text{adj}} = 0.50$ linear vs $r^2_{\text{adj}} = 0.41$ for the exponential function). Reduced major axis (RMA) regression was then applied because we assume that the signal-to-noise ratio of the explanatory variable surface temperature is similar to that of CH₄ flux.

3. Results

3.1. Temperature characteristics and snowmelt dynamic

When CH₄ flux measurements started on 6 April 2008, the surface was completely covered with a snow layer of ~40 cm depth, only some hummocks protruded out of the snow and snowmelt had just started. The meteorological conditions during the study period are shown in Fig. 2. There was minor rain on 9 April (observed but not measured), on 10 April (1.2 mm), 11 April (7.4 mm) and 12 April (4.8 mm). After 12 April, colder weather slowed down snowmelt and caused partial re-freezing of the snowmelt water and peat surface. From 16 April, all snow was melted causing a rise in the WT. Water was standing above the surface in many parts in ombrogenic and minerogenic areas. Hummocks were free of water, but the WT position was usually close to the surface. The precipitation from 18 to 20 April of 9.4 mm contributed to an increase of WT height. From 21

April to 3 May, pronounced fluctuation of daily temperatures caused freezing of water and peat surface during the nights, with the exception of a few nights. During this period, the WT in the minerogenic depression dropped from +17 cm to +11 cm above the peat surface. In the ombrogenic zone, the WT dropped from +12 cm above the peat surface to +3 cm; in the transition zone, from +5 cm above to 2 cm below the surface (Fig. 2).

3.2. CH₄ flux

CH₄ was emitted steadily from the site at the beginning of the measurements. Average hourly CH₄ flux above the snow surface was $\sim 0.54 \pm 0.17 \text{ mg m}^{-2} \text{ h}^{-1}$. April 9 and 10 were windy, and hourly fluxes increased to an average of $\sim 0.78 \pm 0.28 \text{ mg m}^{-2} \text{ h}^{-1}$ and $\sim 0.88 \pm 0.23 \text{ mg m}^{-2} \text{ h}^{-1}$, respectively. Technical problems from 11 to 21 April restrained measurements. From 21 April on, pronounced diurnal variations in CH₄ fluxes were recorded (Fig. 3). The fluxes reached peak values of $> 3 \text{ mg m}^{-2} \text{ h}^{-1}$ in the early afternoon (~ 1400 to 1600 local time (LT); UTC+4), followed by a steady decrease and a minimum in the early morning (~ 0400 to 0900 LT) (Fig. 3). During the period described, the most frequent wind directions were SE and N with winds coming from the minerogenic part (roughly from 120° to 300° ; $0^\circ = \text{N}$) being more common. In general, lowest wind speeds occurred during night and usually highest at late afternoon.

From 21 April to 3 May, the period of strong diurnal changes, CH₄ flux was strongly correlated with T_{sur} ; $r = 0.71$. An empirical linear model based on RMA regression with surface temperature as a predictor was used to model the flux time series (Fig. 3) as follows:

$$F_{\text{CH}_4} = 1.413 + 0.211 T_{\text{sur}}, r^2_{\text{adj}} = 0.50; \text{RMSE} = 0.621. \quad (1)$$

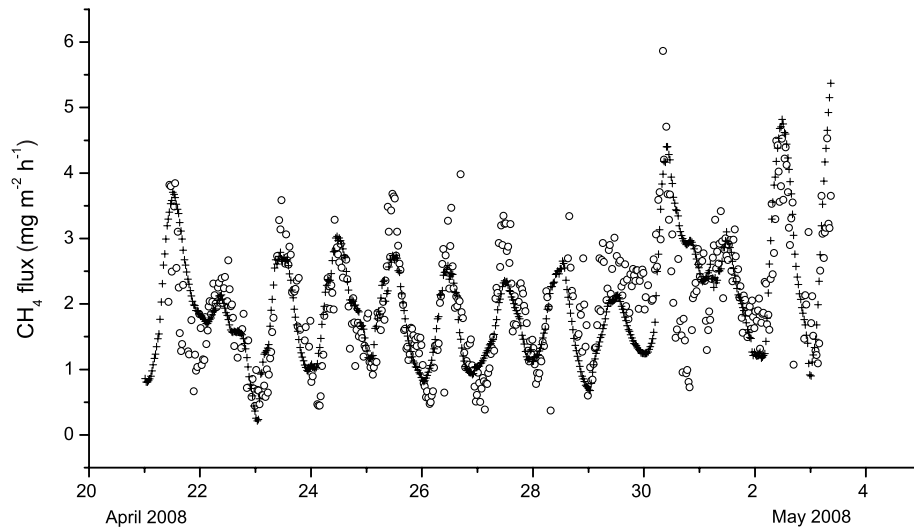


Fig. 3. Diurnal fluctuations in high-resolution CH_4 flux measurements (\circ) and modelled time series ($+$) based on reduced major axis regression using surface temperature as a predictor. The time axis is in UTC.

The modelled fluxes were usually underestimated during the day and overestimated at night.

From 21 to 25 April, the measured CH_4 flux was also well correlated with friction velocity (u^*) $r = 0.66$. When u^* was added as a second parameter to T_{sur} from 21 to 25 April, the model performance increased significantly ($R^2_{\text{adj}} = 0.72$ compared to $r^2_{\text{adj}} = 0.58$ with T_{sur} only, for these particular days). The equation describing this relationship was

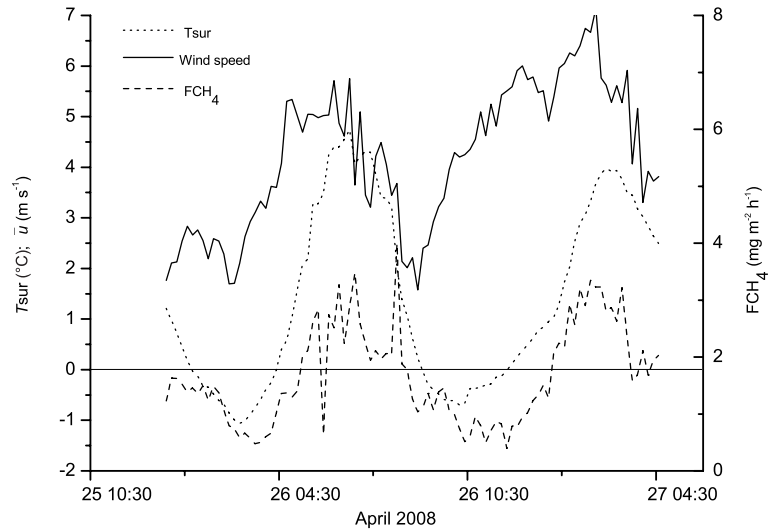
$$F_{\text{CH}_4} = 0.664 + 3.192 u^* + 0.197 T_{\text{sur}}; \text{RMSE} = 0.414. \quad (2)$$

In addition to controls by surface temperature and wind speed, changes in wind direction could also lead to changes in measured flux. At times, wind direction was changing over very short time periods, and spatial differences in the CH_4 flux were observed. For example, on 29 April, the CH_4 flux was increasing, before apparent thaw of the ice layer and an increase in wind speed. On that day, in the morning, the wind direction changed relatively fast from the SE minerogenic depression through S-SW, where more hummocks were present, compared to the minerogenic part in the SE. During the rest of the day, the wind was coming from a relatively narrow region ($\sim 282^\circ \pm 43^\circ$, NW) where the water-logged depression was situated. Wind speed was relatively stable during the day and lower than during the previous days (Fig. 2), and the peak in CH_4 emission as in previous days was not observed (Fig. 3). From 21 to 25 April, the wind direction was changing more or less diurnally from $\sim 150^\circ$ (SE, minerogenic depression) at night, to SW (minerogenic fen) during the day. However, from 26 to 28 April, the wind direction was in a rather narrow range from $226^\circ \pm 18^\circ$ (SW), where the changes in surface coverage are small (Fig. 1), but still strong diurnal variations were observed on these days.

4. Discussion

At our study site, we observed strong diurnal variations of CH_4 fluxes during the early spring period. Diurnal variations of CH_4 fluxes were previously described in different studies (Mikkilä et al., 1995; Thomas et al., 1996; Koch et al., 2007) however, they were referring to controls of diurnal variations during the growing season. During the snow-thaw period analyzed in this study, the ecological conditions are fundamentally different: active vegetation cover is not present, thus no root exudation can fuel CH_4 production, nor can plant-mediated gas transport lead to any significant release of CH_4 . It is possible that some plant-mediated transport still exists, especially through old stalks. However, efflux is nearly exclusively by diffusion across the water-air boundary layer (Heyer et al., 2002) and by ebullition (Hargreaves et al., 2001; Tokida et al., 2007). When considering diffusion as the main way of transport, there should be no diurnal peaks in CH_4 flux due to slow ($10^{-5} \text{ cm}^2 \text{ s}^{-1}$) diffusion of gases in water (close to that of peat) (Clymo and Pearce, 1995). However, transport by diffusion can be affected by atmospheric turbulence, especially above water surfaces (Sachs et al., 2008; Wille et al., 2008). In lakes and inundated soils, gas bubbles adhering to surfaces under water could be released during increase of wind speed and could lead to an increased CH_4 flux (Wille et al., 2008). The same authors observed an exponential dependence of CH_4 emission on atmospheric near-surface turbulence at a study site in polygonal tundra, very likely due to high surface coverage of water bodies. Similarly, Hargreaves et al. (2001) found that turbulent eddies interacting with the vegetation can cause increased efflux of CH_4 by ebullition. They found a short-term relationship between CH_4 flux and momentum flux represented by near-surface turbulence. In our study, the correlation with friction velocity was significant only during the period

Fig. 4. An increase in wind speed (solid line) did not cause an increase in CH₄ flux (dashed line) when the surface temperature (dotted line) fell below zero and the surface was frozen (see the zero line of surface temperature in the figure). The increase in CH₄ flux follows only after the increase of surface temperature. Time on x-axis is in UTC.



from 21 to 25 April. This might be due to the fact that during this period, water was covering most of the peat surface, and the turbulent mixing could be important to release gas bubbles adhering below the water surface.

During the period with strong diurnal variations of CH₄ fluxes, we observed a regular freezing of the top peat and water layers at night. We hypothesize that this frozen layer acted as a barrier to CH₄ efflux and might lead to a layer of peat in which CH₄ concentrations increase during night. During the course of the day, as air and surface temperature increase, the ice layer successively melts, and CH₄ trapped under the ice is released, also through mixing of the upper part of the water or peat surface, resulting in increased measured CH₄ flux (Fig. 4). Tokida et al.

(2007) suggested that high CH₄ concentrations might be caused by rising CH₄ bubbles from deeper layers and their containment under the ice and in the ice by forming ice bubbles. When the surface and water were frozen even a strong increase in wind speed did not have an effect on CH₄ flux (Figs 4 and 5). This might explain the weak relationship of CH₄ flux and u^* after the 25 April, when the night surface temperatures were lower than in the previous days. Thus, the ice layer might have persisted longer into the day. Still, after the melting of the ice layer, turbulent mixing could help to release CH₄. In addition, another factor explaining the weak relationship with friction velocity besides longer persistence of the ice layer during the time after 25 April could be the general decline of the WT, which seems to minimize

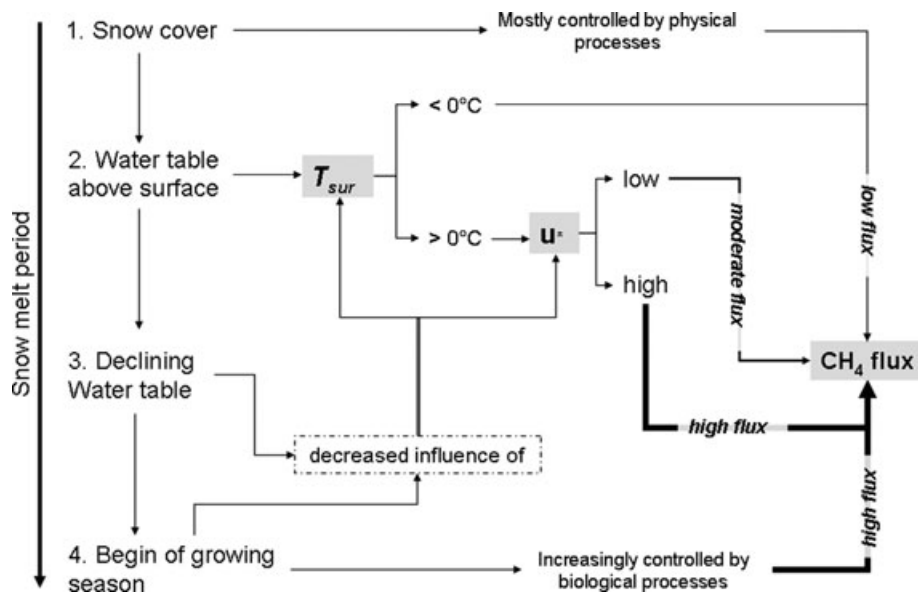


Fig. 5. Conceptual model (flowchart) of the strength in CH₄ flux and its cascade of controlling variables during the four phases (1–4) of the snowmelt period. Most important parameters are surface temperature (T_{sur}) and friction velocity (u^*) (near-surface turbulence), but changes in wind direction and thus source area (not shown here) can also influence the measured CH₄ flux.

the potential effect of turbulent mixing and subsequent increase of CH₄ fluxes (Fig. 4). The factor of changing source area seems to be important on some days; however, it is difficult to consider it without the other controls mentioned earlier. From 21 to 25 April, the source area was changing from the SE at night, where higher WT in combination with low wind speed could be responsible for lower night flux, to SW during the day (minerogenic fen with more hummocks), where higher fluxes could be expected due to higher variability in the surface coverage and the lower WT. However, the following period, 26–28 April, was characterized by winds coming from a narrow region in the SW, similar to the wind direction where the peak CH₄ efflux of previous days was measured. Even with very little variation in the source area, strong diurnal variations have been observed which were apparently not caused by a varying source area, but probably due to factors described earlier. Still, after 25 April, the change of the source area to the minerogenic fen, where more hummocks are present, could be an additional explanation for the decreasing influence of near-surface turbulence.

Evidence of diurnal variation caused by environmental conditions in the early spring might have important implications when the efflux is studied by other methods, for example, closed chambers. In such cases, sampling during the day and extrapolation of results from that one point in time might overestimate early spring fluxes if the mechanism of freezing and thawing as presented in this study is overlooked. In addition, the use of chamber can limit turbulence and thus turbulence-driven efflux as observed in this study, and as a result underestimate CH₄ efflux.

To summarize our findings so far and to fuel further investigation into these phenomena, we propose an idealized flowchart (Fig. 5). The main stages of the snowmelt period (Snow cover, standing water, declining WT and begin of vegetative period) are related to their general flux rates and the possible controlling factors of the measured flux as supported by findings of this study. The highly dynamic spring thaw period seems thus characterized by (1) the transition from low but steady efflux rates mainly controlled by physical properties of the snow cover (Melloh and Crill, 1995) to (2) CH₄ efflux mainly controlled by surface temperature changes, modified by existing turbulence conditions, resulting in diurnally changing CH₄ concentration as found in our study. However, the following transition to the growing season changes the conditions of the environment further leading to higher CH₄ efflux. The high CH₄ efflux during the vegetation period is then mainly driven by increased microbial production, following the increase in soil temperatures and substrate availability (Christensen et al., 2003).

5. Conclusions

In Ust-Pojeg peatland in north-western Russia, diurnal variation in CH₄ flux during the snow-thaw period 2008 occurred as the result of thaw-freeze cycles, enhanced by effects of near-surface

turbulence. These two parameters seem to be strong short-term controlling factors for CH₄ release during the dynamic snow-thaw period, when the peatland is in transition from low and steady efflux during winter to the high efflux during the growing season. When water was covering large parts of the peatland surface during this transition period, the increase of CH₄ concentration under the ice layer at night, and subsequent release after thawing during the day enhanced by mixing of water due to increases in wind speed after calm spells resulted in temporarily increased CH₄ flux during the day. Daily peak efflux during the thaw periods reached values of >3 mg m⁻² h⁻¹ in the early afternoon compared to an average of ~0.8 mg m⁻² h⁻¹ during nights and ~0.5 mg m⁻² h⁻¹ before the snowmelt started. Apparently, during the highly dynamic snow-thaw period, several interactive physical factors influence the gas transport processes and control CH₄ efflux, before other (biological and physical) controls take over in the vegetation period.

6. Acknowledgments

The study was conducted within the framework of the research project EURAPECC- ‘Eurasian peatlands in a changing climate’ and funds were provided by a Sofja Kovalevskaja Research Award and a DFG grant Wi 2680/2–1 to Dr. Martin Wilkming. Michal Gažovič was supported by a KAAD scholarship and a Slovak Gas Industry travel grant. Infrastructure was partially supported by the Carbo North Project (6th FP of the EU, Contract number 036993). We would like to thank all members of the 2007 and 2008 expeditions in Komi Republic, Russia, for mutual patience, understanding and great time.

References

- Becker, T., Kutzbach, L., Forbrich, I., Schneider, J., Jäger, D. and co-authors. 2008. Do we miss the hot spots?—The use of very high resolution aerial photographs to quantify carbon fluxes in peatlands. *Biogeosciences* **5**, 1387–1393.
- Bellisario, L. M., Bubier, J. L., Moore, T. R. and Chanton, J. P. 1999. Controls on CH₄ emissions from a northern peatland. *Global Biogeochem. Cycles* **13**(1), 81–91.
- Bubier, J., Costello, A., Moore, T. R., Roulet, N. T. and Savage, K. 1993. Microtopography and methane flux in boreal peatlands, Northern Ontario, Canada. *Can. J. Bot.* **71**(8), 1056–1063.
- Christensen, T. R., Ekberg, A., Strom, L., Mastepanov, M., Panikov, N. and co-authors. 2003. Factors controlling large scale variations in methane emissions from wetlands. *Geophys. Res. Lett.* **30**, 1414, doi:10.1029/2002GL016848.
- Clymo, R. S. and Pearce, D. M. E. 1995. Methane and carbon-dioxide production in, transport through, and efflux from a peatland. *Philos. Trans. R. Soc. Lond.* **351**, 249–259.
- Comas, X., Slater, L. and Reeve, A. 2008. Seasonal geophysical monitoring of biogenic gases in a northern peatland: implications for temporal and spatial variability in free phase gas production rates. *J. Geophys. Res. Biogeosci.* **113**, G01012, doi:10.1029/2007JG000575.

- Denman, K. L., Brasseur, G., Chidthaisong, A., Ciais, P., Cox, P. M. and co-authors. 2007. Couplings between changes in the climate system and biogeochemistry. In: *Climate Change 2007: The Physical Science Basis. Contribution of Working Group I to the Fourth Assessment Report of the Intergovernmental Panel on Climate Change*. (eds. S. Solomon, D. Qin, M. Manning, Z. Chen, M. Marquis and co-authors). Cambridge University Press, Cambridge, United Kingdom and New York, NY, USA.
- Dise, N. B. 1992. Winter fluxes of methane from Minnesota peatlands. *Biogeochemistry* **17**, 71–83.
- Fischlin, A., Midgley, G.F., Price, J. T., Leemans, R., Gopal, B. and co-authors. 2007. Ecosystems, their properties, goods, and services. In: *Climate Change 2007: Impacts, Adaptation and Vulnerability. Contribution of working group II to the Fourth Assessment Report of the Intergovernmental Panel on Climate Change*. (eds. M. L. Parry, O. F. Canziani, J. P. Palutikof, P. J. Linden van der and C. E. Hanson). Cambridge University Press, Cambridge, 211–272.
- Foken, T. and Wichura, B. 1996. Tools for quality assessment of surface-based flux measurements. *Agric. For. Meteorol.* **78**, 83–105.
- Hargreaves, K. J., Fowler, D., Pitcairn, C. E. R. and Aurela, M. 2001. Annual methane emission from Finnish mires estimated from eddy covariance campaign measurements. *Theor. Appl. Climatol.* **70**, 203–213.
- Heyer, J., Berger, U., Kuzin, I. L. and Yakovlev, O. N. 2002. Methane emissions from different ecosystem structures of the subarctic tundra in Western Siberia during midsummer and during the thawing period. *Tellus* **54B**, 231–249.
- Kettunen, A. 2002. Modeling of microscale variations in methane fluxes. In: *Systems Analysis Laboratory Research Reports*, A83. Helsinki University of Technology. Otamedia Oy, Espoo, Finland, 1–40.
- Koch, O., Tschirko, D. and Kandeler, E. 2007. Seasonal and diurnal net methane emissions from organic soils of the Eastern Alps, Austria: effects of soil temperature, water balance, and plant biomass. *Arct. Antarct. Alp. Res.* **39**, 438–448.
- Mastepanov, M., Sigsgaard, C., Dlugokencky, E. J., Houweling, S., Strom, L., Tamstorf, M. P. and Christensen, T. R. 2008. Large tundra methane burst during onset of freezing. *Nature* **456**, 628–630.
- Melloh, R. A. and Crill, P. M. 1995. Winter methane dynamics beneath ice and in snow in a temperate poor fen. *Hydrol. Proc.* **9**, 947–956.
- Mikkela, C., Sundh, I., Svensson, B. H. and Nilsson, M. 1995. Diurnal variation in methane emission in relation to the water-table, soil-temperature, climate and vegetation cover in a Swedish acid mire. *Biogeochemistry* **28**, 93–114.
- Moncrieff, J., Valentini, R., Greco, S., Seufert, G. and Ciccioli, P. 1997. Trace gas exchange over terrestrial ecosystems: methods and perspectives in micrometeorology. *J. Exp. Bot.* **48**, 1133–1142.
- Moore, C. J. 1986. Frequency response corrections for eddy correlation systems. *Bound.-Layer Meteorol.* **37**, 17–35.
- Panikov, N. S. and Dedysh, S. N. 2000. Cold season CH₄ and CO₂ emission from boreal peat bogs (West Siberia): winter fluxes and thaw activation dynamics. *Global Biogeochem. Cycles* **14**, 1071–1080.
- Sachs, T., Wille, C., Boike, J. and Kutzbach, L. 2008. Environmental controls on ecosystem-scale CH₄ emission from polygonal tundra in the Lena River Delta, Siberia. *J. Geophys. Res. Biogeosci.* **113**, 12, doi:10.1029/2007JG000505.
- Thomas, K. L., Benstead, J., Davies, K. L. and Lloyd, D. 1996. Role of wetland plants in the diurnal control of CH₄ and CO₂ fluxes in peat. *Soil Biol. Biochem.* **28**, 17–23.
- Tokida, T., Mizoguchi, M., Miyazaki, T., Kagemoto, A., Nagata, O. and co-authors. 2007. Episodic release of methane bubbles from peatland during spring thaw. *Chemosphere* **70**, 165–171.
- Wille, C., Kutzbach, L., Sachs, T., Wagner, D. and Pfeiffer, E. M. 2008. Methane emission from Siberian arctic polygonal tundra: eddy covariance measurements and modelling. *Glob. Change Biol.* **14**, 1395–1408.

Chapter 3

Temperature and plant phenology control the seasonal variability of CO₂ and CH₄ fluxes from a boreal peatland in North-West Russia*

Abstract

The micrometeorological eddy covariance method was used to study exchange fluxes of carbon dioxide (CO₂) and methane (CH₄) between a boreal peatland in North-West Russia and the atmosphere. The aim of the study was to quantify the emissions of CO₂ and CH₄, and to study sub-seasonal environmental mechanisms of carbon (C) turnover which control the measured fluxes on the landscape scale. The study site is the Ust-Pojeg mire complex (61°56'N, 56°13'E) in the Komi Republic and is characterised by a boreal humid continental climate. Eddy covariance flux measurements took place from April 2008 until February 2009. After the snowmelt period, the net ecosystem exchange of CO₂ (NEE) was found to be primarily controlled by temperature and by changes in vegetation phenology. The highest upward and downward directed CO₂ fluxes were measured in the period of the highest leaf area of the vascular plants at the end of July. With senescing vegetation, from the beginning of August, the photosynthesis slowly decreased, while the ecosystem respiration continued during autumn at substantial rates, and positive CO₂ fluxes were measured during the winter time. Moving response functions were used to address ecological changes in CO₂ flux control throughout the season and appear to be a good tool to study physiological drivers of the carbon cycle processes on sub-seasonal scale. Methane flux in its annual course was well explained by soil temperature, the seasonal course of which is closely connected to vascular plant development. Our study site was observed to be a net C

* Manuscript to be submitted in 07/2011.

sink with an estimated annual net ecosystem CO₂ exchange of -458 ± 45 g CO₂ m⁻², and a CH₄ source with an annual flux estimate of 30 ± 3 g CH₄ m⁻².

3.1 Introduction

The largest areas of peatlands are located in sub-arctic and boreal regions storing between 400-500 Gt of carbon (C) (Gorham, 1991; Davidson and Janssens, 2006a). For comparison, today's C content of the Earth's atmosphere is ~730 Gt, and C stored in the global vegetation amounts to ~650 Gt (Zimov et al., 2006). Plant primary production rates are limited by short growing seasons, but soil organic matter decomposition is strongly limited as well by the usually wet and cold subsurface conditions (Gorham, 1991). Generally, these peatlands represent net sinks of atmospheric carbon dioxide (CO₂) and sources of methane (CH₄) over long time scales. In recent years, a number of peatland C flux studies in arctic tundra and the boreal zone were conducted, many of them focusing on CO₂ (e.g. Shurpali et al., 1995; Arneeth et al., 2002; Aurela et al., 2002; Lindroth et al., 2007; Kutzbach et al., 2007), CH₄ (e.g. Suyker et al. 1996; Hargreaves et al., 2001; Rinne et al., 2007; Sachs et al., 2008; Wille et al., 2008), or both gases simultaneously (e.g. Friborg et al., 2003; Heikkinen et al., 2004; Riutta et al., 2007). In general, carbonaceous gas dynamics show high spatial variation between peatland sites, and annual CO₂ emissions can differ substantially between tundra and taiga sites. Reported annual CO₂ flux estimates from a Russian tundra peatland region measured by eddy covariance were -71 g CO₂ m⁻² (Kutzbach et al., 2007), which is similar to the annual balance of -68 g CO₂ m⁻² measured from a subarctic fen in northern Finland (Aurela et al., 2002). Much higher annual estimates of -396 g CO₂ m⁻² were reported for a Russian taiga peatland region (Friborg et al., 2003). Similar spatial variation can be observed in CH₄ fluxes from different studies. For example, measured annual CH₄ emissions from Finnish and Russian tundra sites estimated by eddy covariance were 5.5 g CH₄ m⁻² and 3 g CH₄ m⁻², respectively (Hargreaves et al., 2001, Wille et al., 2008). However, much higher average CH₄ fluxes were reported from Finnish boreal peatlands measured by the static chamber technique (23 g m⁻² yr⁻¹) and by eddy covariance (12.5 g m⁻² yr⁻¹) (Huttunen et al., 2003; Rinne et al., 2007). The seasonal CH₄ budget measured by eddy covariance for the period 11 May to 26 December 2007 at the boreal fen Salmisuo in eastern Finland was

11.7±0.2 g m⁻² (Forbrich et al., 2011). Considering the vast area of Russian tundra and boreal peatland and the studies already conducted (e.g. Panikov and Dedysh, 2002; Arneth et al., 2002; Friborg et al., 2003; Kutzbach et al. 2007; Golovatskaya and Dyukarev, 2009), still little is known about their C cycling compared to Fennoscandinavia and North America. Especially continuous C-flux data from peatlands in the Russian boreal region are very limited (but see Arneth et al., 2002; Friborg et al., 2003). In this paper we present continuous measurements of CO₂ and CH₄ fluxes from a boreal peatland in the Komi Republic, Russian Federation.

When studying relationships between measured fluxes and environmental variables, linear or nonlinear response functions determined by regression are typically used to describe these relationships. Often, these regressions functions are not computed for multiple time intervals, and so the time-dependent changes in the relationships are not easily identified (Biondi, 1997). To capture dynamical variability of the signal, moving response function analysis can be applied. This technique employs a fixed time interval progressively slid across the time series of the fluxes (predictand) and the respective environmental control variables (predictors) to compute the response coefficients (Biondi, 1997, Mahecha et al., 2010). “Moving windows” were previously used for the estimation of short-term temperature sensitivity of ecosystem respiration (Reichstein et al., 2005). A similar concept of temporally variable parameters is incorporated in the Kalman filter method (e.g Visser, 1986; Rastetter et al., 2010).

The objective of this study was to quantify the annual emissions of CO₂ and CH₄, and to study sub-seasonal environmental mechanisms which control the carbon (C) turnover and the measured fluxes on the landscape scale.

3.2 Methods

3.2.1 Study site

Measurements of CO₂ and CH₄ fluxes were conducted at the boreal peatland complex Ust- Pojeg (61°56'N, 56°13'E), about 60 km north-west of Syktyvkar, the capital of the Komi Republic, Russian Federation. The Ust- Pojeg peatland complex (ca. 25 km²) is situated between the Pojeg River (in the West) and the Vychegda River (in the North). The peatland complex is composed of a mosaic of different landscape units in terms of

nutritional state and hydrology and can be described as a transition peatland composed of both ombrogenic bog and minerogenic fen types (Fig.1). We differentiated between 1) the ombrogenic bog part where the dominant moss vegetation cover is *Sphagnum angustifolium* and *S. fuscum*, 2) the minerogenic fen part with *S. jensenii* and *S. fuscum* and 3) a transition zone between the bog and fen parts which was dominated by *Carex rostrata* (Fig. 3.1). A special feature 4) was a minerogenic depression zone which was a stripe between the minerogenic and the transition zones characterised by generally higher water table levels. At small scales, *Carex limosa* and *Scheuchzeria palustris* dominated in hollows, the wettest microforms, while *Andromeda polifolia*, *Chamaedaphne calyculata*, *Betula nana* and stunted *Pinus sylvestris* dominated on hummocks, the driest microforms. Vegetation on lawns as intermediate microforms was a mixture of hummock and hollow vegetation with *Vaccinium oxycoccus*. The occurrence of *Menyanthes trifoliata* and *Utricularia intermedia* indicated greater nutrient supply in the minerogenic part of the peatland complex. The average depth of the peat was ca. 1.5 m.

The climate is boreal, continental and humid. The average temperatures for Syktyvkar in the period 1999-2008 were 18.2 °C and -12.7 °C for July and January, respectively (<http://meteo.infospace.ru>). The mean annual precipitation for the same period was 465 mm. Snow cover persists usually from November until the end of April. In April 2008, the eddy covariance (EC) system was set up in the South-West part of the peatland complex Ust-Pojeg. The area of interest in this study is defined as a circle with a radius of 300 m around the eddy covariance (EC) system (Fig. 3.1).

3.2.2 Experimental setup

The fluctuations of the wind speed components were measured using a three-dimensional sonic anemometer (Solent R3, Gill Instruments Ltd., UK) installed 3 m above ground level. From the sample intake 15 cm below the central point of the sensor array of the anemometer, a vacuum pump drew the sample air through a CO₂/H₂O infrared gas analyser (LI-7000, LI-COR Inc., USA) and through a CH₄ fast methane analyser (RMT-200, Los Gatos Research Inc., Mountain View, CA, USA). Both analyzers and the PC were housed in temperature-regulated boxes (InsituFlux, AB, Sweden). In October 2008, heating cables were installed at the intake tubes.

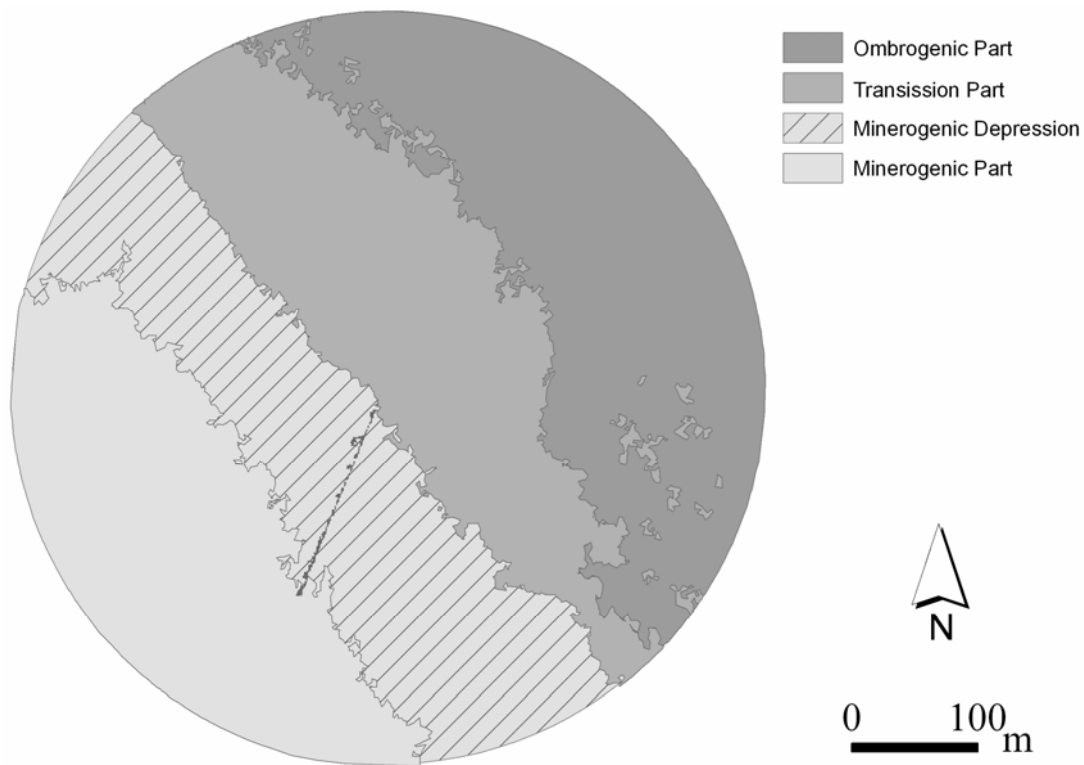


Figure 3.1 Location of ombrogenic, transition and minerogenic mire zones with a special feature in the minerogenic part, the minerogenic depression at the Ust-Pojeg study site (derived from Quickbird satellite image). Black line represents a boardwalk. The eddy covariance tower is situated at the northern end of the boardwalk at the border between the minerogenic and transition mire parts.

Additional instruments installed near the EC tower include sensors for air temperature and relative humidity (CS215, Campbell Scientific Ltd., UK), wind speed and direction (M15103, R.M. Young, MI, USA), incoming and outgoing shortwave and longwave radiation (CNR 1, Kipp and Zonen B.V, The Netherlands), incoming photosynthetically active radiation (QS2 Delta-T Devices Ltd., UK) and barometric pressure (RPT 410, Druck Messtechnik, GmbH, Germany). Liquid precipitation was monitored with a tipping bucket rain gauge. All signals from additional sensors were logged on a data logger (CR-1000, Campbell Scientific Ltd., UK). Soil temperature was measured at depths of 5 cm, 10 cm, 20 cm and 40 cm with automatically logged soil temperature sensors (HOBO U12 Outdoor/Industrial, Onset Computer Corp., Bourne, USA) under the surfaces of various representative microforms. At these

microforms, additional chamber measurements of CO₂ and CH₄ fluxes were conducted, as well as measurements of the green leaf area index (LAI). LAI of vascular plants was calculated as a product of the leaf size and number of green leaves. The green leaf area of mosses was estimated as the projection coverage of living moss capitula (about 0.75 m² m⁻²). The estimated moss cover was set constant over the growing season. Total LAI was calculated as a sum of both vascular plants and mosses (Schneider et al., in review) Water table (WT) fluctuations were monitored using water level loggers (type MDS, Seba Hydrometrie GmbH, Kaufbeuren, Germany) installed at four different locations in the peatland, representing ombrogenic bog, minerogenic fen, the transition zone mostly consisting of *Carex* and *Sphagnum* lawns and the minerogenic depression.

3.2.3 Raw data processing and flux calculation

Data were logged at 20 Hz, and eddy covariance fluxes were calculated over 30 min intervals. The time lag between wind and scalar concentration measurements was determined and removed for every averaging period. Turbulent fluxes were calculated using the EdiRe software (Robert Clement, University of Edinburgh, UK). Two coordinate rotations were applied to the wind components so that the mean transverse and the mean vertical wind components were reduced to zero. Flux losses due to the limited frequency response of the eddy covariance system were corrected in the flux calculation process. The fluxes were corrected for the frequency attenuation due to tube attenuation, sensor path separation and spectral response of the instruments (Moore, 1986; Moncrieff et al., 1997). The frequency correction in our study was on average 12.8±1.1 % and 10.4±0.4 % for CO₂ and CH₄ fluxes, respectively. The Webb correction adapted for closed-path eddy covariance systems was applied to the CO₂ flux (Ibrom et al., 2007). The Webb correction for open path eddy covariance system was applied for CH₄ fluxes as well. Integral turbulence characteristics (ITC) were calculated, and data were screened accordingly (Foken and Wichura, 1996). Data were removed if the deviation from the ITC parameter was greater than 30%. Instationarity characteristics were calculated and used to discard the data obtained during non-stationary conditions (Foken and Wichura, 1996).

Due to technical problems, instrument calibration and maintenance, gaps in the data series were introduced lasting from a few hours to days. The largest gap occurred from

29 June -10 August in the CH₄ measurements due to malfunctioning of the analyzer and shipment problems for the spare parts. In total, fraction of gaps after quality control screening was 40% for CO₂ and CH₄ data, respectively. For this study, positive flux values indicate upward fluxes, e.g. emission from the peatland ecosystem; negative flux values indicate the contrary, e.g. uptake by the peatland ecosystem.

3.2.4 Gap-filling models

To properly estimate the annual carbon balance, the gaps in the CO₂ and CH₄ flux time series were filled by empirical models of net ecosystem exchange of CO₂ and CH₄.

3.2.4.1 CO₂ flux model

In this study, we used a moving window analysis to determine the model parameters at smaller than seasonal scale. Data were divided into night (PAR < 20 μmol m⁻² s⁻¹) and day (PAR > 20 μmol m⁻² s⁻¹) measurements. The term net ecosystem exchange (NEE), which is the sum of gross photosynthesis (P_g) and ecosystem respiration (R_{eco}), is equivalent to the calculated CO₂ fluxes. In our study we adapted a multiplicative nonlinear model based on Michaelis-Menten kinetics for gross photosynthesis P_g (Kettunen, 2000):

$$P_g = aI * PAR / (PAR + kI) \quad (3.1)$$

where *aI* indicates maximum photosynthesis (P_{max}), PAR is photosynthetically active radiation, and *kI* is the PAR value for which the P_g reaches half of P_{max}. For ecosystem respiration, relationships with air and soil temperatures were studied, using data representing fluxes during dark periods (PAR < 20 μmol m⁻² s⁻¹). After the initial inspection, respiration rates R_{eco} were modelled using the following exponential function

$$R_{eco} = pI * e [p2 * T] \quad (3.2)$$

where T is air temperature (T_{air}) or soil temperature (T_{soil}), parameter $p1$ represents y-axis offset (magnitude of R_{eco} during the specific period/temperature regime) and parameter $p2$ represents the curvature of the exponential function. The NEE time series was modelled by combining equations 1 and 2, resulting in the following equation

$$\text{NEE} = a1*\text{PAR} / (\text{PAR}+k1) + p1* \exp (p2*T) \quad (3.3)$$

with parameters and predictor variables as described above. We expected P_g to be zero during the night-time, and thus the CO_2 flux should represent R_{eco} . For this reason we fitted equation (2) to the night-time data with soil temperature in 20 cm as a predictor. Equation (3) was fitted to the day-time data as we expected non-zero respiration during the day with air temperature as a predictor. This was done on raw data prior to gap filling. The empirical models were fitted to the flux data with a 10-day long window. The window was then slid one day forward to produce a second set of fit coefficients and so on. As a result we obtained time series of model parameters, coefficients of determination (R^2_{adj}) and root mean square errors (RMSE) indicating the performance of the fit function between measured fluxes and environmental predictor variables within the window. Thus we could analyze the changes of the parameters over time and use them for CO_2 flux modelling and gap-filling.

The results of the moving response analysis in this manuscript were always plotted in a way that each single plotted parameter or coefficient value belonged to the centre of the 10-day long window (± 5 days) and thus was representative for the whole window period. For convenience to follow the results, we will refer to the time of the year as: beginning (spring), middle (summer) and end (autumn/winter). During periods when we could not successfully model the time series with the described models (for CO_2 before 4 May and after 5 November), the existing flux data sets were linearly interpolated. In order to estimate reasonable winter emissions during the period 19 February to 6 April when no data were available, the average flux values of the last three measurement days during the winter campaign in February 2009 were used as estimates.

3.2.4.2 CH₄ flux model

We did not use the moving window approach for the CH₄ fluxes due to the long data gap in summer. CH₄ fluxes were exponentially related to temperature and were modelled as

$$F_{CH_4} = a * \exp [b * T_{soil}] \quad (3.4)$$

where T_{soil} is soil temperature in 20 cm, a represents y-axis offset (magnitude of CH₄ flux during the specific period/temperature regime) and parameter b represents the curvature of the exponential function. This model was used from 3 May until the end of the measurements on 12 February. From 6 to 21 April and from 5 November to 12 February, the existing data sets were linearly interpolated, and from 21 April until 3 May an empirical model with surface temperature as regulating variable describing diurnal variations during the snow melt period was applied (Gažovič et al., 2010). To estimate the winter emissions during the period 12 February to 6 April when no data were available, the average flux values of the last three measurement days during the winter campaign in February 2009 were used as estimates.

3.2.5 Footprint modelling

To estimate the EC source area fractions (Ω_i) of the landcover classes (i) in the area of interest, an analytical footprint model (Kormann and Meixner, 2001) was combined with landcover raster maps with 1 m resolution. These maps contain the information about the absence or presence of a class coded as 0 or 1, respectively. For each 30 min flux calculation interval and each class, each pixel was weighted with the footprint model function and multiplied with the code value (0 or 1) and the pixel area (1 m²). Ω_i was then calculated as the sum of the pixels belonging to each class (Forbrich et al., 2011). The time series was filtered for low turbulence (friction velocity $u^* < 0.1$ m/s), high crosswind fluctuations ($\sigma_v > 1$ m/s) and periods when sensible heat flux was zero, leading to the removal of 43% of the data points of the 11-month time series. The gaps were filled with means of Ω_i which were calculated for one-degree intervals of wind direction for stable and unstable atmospheric conditions, respectively.

3.2.6 Estimating the annual C balance

The estimates of annual CO₂ and CH₄ emissions were calculated by integrating the gap-filled half-hour flux time series over time. When quantifying the annual budget based on EC measurements, various types of errors have to be considered (Moncrieff et al., 1996) as they are introducing uncertainty to the final estimate. For CO₂ estimates, we calculated the random error from the difference between the observed and modelled half-hourly fluxes using equation B1 in Aurela et al. (2002). The random error was calculated for three periods with different gap filling methods: a) linear interpolation before 4 May, b) empirical model (equation 3) from 4 May until 4 November and c) linear interpolation after 5 November. To estimate the random error for periods when linear interpolation was used, we linearly interpolated between beginning and end points of the groups of measured data, and the random error was calculated as a difference between measured and linearly interpolated values (Rinne et al., 2007). Systematic errors in EC measurements have their origin in the limited frequency response of the EC system. An uncertainty of 30% was assumed for the frequency and Webb correction procedures itself (Aurela et al., 2002). For winter measurements with no data coverage where average values were used, 20% uncertainty of the balance of this season was assumed (Aurela et al., 2002). Additionally, the systematic error associated with selection of the gap filling method with moving and fixed parameters was estimated.

For CH₄, the random errors were estimated for the two periods when linear interpolation and the empirical models were used for gap filling. Systematic errors were considered, due to frequency and Webb corrections, and for winter estimations. The biggest source of possible systematic error in the annual CH₄ estimate was a 5-week gap in the summer period. Although the gap-filling procedure was shown not to have a strong effect on annual methane emission estimation (Rinne et al., 2007), we have used different gap-filling methods in our case in order to fill the gap during the summer, namely 1) linear interpolation, 2) gauss function and 3) an exponential function. The difference between the methods giving the smallest and the highest annual emission was considered as a systematic error for this period.

3.3 Results

3.3.1 Weather characteristics

When instruments were set up at the end of March, the peatland was snow-covered (ca. 40 cm, P. Schreiber, personal communication) with a few snow-free hummocks. Mean daily temperatures were below 0 °C rising rapidly reaching 3.5 °C on 1 April. High daily mean temperatures and rainfall accelerated snowmelt. From 12 to 16 April, mean daily temperatures decreased again below zero (Fig. 3.2a). All snow had disappeared by 17 April. No snow cover was established before the end of October (field observations). After this time, direct observations of snow accumulation are not available, but values of incoming and outgoing solar radiation indicate, that snow cover started to establish only at the end of November and probably even later. The first week in December was characterized by high -for this time of the year- temperatures, and thus we expect that the permanent snow cover was present only from the second third of December onwards.

After snowmelt, the WT stayed close to the surface in the ombrogenic, the minerogenic and the transition zone, at times rising slightly above the surface. The WT in the minerogenic depression stayed above the peat surface until 18 June, and hence only hummocks were protruding out of the water surface. The WT was at its lowest reaching around 22 cm below the peat surface on 19 August in the ombrogenic part, while in the minerogenic depression it only fell to around 5 cm below the peat surface. Frequent rainfall in the second half of August amounting to 115 mm (29 % of all liquid precipitation measured from April to October) caused a considerable rise in the WT (Fig. 3.3).

The average July and January temperatures were 18.3 °C and -15.6 °C, respectively, which was 0.1 °C above and 2.9 °C below long term mean, respectively. Liquid precipitation measured from April to October was 388 mm. Mean daily temperatures during the study period reached a peak of 25 °C (diurnal maxima 31.1 °C) on 20 July. Lowest mean daily temperature of -32.8 °C (diurnal minima -40.1°C) was measured on 6 February 2009. Interestingly, the air temperatures during winter showed high variability, and differences between night and day temperatures of up to 40 °C were

observed. Soil temperatures measured in different depths reached mean seasonal peak values of 19.7 °C

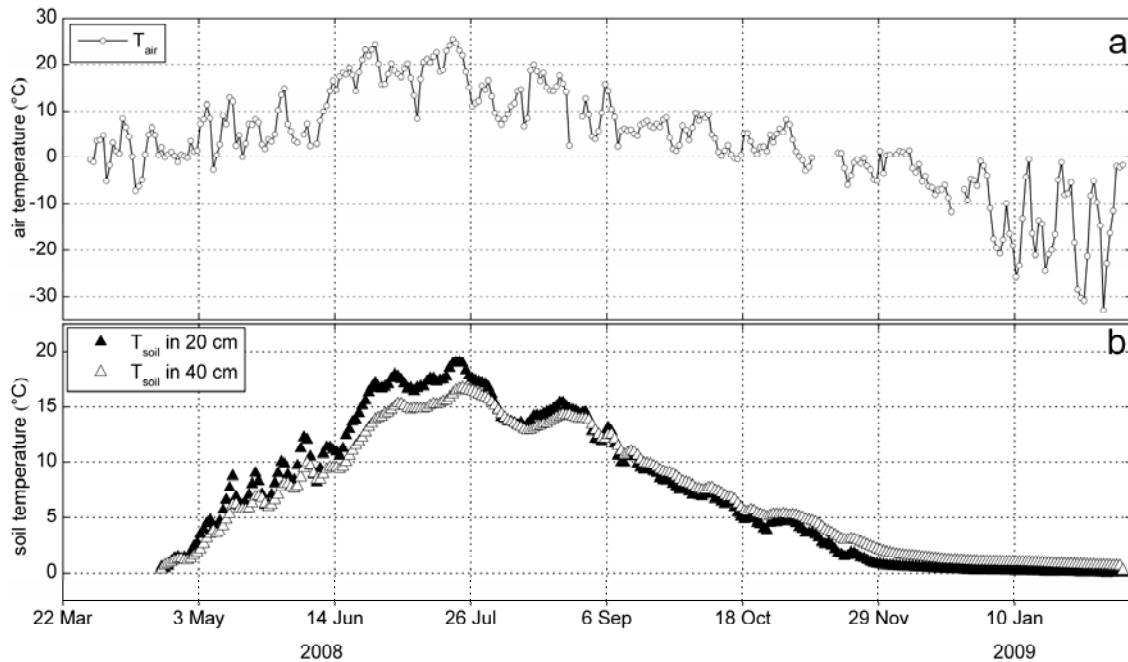


Figure 3.2 Development of a) average daily air temperatures (○) and b) average daily soil temperatures in 20 cm (▲) and 40 cm (△) depth at Ust-Pojeg site from April 2008 until February 2009.

in 10 cm and 16.5 °C in 40 cm, respectively, on 20 July and were decreasing thereafter. Soil temperatures in 20 cm and 40 cm depth did not reach the freezing point until the end of measurements in February. Soil temperatures in 5 cm and 10 cm depth occasionally dropped below zero in January and February 2009, with the lowest temperature -0.5 °C in 5 cm depth measured on 7 February, when the lowest night air temperature -40.1 °C was measured.

Vascular plants appeared within few days after the snowmelt (field observation). Leaf area index (LAI) of vascular plants measured manually starting 14 June was rapidly increasing, reaching peak LAI values from the end of July to the beginning of August, and was decreasing moderately thereafter with senescing vegetation.

Winds from south-east were predominant, but south, south-west and north-west winds also frequently occurred (Fig. 3.4). The mean wind speed during the study period was $2.3 \pm 1.4 \text{ m s}^{-1}$.

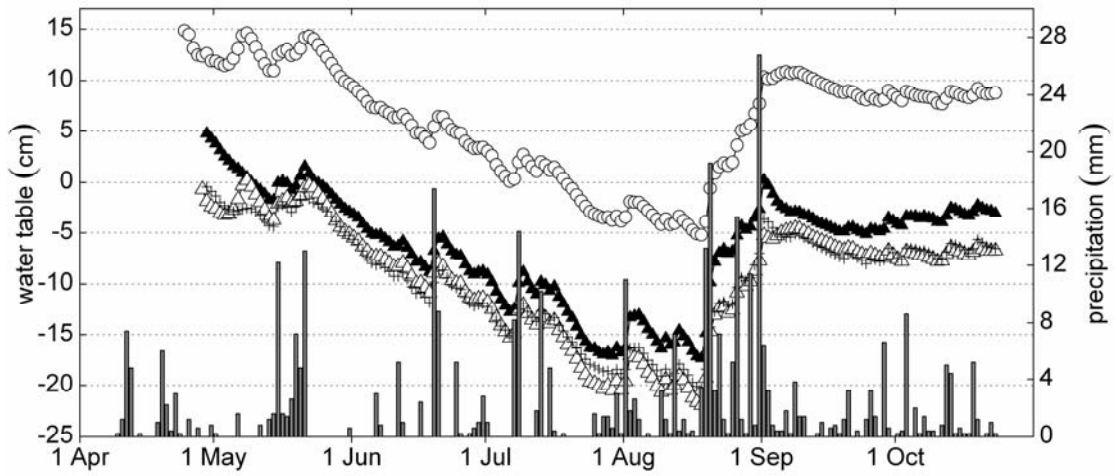


Fig. 3.3 Average daily values of water table (cm) and precipitation (mm, bar plot). Water table was measured in the minerogenic depression (○), the ombrogenic (▲), minerogenic (Δ) and transition (+) mire parts.

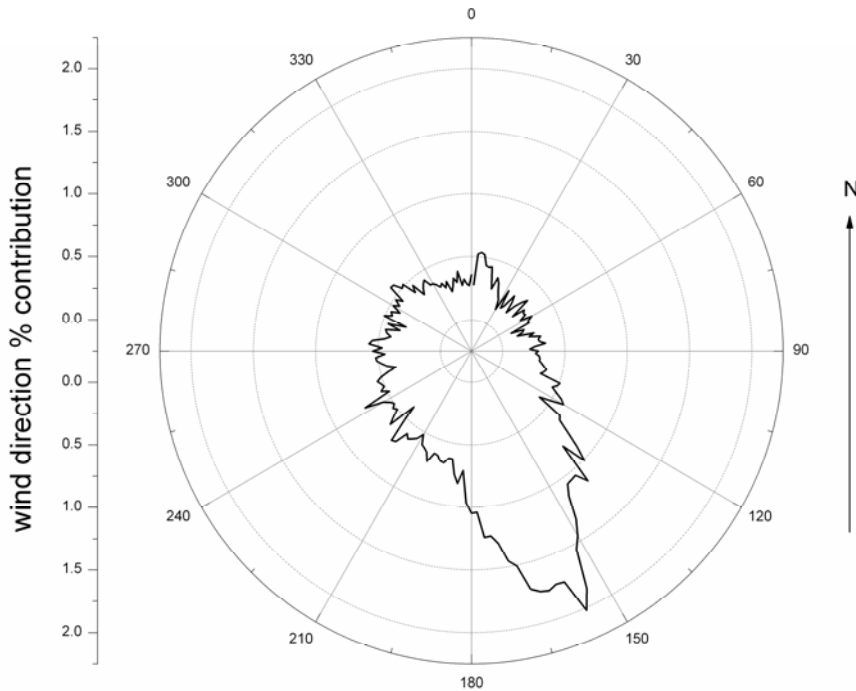


Figure 3.4 Frequency distribution of wind directions at the Ust-Pojeg peatland during the study period (5° intervals)

3.3.2 CO₂ flux

The late winter from 6 April to 16 April 2008 was characterised by moderate but variable CO₂ fluxes, on average $26 \pm 23 \text{ mg m}^{-2} \text{ h}^{-1}$. After 16 April, when all snow disappeared, the fluxes were increasing and reached $187 \text{ mg m}^{-2} \text{ h}^{-1}$ on 19 April, followed by a decline due to increasing photosynthesis. Diurnal oscillations were observed from 16 April right after the snowmelt, and several half-hourly fluxes during midday showed small CO₂ uptake. The daily NEE was oscillating between a small sink and a small source from the beginning of May. Afterwards, the photosynthesis was increasing, and on 20 May the peatland turned into a net daily CO₂ sink. A steeper increase in day and night NEE was observed after 8 June. CO₂ uptake during daytime culminated in the second half of July with NEE values of up to $-1900 \text{ mg m}^{-2} \text{ h}^{-1}$, while the nighttime CO₂ releases reached $1000 \text{ mg m}^{-2} \text{ h}^{-1}$. In the beginning of August, a decrease in both day and night fluxes was observed although the CO₂ flux increased again in the middle of August, prior to autumnal decline (Fig. 3.5). At the end of September, respiration dominated the CO₂ flux and the peatland turned into a net daily CO₂ source with increasing positive fluxes, reaching up to $150 \text{ mg m}^{-2} \text{ h}^{-1}$ at the end of October. Since then, the positive CO₂ release was decreasing towards winter minima. Diurnal oscillations, however small, could be observed until beginning of November. The winter measurements in January 2009 showed positive CO₂ fluxes with an average of $16.7 \pm 9.3 \text{ mg m}^{-2} \text{ h}^{-1}$.

3.3.3 Moving window analysis of CO₂ fluxes

The results of the moving window analysis showed clear changes in the model parameters through the year. For daytime NEE, the maximum photosynthesis (P_{max}) was steadily increasing from the beginning of May (Fig. 3.6a). The increase in P_{max} was slightly delayed after the steep increase in soil temperature in the beginning of June (Fig. 3.6b) although it seemed to follow the development of the green LAI (Fig. 3.6c), with the peak of P_{max} coinciding with the peak in LAI. After the peak LAI and P_{max} was reached and LAI was decreasing in August, P_{max} seemed to be influenced more by the temperature.

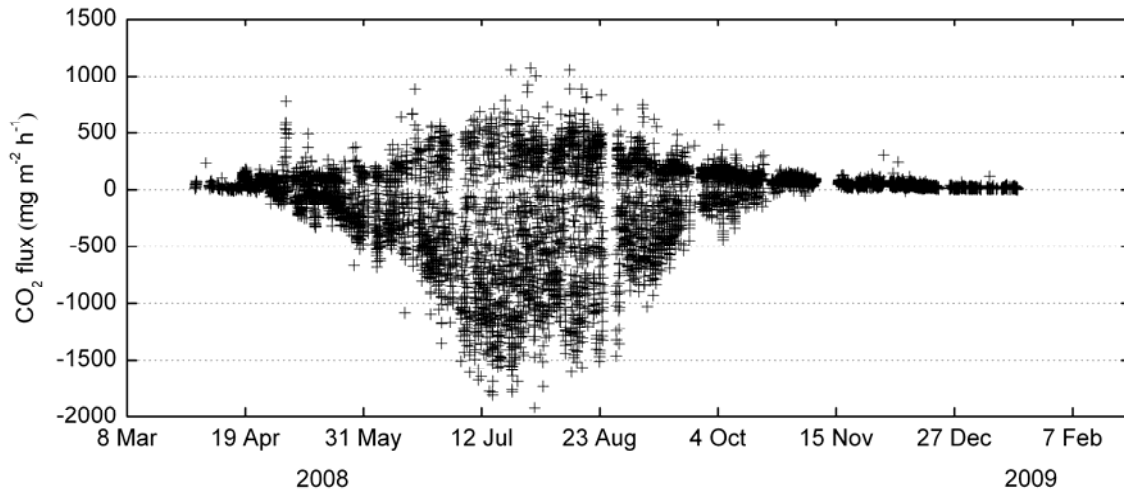


Figure 3.5 Annual pattern of half-hourly measured CO₂ fluxes. Negative values indicate uptake of CO₂, positive values indicate CO₂ release.

For nighttime NEE- R_{eco} , the parameter $p1$ indicating the level of R_{eco} during a specific phenological period was increasing from the spring time, reached peak values in the end of July, and was decreasing thereafter (Fig. 3.7a). The parameter $p2$ representing the curvature of the exponential function and so the temperature sensitivity of R_{eco} during a specific phenological period was increasing from the end of May although a strong decrease was observed from the middle of June indicating a lower sensitivity of R_{eco} to T_{soil} during this period (Fig. 3.7b). An increase of the parameter $p2$ was observed again from the beginning of August indicating a more pronounced temperature sensitivity of R_{eco} .

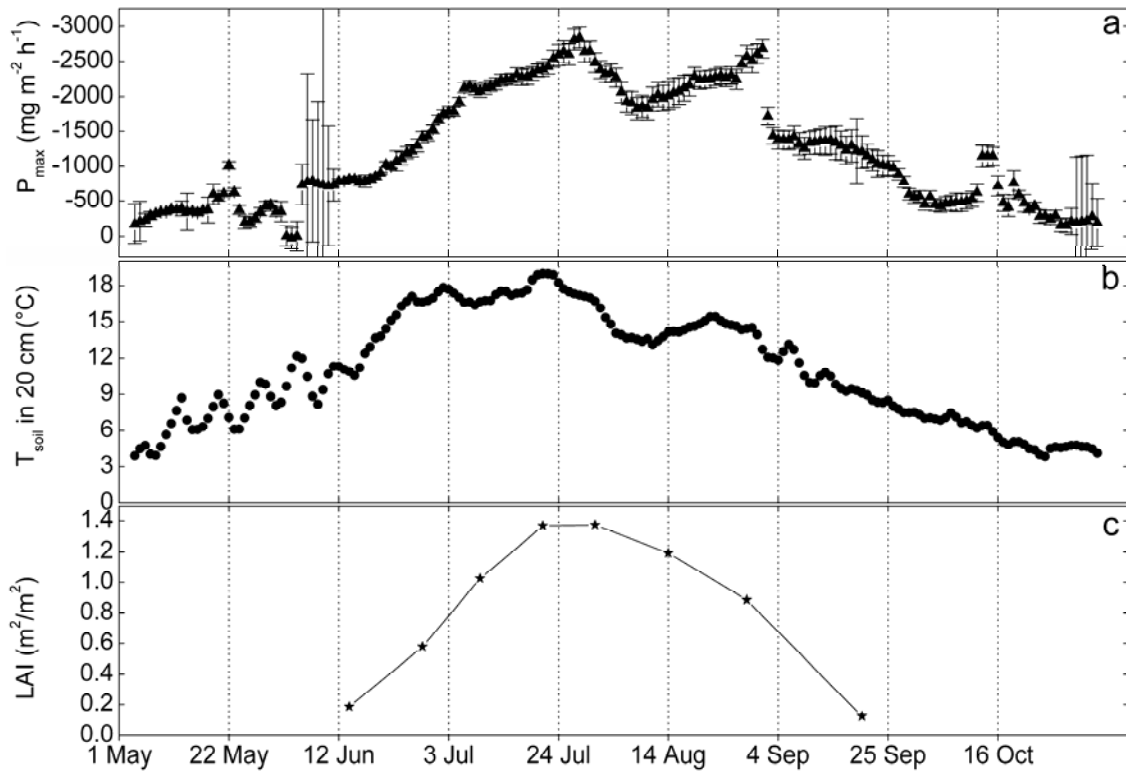


Figure 3.6 Time series of a) maximum photosynthesis P_{\max} (\blacktriangle) obtained by moving window analysis with 10- day long window, b) soil temperature in 20 cm depth (\bullet), and c) green leaf area index ($*$) at the Ust-Pojeg mire from May to November. Note that the y-axis for P_{\max} is reversed.

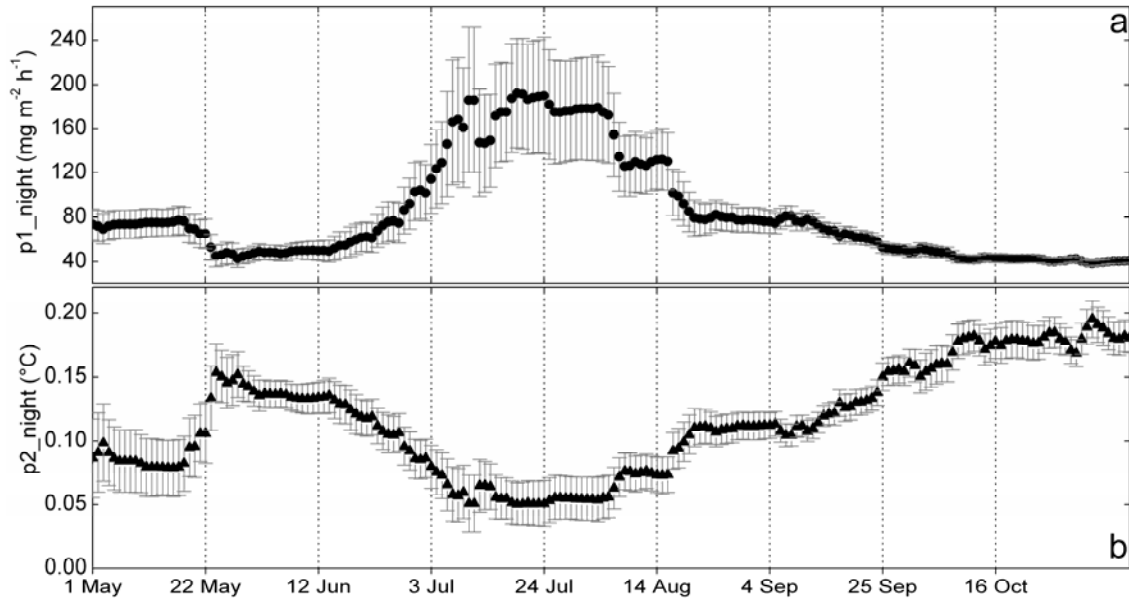


Figure 3.7 Results of moving window analysis on CO_2 night fluxes as exponential functions of soil temperature in 20 cm (Eq. 3.2). a) Estimated parameter $p1$ (•) and b) parameter $p2$ (▲) of the exponential model for 10-day window with 95% confidence intervals.

3.3.4 CH_4 flux

The Ust-Pojeg peatland acted as a CH_4 source throughout the investigation period (Fig. 3.8). The lowest, but positive fluxes with on average $0.53 \pm 0.13 \text{ mg m}^{-2} \text{ h}^{-1}$ were measured from the snow-covered surface at the beginning of April 2008. In the beginning of May, the highest emissions were $5 \text{ mg m}^{-2} \text{ h}^{-1}$, followed by a slight decline. The fluxes were increasing from the end of May; however, a steep increase in CH_4 fluxes was observed from 12 June until 29 June. The highest emissions before and after the gap from 29 June to 10 August in the measurements were about $13 \text{ mg m}^{-2} \text{ h}^{-1}$. From the beginning of September, CH_4 emissions were decreasing until reaching the winter minima. Beside diurnal variations observed in the period from 21 April to 3 May (Gažovič et al., 2010), no systematic diurnal variation was found based on the normalized medians method (Rinne et al., 2007). The empirical model driven by soil temperature showed a good performance ($R^2_{\text{adj}}=0.82$; $\text{RMSE}=1.18 \text{ mg m}^{-2} \text{ h}^{-1}$) and was used to fill missing data gaps.

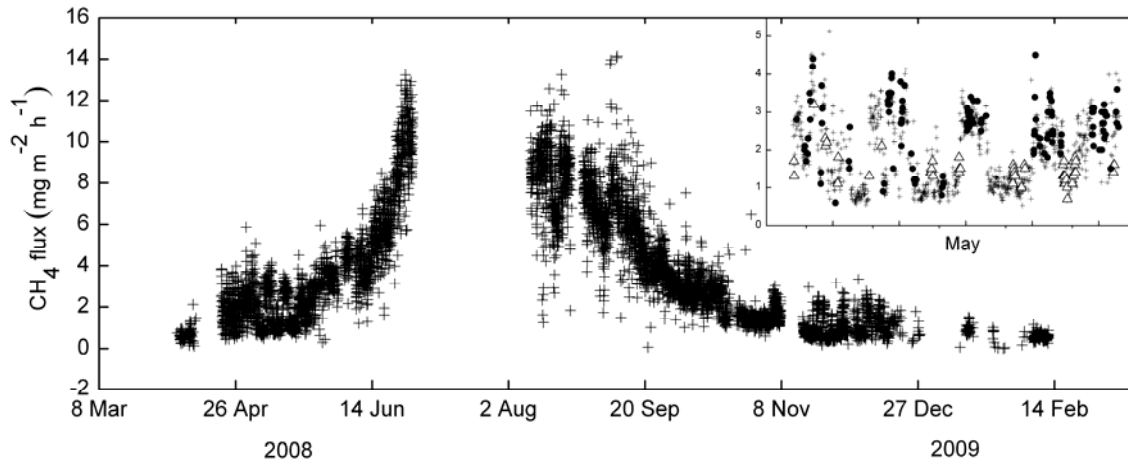


Figure 3.8 Annual course of methane fluxes measured half-hourly. The inset illustrates spatially weighted CH_4 flux from minerogenic (Δ) and transition part (\bullet) during May. The y-axis of the inset is in the same units as the main plot.

3.3.5 Footprint analysis

Because the source area of the measured flux regularly extended over the area of interest, the sum of source area fraction Ω_i for each 30-min period ranged between 53–100 %. We restricted the analysis on the 92 % of all the flux data points which originated at least by 70 % in the area of interest, after this restriction the sum of Ω for the minerogenic area (Ω_{min}) ranged from 0 to 87 % (mean: 37%), for the ombrogenic area (Ω_{omb}) from 0 to 29 % (mean: 5 %) and for the transition zone (Ω_{trans}) from 4 to 100 % (mean: 46 %). As the main wind direction was South (Fig. 3.4), the ombrogenic part situated in the north was under-sampled and in 60 % of the cases its area contribution was approximately 0 %. On the other hand, the minerogenic and transition parts of the peatland were sampled evenly. Thus, further analysis was restricted to the minerogenic and transition parts by filtering the time series of measured fluxes for Ω_{min} or $\Omega_{\text{trans}} \geq 80$ %.

Filtering the time series of measured fluxes did not result in significantly different model parameters ($p < 0.05$) for CO_2 or CH_4 , respectively. Hence, we applied the gap-filling models for CO_2 (eq. 3.3) and CH_4 (eq. 3.4) on all fluxes which remained after the flux evaluation with no footprint function weighing.

3.3.6 Annual carbon balance and uncertainty estimates

The cumulative gap-filled NEE flux in our study was $-458 \text{ g CO}_2 \text{ m}^{-2} \text{ yr}^{-1}$. The random errors associated with the annual CO_2 estimate were $\pm 3.8 \%$, $\pm 4.1 \%$ and $\pm 1.3 \%$ and correspond to 1.2 g , 24 g and $0.9 \text{ g CO}_2 \text{ m}^{-2}$ for the time periods of different gap-filling procedures: a) linear interpolation before 4 May, b) empirical model (equation 3.3) from 4 May until 4 November and c) linear interpolation after 5 November, respectively. The wintertime (February to April) uncertainty was $5.6 \text{ g CO}_2 \text{ m}^{-2} \text{ yr}^{-1}$ which corresponds to $\pm 1.2 \%$ of the annual balance. The uncertainty associated with the CO_2 flux frequency correction was 3.8% or $\pm 17.4 \text{ g CO}_2 \text{ m}^{-2} \text{ yr}^{-1}$. The uncertainty introduced by applying the Webb correction to the CO_2 flux of 5% , corresponded to $\pm 22.9 \text{ g CO}_2 \text{ m}^{-2} \text{ yr}^{-1}$. Systematic error associated with selection of the gap-filling method by comparing the models with fixed and moving parameters in our case accounted for an error of 13% . Combining these errors following the standard error propagation, a relative uncertainty of 15.6% was obtained, which corresponds to $\pm 48 \text{ g CO}_2 \text{ m}^{-2} \text{ yr}^{-1}$.

In terms of CH_4 , the peatland was a source of methane to the atmosphere of $30 \text{ g CH}_4 \text{ m}^{-2} \text{ yr}^{-1}$. For CH_4 , the random errors of gap filling were 3% and 0.4% and correspond to 0.01 and $0.11 \text{ g CH}_4 \text{ m}^{-2} \text{ yr}^{-1}$ for linear interpolation and empirical model data gap-filling. During the winter period when average fluxes were used, an uncertainty of 0.47% corresponds to $0.14 \text{ g CH}_4 \text{ m}^{-2}$ of the annual balance. The uncertainty of the frequency correction procedure was 3.1% , corresponding to $0.93 \text{ g CH}_4 \text{ m}^{-2}$ in the annual balance. The systematic error associated with the long gap in summer was 7.2% or $2.12 \text{ g CH}_4 \text{ m}^{-2} \text{ yr}^{-1}$. Standard error propagation resulted in a combined error of 8.5% or $\pm 2.5 \text{ g CH}_4 \text{ m}^{-2} \text{ yr}^{-1}$.

Taking the uncertainty in the measurements into account, the studied peatland acted as a CO_2 sink with an accumulation of $\sim 458 \pm 48 \text{ g CO}_2 \text{ m}^{-2} \text{ yr}^{-1}$. In terms of CH_4 , the peatland was a source of methane to the atmosphere of $\sim 30 \pm 2.5 \text{ g CH}_4 \text{ m}^{-2} \text{ yr}^{-1}$. Considering the balances of both gases measured in our study, the peatland represented a net carbon sink of $\sim -102 \pm 14 \text{ g C m}^{-2} \text{ yr}^{-1}$.

3.4 Discussion

3.4.1 Annual carbon balance

The CO₂ and CH₄ estimates from our study of $-458 \pm 48 \text{ g CO}_2 \text{ m}^{-2} \text{ y}^{-1}$ and $\sim 30 \pm 3 \text{ g CH}_4 \text{ m}^{-2} \text{ yr}^{-1}$, respectively, are consistent with a range of other studies from the Russian boreal region. Friberg et al. (2003) reported an annual CO₂ flux estimate of $-396 \text{ g CO}_2 \text{ m}^{-2} \text{ yr}^{-1}$ based on eddy covariance measurements from the boreal peatland Bagchar Bog in western Siberia. The annual CO₂ balance from a sedge-Sphagnum fen in the same peatland complex estimated by combining biomass sampling and CO₂ emissions was $-443 \text{ g CO}_2 \text{ m}^{-2} \text{ yr}^{-1}$ (Golovatskaya and Dyukarev, 2009). Usually, annual CO₂ estimates from tundra peatland sites are lower due to smaller primary production, and annual CO₂ balances of $-68 \text{ g CO}_2 \text{ m}^{-2} \text{ yr}^{-1}$ and $-71 \text{ g CO}_2 \text{ m}^{-2} \text{ yr}^{-1}$, respectively, were reported (Aurela et al., 2002; Kutzbach et al., 2007). However, a very low annual NEE of $-34 \pm 49 \text{ g CO}_2 \text{ m}^{-2}$ was also reported during a dry summer at an ombrotrophic boreal bog in Canada (Lafleur et al., 2003).

For Finnish boreal mire sites, relatively low annual CH₄ estimates determined by eddy covariance measurements of $12.6 \pm 1 \text{ g CH}_4 \text{ m}^{-2}$ were reported (Rinne et al., 2007). Forbrich et al. (2011) estimated growing season (May-September) CH₄ emissions measured by eddy covariance of $9.4 \pm 0.15 \text{ g CH}_4 \text{ m}^{-2}$. Annual CH₄ budgets in Russian boreal sites show higher values. Friberg et al. (2003) reported an annual CH₄ estimate for boreal site Bagchar Bog of $26 \text{ g CH}_4 \text{ m}^{-2} \text{ y}^{-1}$, which is similar to $30 \pm 3 \text{ g CH}_4 \text{ m}^{-2} \text{ yr}^{-1}$, calculated in this study.

To explain the relatively high CO₂ uptake and CH₄ emission in our study, we have to consider the conditions at the site during the measurements. As was shown above, there was a bias in the wind directions during the study, causing uneven sampling of different parts of the peatland, visible in an undersampling of the ombrogenic part. Thus the measured fluxes are representative for the nutrient-richer and more productive minerogenic and transition mire parts. The high NEE from our study could be a result of combination of high primary production and lower soil respiration in the minerogenic and the transition zones due to high WT. Although it was previously shown that in forest and crop ecosystems there is no indication that R_{eco} is much larger

than soil respiration (Reichstein et al., 2005), a smaller soil respiration contribution to R_{eco} due to a smaller oxidation layer at the studied mire where the daily mean WT did not fall below 22 cm below the peat surface, appears likely. Due to the waterlogged conditions, soil respiration is most likely limited by insufficient oxygen supply which is a substrate for respiration of soil microbes and roots (Davidson et al., 2006b), and the reduction of organic matter to CH_4 might be a more important mechanism for mineralization of organic matter than CO_2 soil respiration. Substrate supply is a master control for methane production once the anaerobic conditions are established (reviewed in Lai, 2009), and thus higher primary production could be responsible for a high soil substrate input which in the presence of high WT could be transformed into CH_4 , resulting in high CH_4 flux. On the other hand, greater methane oxidation might be expected at hummocks in the thicker aerobic layers (Lai, 2009).

3.4.2 Seasonal development of photosynthesis and ecosystem respiration

After the snowmelt, without the presence of vascular plants and mosses being the only active green plants, R_{eco} – though at low levels – dominated the CO_2 flux. We can assume that during spring time the activity of microbial communities in the soil was increasing with rising soil temperatures leading successfully to higher rates of R_{eco} . With the progression of the vegetation period, the influence of T and PAR on day-time NEE increased steadily. The effects of rapidly rising temperatures since 8 June was followed by the rapid increase of vascular plants LAI from 14 June on when the first LAI measurements were conducted. The increase of R_{eco} at night indicated by parameter $p1$ seemed to follow after the increase of LAI. The rapid increase in the temperatures after 8 June (Fig. 3.2) seemed to be responsible for changing the exponential relationship between R_{eco} and temperature (parameter $p2$). This supports the modelling approach with changing, rather than constant parameters (e.g. Atkin and Tjoelker, 2003; Reichstein et al., 2003; Davidson et al. 2006b). The change in parameters of our model used on sub-seasonal scale confirms that the temperature sensitivity of R_{eco} derived from annual data does not reflect short-term temperature sensitivity (Reichstein et al., 2005). With the culmination of plant growth and starting senescence, photosynthesis and plant-mediated respiration during the night slowly

declined. The night- and day- time NEE at the end of the vegetation season was due to soil respiration controlled by soil temperature.

3.4.3 Effects of abiotic and biotic factors on CH₄ fluxes

The seasonal trend of CH₄ fluxes was well explained by the influence of temperature in combination with changes in plant phenology induced by changes in temperature. Methane emissions are typically increasing with rising temperatures (Williams and Crawford, 1984; Christensen et al., 2003). Vascular plants have double influence on CH₄ flux: first as substrate suppliers for anaerobic microbial CH₄ production (Whitting and Chanton, 1993; Christensen et al., 2003) and second as CH₄ transport mediators (Morrissey and Livingstone, 1992; Lai, 2009). At our study site, a rapid increase of temperatures after 8 June was closely followed by LAI development and the senescence phase was also closely related to the temperature course. We can assume a substantial influence on the CH₄ fluxes by the rapid development of vascular plants as substrate suppliers and CH₄ transport mediators in conditions with high and relatively stable WT level as in our study.

Beside a clear seasonal trend, the CH₄ fluxes normally showed short-term fluctuations ranging from diurnal to several days. While diurnal cycles were mostly attributed to plant activity (e.g. Kim 1998, Hendriks et al. 2009, Long et al. 2009) or freeze-thaw cycles (Gažovič et al., 2010), an additional explanation for the variability of the eddy covariance CH₄ flux measurements is the variation of the strength of the CH₄ source within the EC source area (Fan et al. 1992, Edwards et al. 1994, Forbrich et al., 2011). These variations are not restricted to diurnal cycles of temperature and/or radiation, so that they could explain the lack of a clear diurnal trend in the CH₄ flux data. Furthermore, they would explain the large scattering in fluxes from both the minerogenic and transition part. Both parts consist of a mosaic of hollows, lawns and hummocks, with CH₄ flux strength decreasing strongly from hollows and lawns towards hummocks (Wolf, U., personal communication). However, a detailed analysis on this scale requires high-resolution (<1 m²) landcover maps (e.g. Becker et al. 2008, Forbrich et al., 2011) which are lacking for this site. To detect differences in CH₄ flux from the minerogenic and transition parts with the applied techniques, the CH₄ source strength of the two parts have to be similarly distinct as e.g. between hollows and

hummocks on the microform scale. This seems not to be the case for the entire vegetation period because we could not identify significantly different model parameters for the minerogenic and transition peatland parts.

During May, CH₄ fluxes from the transition part are higher than from the minerogenic part (Fig. 3.8, inset). One explanation of this difference could be the WT level. The WT was above the peat surface in the minerogenic depression, whereas it was below the surface in all other parts of the area of interest (Fig. 3.3). In turn, water standing above the surface represents a high diffusion resistance; therefore the fluxes from the waterlogged part could be smaller. However, we did not detect similar clear differences between the two parts in autumn, when the difference in water table position was similar as during May.

3.4.4 Winter Fluxes: an important constituent of annual C budget

Winter (snow-covered surface) CO₂ and CH₄ fluxes amounted to 16.7-26 mg m⁻² h⁻¹ and 0.53±0.13 mg m⁻² h⁻¹, respectively from the peatland Ust Pojeg, show very little variation and were in agreement with the range of former winter flux studies. In a subarctic fen, Aurela et al. (2002) measured winter CO₂ fluxes of 20 mg m⁻² h⁻¹ in Finland, while a study from a boreal peatland in Siberia reported pre-snowmelt CO₂ flux of 36 mg m⁻² h⁻¹ (Arneeth et al., 2007). Average winter CO₂ emissions from Finish bog and fen sites measured by the chamber method of 20 mg m⁻² h⁻¹ and 37 mg m⁻² h⁻¹, respectively, were reported by Alm et al. (1999).

Winter CH₄ fluxes from Minnesota peatlands ranged from 0.125 - 0.66 mg m⁻² h⁻¹ (Dise, 1992), whereas Panikov and Dedysh (2000) measured winter emissions from a West Siberian peatland of 0.054 - 0.36 mg m⁻² h⁻¹. We did not find a relationship which could explain the emission controls of either of the gases measured during the winter in our study. Aurela et al. (2002) explained part of the CO₂ flux variation by the correlation with the friction velocity (u*). We did not find a similar relationship in our study. During winter, several occasions with positive winter air temperatures were observed. Considering the strong influence of snow and ice on winter fluxes (Melloh and Crill, 1995), positive temperatures can cause melting of snow, and flux barriers in the form of thin ice layers within the snow-pack can occur during refreezing. This would effectively decrease the wind-induced emission. Winter methane emission can

correlate with CO₂ flux (Panikov and Dedysch, 2000) which could be an indication of a common emission control. We did not find such a relationship in our study; however, no final conclusion on winter emission controls can be drawn at this stage, as only few CH₄ flux data are available, and parallel measurements of both gas species from snow covered surface are rare.

3.5 Conclusions

The results of our study brought additional estimates of carbon accumulation in the boreal peatlands of the Russian Federation. Net annual carbon accumulation in the Ust-Pojeg peatland was $-102 \pm 14 \text{ g C m}^{-2} \text{ y}^{-1}$. The results show that the CH₄ emissions play an important role in annual estimates and in our study amount to 19% ($22.5 \text{ g C m}^{-2} \text{ yr}^{-1}$) of the annual carbon balance. No differences in trace gas exchange among the minerogenic and the transition mire parts could be identified during the entire vegetation period; the ombrogenic part was under-sampled. Using moving-window analysis, we could show a changing strength of the parameters of the CO₂ flux model at sub-seasonal scale. Over the course of a season, the CO₂ exchange was predominately influenced by soil and air temperatures, in combination with changes in PAR and in plant phenology. The seasonal trend of CH₄ exchange was strongly influenced by changes in soil temperature covarying with plant phenology, and no relationship with WT was detected.

Acknowledgements

The study was conducted within the framework of the research project EURAPECC-“Eurasian peatlands in a changing climate”, and funds were provided by a Sofja Kovalevskaja Research Award and a DFG grant # Wi 2680/2-I to Dr. M. Wilmking. Michal Gažovič was supported by a KAAD scholarship and a Slovak Gas Industry travel grant. During the phase of data analysis and manuscript writing, L. Kutzbach and C. Wille were supported through the Cluster of Excellence “CliSAP” (EXC177), University of Hamburg, funded through the German Research Foundation (DFG). Infrastructure was partially supported by the Carbo North Project (6th FP of the EU, Contract # 036993).

Chapter 4

Hydrology driven ecosystem respiration determines the carbon balance of a boreal peatland*

Abstract

Carbon dynamics in boreal peatlands are controlled by several factors that interact to result in an annual carbon balance. In this study, the main carbon (C) balance components, the carbon dioxide (CO₂) fluxes, the lateral export of dissolved organic carbon (DOC) and the methane (CH₄) fluxes, were measured at a boreal peatland in eastern Finland during one dry year 2006 and one wet year 2007. Contrasting environmental conditions allowed identification of the main factors responsible for inter-annual variations in CO₂, DOC and CH₄ fluxes which resulted in an annual net ecosystem production of $-83.7 \pm 14 \text{ g C m}^{-2}$ and $-134.5 \pm 21 \text{ g C m}^{-2}$ in the dry and the wet year respectively. We observed high, three- and two- fold differences in the DOC and CH₄ fluxes between the dry and the wet year, respectively. However, the higher DOC and CH₄ fluxes in the wet year did not compensate the higher CO₂ uptake in the wet year. We postulate that high variations in C uptake and annual net ecosystem exchange (NEE) were caused by the variation in water table (WT) and its influence mainly on soil respiration as a contributing factor to ecosystem respiration. Thus, in our study, WT was identified as the most important factor responsible for inter-annual variations in the C balance.

* This article was submitted to *Oecologia* as: M. Gažovič, I. Forbrich, D. Jager, L. Kutzbach, C. Wille and M. Wilmking, Hydrology driven ecosystem respiration determines the carbon balance of a boreal peatland (06/2011).

4.1 Introduction

The low productivity of boreal peatlands coupled with its unique hydrological and thermal regimes results into significant carbon (C) storage in these ecosystems (Gorham, 1991). Typically, net ecosystem C storage is a fine balance between gross primary production (GPP) and ecosystem respiration (ER), representing the two strongest C fluxes of equal importance (Houghton et al., 1998, Davidson et al., 2006). The sum of the opposing CO₂ fluxes GPP and ER is called net ecosystem exchange (NEE) of CO₂. For a more complete C balance of boreal peatlands, lateral fluxes of dissolved organic carbon (DOC) and methane (CH₄) emissions have to be taken into account as well. In an upland catchment covered mainly by blanket peat, Worrall et al. (2009) identified GPP as the biggest single component of the C budget, followed by ER and the loss of DOC from the soil. Not including the CH₄ component into the C balance calculation was shown to possibly overestimate net C storage by as much as 19% (Friborg et al., 2003). In northern peatlands, CH₄ flux represented on average 4% of net ecosystem production (Bellisario et al. 1999). However, in some circumstances (e.g. low WT position) non-CO₂ fluxes can account for less than 1% of the carbon exchange, and NEE can account for up to 99% of net carbon storage (Waddington and Roulet, 2000).

Despite the relative importance of non-CO₂ fluxes for net C storage, the close connections between the major C balance components can help us to understand ecological functioning of peatland ecosystems. For example, CH₄ production was shown to be related to GPP by stimulation of methanogenesis through increased substrate supply to the soil (Whitting and Chanton, 1993; Bellisario et al., 1999; Segers, 1998; Christensen et al., 2003; Lai, 2009).

Lateral export of DOC from the peatlands is typically influenced by precipitation patterns during the year and in turn by fluctuations of WT and water discharge with usually highest DOC export during the spring thaw (Jager et al., 2009; Dyson et al., 2011). Fluxes of dissolved inorganic and particulate organic carbon are much lower compared to DOC fluxes (Dyson et al., 2011). Freeman et al. (2004) observed a decrease in DOC export from an upland peatland with simulated drought because gaseous CO₂ rather than dissolved organics tends to be the major end product of

decomposition. However, highest concentrations of DOC in the peat column appear during summer months, and the precipitation patterns during the summer months could have an influence on DOC export patterns (Worrall et al., 2009), which was previously shown also in the study by Jager et al. (2009). In case of low water discharge, retention of DOC can appear causing exponentially increased emissions of CO₂ and CH₄ (Pastor et al., 2003). Besides, DOC increase can be induced by increase in primary production and DOC exudation from plants, caused by elevated atmospheric CO₂ concentrations (Freeman et al., 2004).

Carbon uptake can be affected by ecological responses of plants to recent climate changes as represented by changes in phenology and subsequent changes in length of the growing season (Menzel, 2002; Walther et al., 2002, Badeck et al., 2004). For example, higher CO₂ uptake was measured in years with an earlier onset of the growing season (Rocha and Goulden, 2008; Sottocornola and Kiely, 2010). However, predicted longer growing seasons do not necessarily have to lead to higher uptake of CO₂ as higher plant activity may enhance ecosystem respiration and thus shift the ecosystems to a C source, rather than a C sink (Houghton et al., 1998, Davidson et al., 2006). Furthermore, shorter growing seasons might be induced by drought effects and early plant senescence (Sonntag et al., 2010). Changes in primary production induced by phenological changes together with changed precipitation patterns might have thus an effect not only on the CO₂ balance but also on DOC and CH₄ fluxes.

Various flux measurement methods determining trace gas emissions from peatlands have been described and used (e.g. Alm et al., 2007); however, the eddy covariance (EC) method (Baldocchi, 1988; 2003) which is able to continuously measure CO₂ and CH₄ fluxes on the landscape scale was increasingly used (e.g. Hargreaves et al., 2002; Lafleur et al., 2005; Rinne et al. 2007; Lasslop et al., 2010). Several EC studies measuring C exchange over peatlands have been limited to single-year measurements (e.g. Aurela et al., 2002; Friberg et al., 2003; Kutzbach et al., 2007b); however, only longer time series allow us to understand inter-annual variations in C exchange and possible effects of changing ecological responses to climate change (Sottocornola and Kiely, 2010). Unfortunately, multi-annual measurements of CO₂ exchange over peatlands are still very limited (but see Arneeth et al., 2002; Lafleur et al., 2003; Rocha

and Goulden, 2009; Sottocornola and Kiely, 2010), and thus new peatland studies extending beyond single-year measurements are needed.

Here we present a) eddy covariance CO₂ flux measurements, b) DOC export measurements and c) CH₄ chamber measurements during two years 2006 and 2007, which were characterized by contrasting environmental conditions, in the boreal fen Salmisuo in Eastern Finland. Evapotranspiration dynamics and detailed DOC and CH₄ dynamics of this peatland during the years 2006 and 2007 have been reported elsewhere (Becker et al., 2008; Jager et al. 2009; Wu et al., 2010, Forbrich et al., 2011, submitted).

The main objectives of this study were

- 1) to quantify and compare inter-annual variation of NEE, GPP and ER in two meteorologically contrasting years and,
- 2) to study the relative influence of each C-flux components to the total C budget and identify their main environmental drivers.

4.2 Methods

4.2.1 Study area

The Salmisuo mire complex is situated in eastern Finland (62°47'N, 30°56'E), and represents an oligotrophic low sedge *Sphagnum papillosum* pine fen (Saarnio et al., 1997). Three micro-forms can be distinguished based on vegetation communities: hummocks: elevated, drier areas with *Sphagnum fuscum*, *Andromeda polifolia* and *Pinus sylvestris*; lawns: intermediate areas with *Sphagnum papillosum*, *Sphagnum balticum* and *Eriophorum vaginatum* and flarks: low and wet areas with *Scheuchzeria palustris* and *Sphagnum balticum*. The average yearly temperature is +2 °C; average yearly rainfall is 667 mm, of which one third falls as snow during the winter (Drebs et al., 2002). The area of interest for NEE measurements was defined as a circle with a radius of 200 m around the eddy covariance tower. The catchment area for the DOC measurements was 46.0 ha with peatland forming 79 % of the area. The peatland represents a mainly undisturbed ecosystem; only in the north-western edge of the

peatland a drainage ditch runs parallel to a road constructed in 1960 (Jager et al., 2009). More detailed site characteristics with respect to vegetation and hydrological properties at the site were previously described in other studies (see for example Saarnio et al., 1997, Jager et al., 2009, Wu et al., 2010).

4.2.2 Net ecosystem exchange measurements

Landscape-scale CO₂ fluxes were determined using a closed path eddy covariance system with infrared CO₂/H₂O gas analyzer (LICOR 7000; Licor Inc., USA). The head of a three-dimensional sonic anemometer (Solent R3, Gill Instruments Ltd., UK) was located in 2 m height above the peat surface. Meteorological characteristics, air and soil temperatures, air relative humidity, water table fluctuation at lawn microform and radiation, were measured at the site.

Eddy covariance fluxes were calculated over 30 min intervals. The time lag between wind and scalar concentration measurements was determined and removed for every averaging period. Turbulent fluxes were calculated using the EdiRe software (Robert Clement, University of Edinburgh, UK). Two coordinate rotations were applied to the wind components so that the mean transverse and the mean vertical wind components were reduced to zero. The fluxes were corrected for the frequency attenuation due to tube attenuation, sensor path separation and spectral response of the instruments (Moore, 1986; Moncrieff et al., 1997). The mean average CO₂ frequency correction in our study was 17.2 % in 2006 and 16.9 % in 2007. The Webb correction adapted for closed-path eddy covariance systems was applied to the CO₂ flux (Ibrom et al., 2007). Integral turbulence characteristics (ITC) were calculated, and data were screened accordingly (Foken and Wichura, 1996). Data were removed if the deviation from the modeled ITC parameter was greater than 30%. Instationarity characteristics were calculated and used to discard the data obtained during non-stationary conditions (Foken and Wichura, 1996).

Details of the eddy covariance system setup and supporting measurements were previously described in Wu et al. (2010). The only difference in this study is the use of precipitation measurements from Mekrijärvi research station situated 4 km south-west from the site.

For this study, positive fluxes indicate upward flux, i.e. emission from the peatland, and negative fluxes indicate the contrary, i.e. uptake by the peatland.

4.2.3 Gap-filling and flux-partitioning

In total 41 % of CO₂ flux data points were missing due to technical problems or were removed during the data quality check. The gaps in the time series were filled using the online gap filling tool available at <http://gaia.agraria.unitus.it/database/eddyproc/> (Reichstein et al. 2005). This tool is filling the gaps considering both the co-variation of fluxes with meteorological variables and the temporal auto-correlation of the fluxes using a look-up table with similar meteorological conditions within a certain window length. CO₂ flux-partitioning was performed using this tool with air temperature (T_{air}) set as a driver for ER and the vapor pressure deficit (VPD) algorithm included (Lasslop et al., 2010).

4.2.4 Regression analysis of relationships between environmental parameters and CO₂ fluxes

Non-linear and linear regression analysis was used to study the relationships between measured daytime and nighttime CO₂ fluxes and environmental parameters such as soil and/or air temperature, photosynthetic photon flux density (PPFD) and water table (WT). A PPFD value 20 $\mu\text{mol m}^{-2} \text{s}^{-1}$ was used as a threshold between day and night time. Night time NEE values represent ER as no photosynthesis is present. The regression analysis was performed on day-time and night-time means of raw flux data with no gap-filling applied to prevent any confounding effects introduced by the gap-filling method.

4.2.5 Discharge and DOC concentrations measurements

Discharge and DOC concentration measurements were done in the stream behind the drainage pipe of the ditch under the road. The measurements were initiated after the snow melt when outflow was possible to measure. This occurred on 19 April in 2006 and on 16 March in 2007. Discharge was measured using a sharp-crested v-notch weir, and samples for DOC concentration measurements were taken at a two- to three- day

basis, except for snowmelt when the samples were taken several times a day to capture fast changes in the water discharge. Daily DOC flux was calculated by multiplying total daily runoff with the average (volume weighted) daily DOC values. The monthly seasonal DOC fluxes were subsequently calculated by summing the calculated daily values. For details on DOC and discharge measurements from the Salmisuo site see Jager et al. (2009).

4.2.6 CH₄ flux measurements

Closed-chamber measurements of CH₄ were carried out during the growing season from 10 May to 18 October in 2006 and from 9 May to 10 October in 2007 on 6-8 replicates of the three typical microform types in the area of interest. Four samples of the chamber headspace air were taken during the closure periods and were analyzed using a gas chromatograph equipped with a flame ionization detector (Shimadzu 14-A). The calculated fluxes were filtered using the standard deviation of residuals as criterion to exclude measurements which were characterized by excessive noise or strongly non-linear concentration increases (Kutzbach et al., 2007a). An empirical model based on soil temperature in 50 cm and WT depth was used for modeling the data, and CH₄ fluxes were then spatially weighted with the distribution of microforms in the area of interest represented by the eddy covariance measurements. Detailed description of CH₄ measurements from this site can be found elsewhere (Forbrich et al., 2011, submitted). To estimate annual CH₄ balance, we assumed non-zero winter CH₄ emissions to be 6% of the growing season emission, similar to winter emissions estimated by Rinne et al. (2007). The winter emission was evenly divided during six months when no CH₄ measurements were available although we are aware that the snowmelt CH₄ emissions might sometimes account for a large portion of the annual CH₄ emission (Comas et al., 2008).

4.3 Results

4.3.1 Hydro-meteorological variables

In general, air temperatures (T_{air}) in both years were very similar, except in March when mean monthly temperature was $-11\text{ }^{\circ}\text{C}$ in 2006, but $1.2\text{ }^{\circ}\text{C}$ in 2007 (Fig. 4.1a). The lowest monthly T_{air} were measured in February in both years; the highest monthly temperatures were measured in July in 2006 and in August in 2007.

The monthly means of day-time PPFD showed small inter-annual variation (Fig. 4.1b). The annual precipitation was 591 mm and 700 mm in 2006 and 2007, respectively, which was 76 mm below and 33 mm above the long-term average annual precipitation, respectively. In 2007 there was more precipitation in all months from January to September (Fig. 4.1c).

In both years 2006 and 2007, the WT measured at lawn microforms fell below the peat surface and reached the lowest monthly averages of -27 cm and -12 cm in August in 2006 and 2007, respectively. The range of monthly mean WT was $\pm 21\text{ cm}$ in the dry year, while in the wet year WT stayed in a narrow range of $\pm 7\text{ cm}$ (Fig. 4.1d).

Soil temperature (T_{soil}) measured at 10 cm depth at lawn microforms (Fig. 4.1e) reached highest values in July and August. In the months May and June in 2006, T_{soil} was $1.3\text{ }^{\circ}\text{C}$ higher compared to 2007.

4.3.2 Carbon balance components: Comparison between dry and wet year

4.3.2.1 Monthly NEE

Winter NEE measured from January-April showed higher positive values in 2006 compared to 2007 indicating net release of CO_2 from the peatland (Fig. 4.2a) with ER dominating the NEE (Fig. 4.3b). In May, the peatland turned into a net sink of CO_2 (Fig. 4.2a), with the net uptake starting 10 days later in 2006 compared to 2007. In both years, the peatland acted as a net CO_2 sink for 5 months from May through September, with inter-annual differences. In August 2006 the NEE of $-18.8\text{ g C-CO}_2\text{ m}^{-2}$ was two times lower compared to $-40.3\text{ g C-CO}_2\text{ m}^{-2}$ in August 2007. In September, NEE was $-1.9\text{ g C-CO}_2\text{ m}^{-2}$ and $-11.7\text{ g C-CO}_2\text{ m}^{-2}$ in 2006 and 2007, respectively. These highest

differences in NEE were coinciding with the highest rates of ER (Fig. 4.3b) and lowest WT in 2006 (Fig. 4.1d). From October, CO₂ release was higher in 2006 than in 2007. Such seasonal pattern resulted in a big difference in the cumulative NEE which was $-92.5 \pm 13 \text{ C-CO}_2 \text{ m}^{-2} \text{ yr}^{-1}$ and $-154.6 \pm 19 \text{ g C-CO}_2 \text{ m}^{-2} \text{ yr}^{-1}$ in 2006 and 2007, respectively.

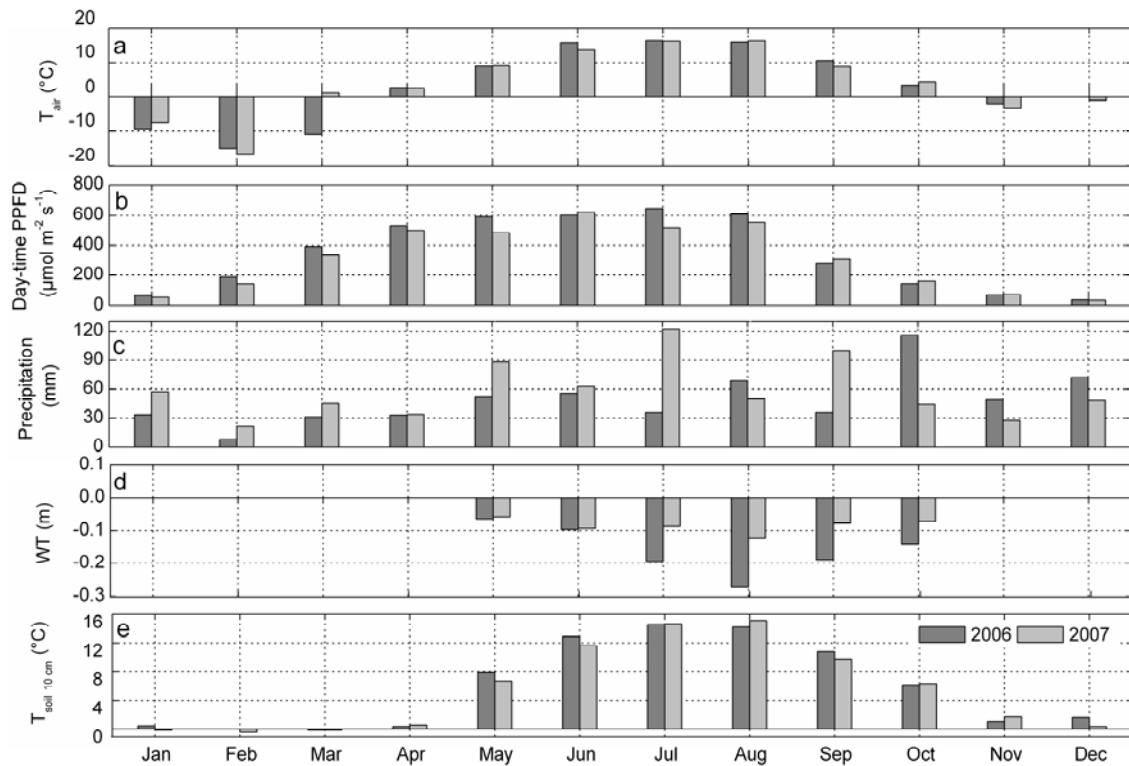


Figure 4.1 Monthly means of environmental variables at Salmisuo site during the years 2006 and 2007: a) air temperature T_{air} ; b) day-time photosynthetic photon flux density PPFD; c) precipitation; d) water table level WT and e) soil temperature in 10 cm $T_{\text{Soil } 10 \text{ cm}}$

4.3.2.2 Regulation of photosynthesis and respiration

From May to October in 2006, measured ER (night-time NEE) was best related to T_{soil} in 10 cm and could be well estimated by an exponential function. ($r^2_{\text{adj}}=0.65$; RMSE=0.58), similar to 2007 ($r^2_{\text{adj}}=0.66$; RMSE=0.54). A statistically significant positive linear relationship between the residuals of the soil temperature model and WT level was observed in 2006 ($r=0.34$, $\alpha=0.05$). Higher residuals (flux overestimation) were associated with higher WT level and vice versa. In 2007 only a weak, non-

significant positive linear relationship between the temperature model residuals and WT level was observed ($r=0.044$, $\alpha=0.05$).

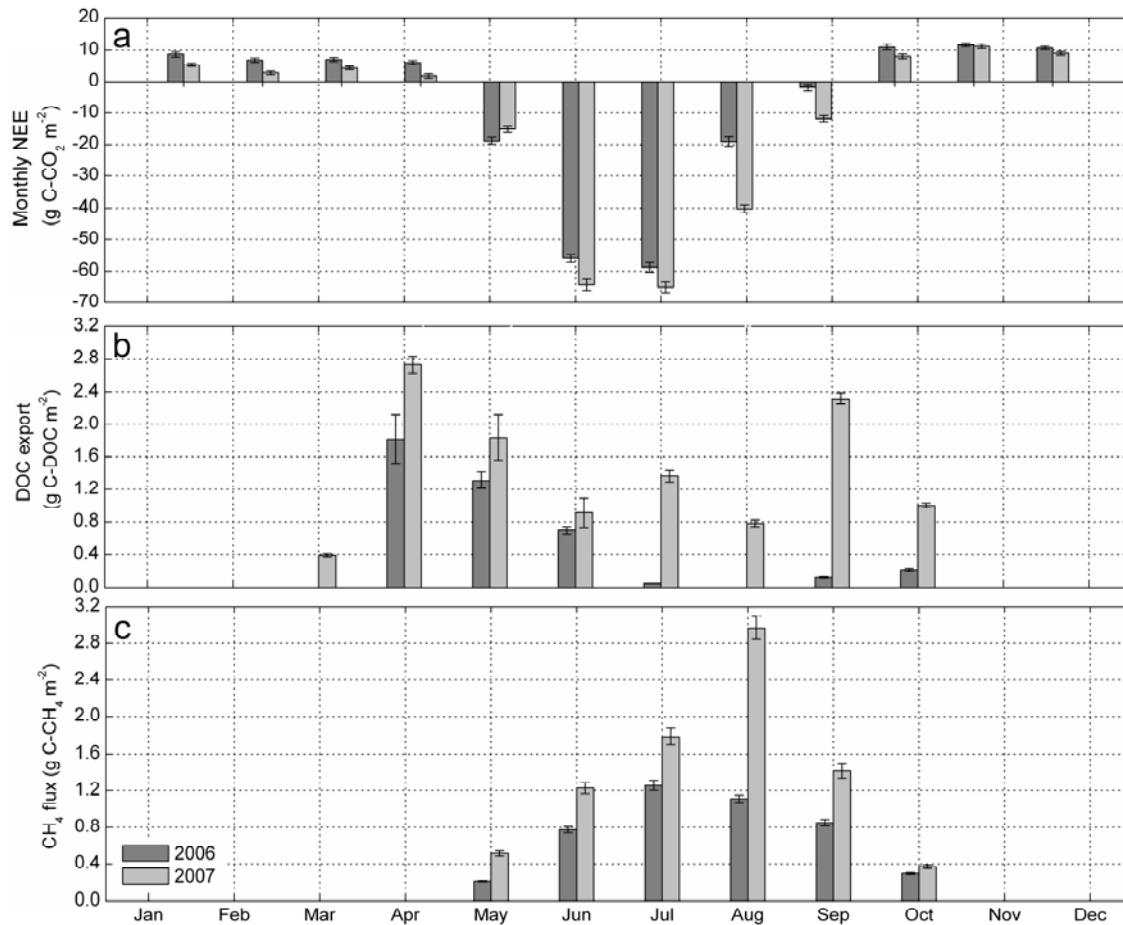


Figure 4.2 Monthly sums of measured a) net ecosystem exchange NEE; b) dissolved organic carbon export DOC and c) methane CH₄ emissions with standard errors during 2006 and 2007

Daily mean day-time NEE was best related to PPFD changes. It was positively linearly related to WT in 2006 ($r=0.37$) and 2007 ($r=0.53$); however, this relationship was not significant in 2007. The PPFD model residuals showed a positive linear relationship with T_{air} in both years 2006 ($r=0.35$) and 2007 ($r=0.54$), respectively). A negative linear relationship of the PAR model residuals with WT was observed in both years in 2006 ($r=-0.42$) and 2007 ($r=-0.47$), respectively.

4.3.2.3 NEE partitioning

The NEE partitioning showed the highest monthly GPP in July in both years, while the highest ER lagged one month behind the highest GPP and was observed in August. In general, the highest rates of both GPP and ER were observed in the dry year 2006 with the exception of August when higher GPP was observed in 2007 (Fig. 4.3).

4.3.2.4 Monthly DOC export

Water discharge was detectable already in March in 2007, but only in April in 2006. In 2006, lower water discharge and lower DOC export compared to 2007 was observed in all months. The DOC export from the peatland was highest during and after thawing. In July and September of 2006 very low DOC export was observed, and no DOC export was measured in August in 2006; however, high DOC export was measured in summer and autumn in 2007 with DOC export in September nearly reaching the maximum export from the spring period (Fig. 4.2b). The DOC export pattern in the dry and the wet year resulted in a high inter-annual difference with annual DOC export of 4.2 ± 0.5 g C-DOC m^{-2} and 11.3 ± 0.8 g C-DOC m^{-2} in 2006 and 2007, respectively, assuming no relevant winter DOC export.

4.3.2.5 Monthly CH₄ emissions

Monthly mean CH₄ emissions were increasing from May with increasing temperatures. Lower CH₄ emissions than in 2007 were measured in all months of 2006. Highest monthly CH₄ emissions were measured in July in 2006 and in August in 2007, respectively, and were decreasing thereafter (Fig. 4.2c). August CH₄ emissions in 2007 were more than twice as high as in 2006. Methane emissions during the growing season were 3.4 ± 0.3 g C-CH₄ m^{-2} and 6.4 ± 0.6 g C-CH₄ m^{-2} in 2006 and 2007, respectively, representing a nearly two-fold difference between the dry and the wet year. Considering measured CH₄ emissions from the growing seasons and winter estimates gives annual CH₄ emissions of 3.6 ± 0.3 g CH₄ m^{-2} in 2006 and 6.6 ± 0.6 g CH₄ m^{-2} in 2007, respectively.

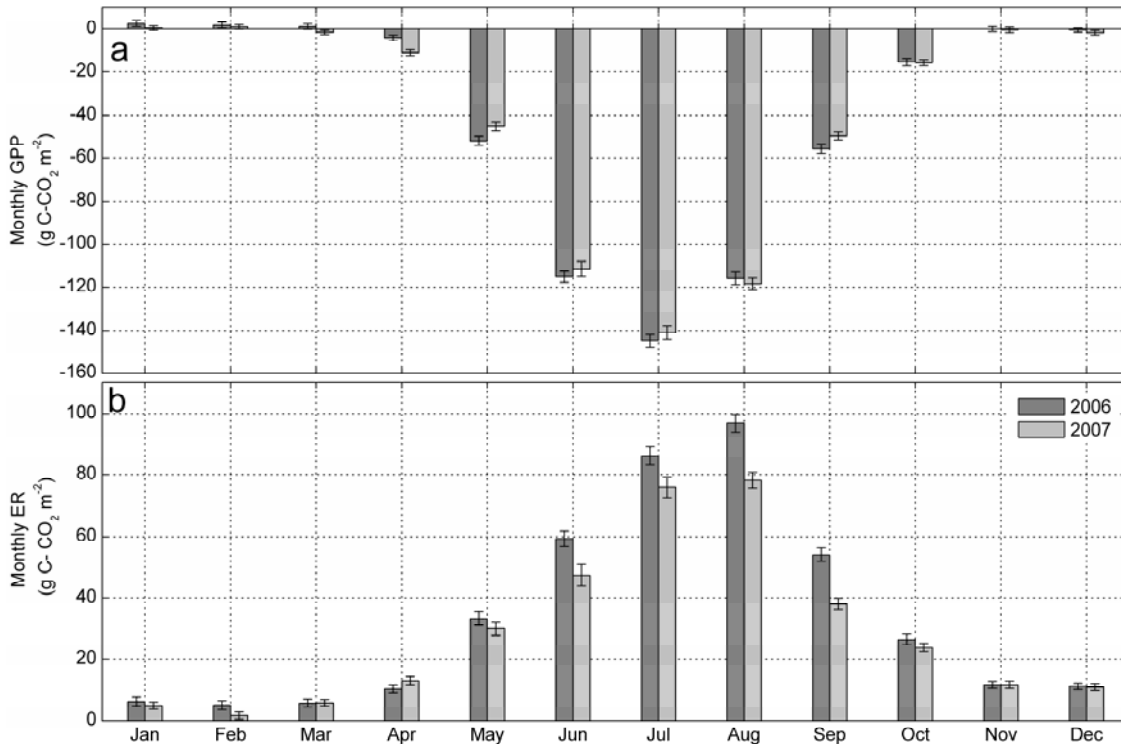


Figure 4.3 NEE partitioning during 2006 and 2007. Monthly sums of a) gross primary production (GPP) and b) ecosystem respiration (ER) with standard errors

4.3.2.6 Annual C balance

Considering the three main C fluxes of CO₂, CH₄ and DOC, Salmisuo acted as a net C sink with an annual balance of -85 ± 14 g C m⁻² and -136 ± 21 g C m⁻² during one dry and one wet year, respectively. In both years, the NEE represented the biggest C balance component. The contributions of DOC and CH₄ fluxes were higher in the wet year compared to the dry one (Fig. 4.4).

4.4 Discussion

The annual NEE from our study of -92.5 ± 13 g C m⁻² and -154.6 ± 19 g C-CO₂ m⁻² in 2006 and 2007, respectively, were in the upper range of previously reported values from peatland ecosystems (e.g. Sottocornola and Kiely, 2010; Friberg et al., 2003; Golovatskaya and Dyukarev, 2009) and confirm high inter-annual NEE variations observed in other studies. Much lower annual NEE of 9 ± 13 g C m⁻² during a dry year was reported by Lafleur et al. (2003), while Sottocornola and Kiely (2010) measured

high inter-annual variations in NEE from an Atlantic blanket bog ranging between -16.5 ± 5.1 and -96.5 ± 23.2 g C-CO₂ m⁻².

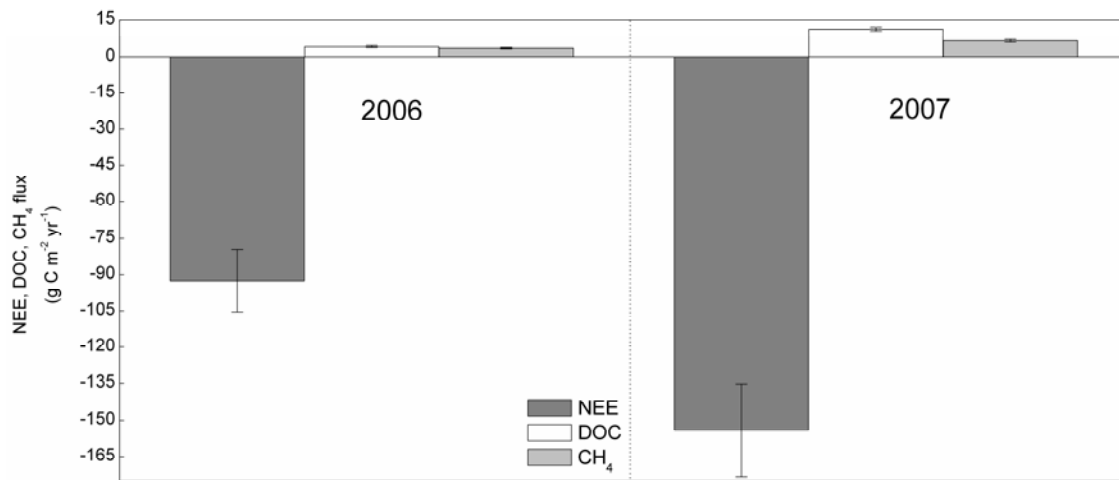


Figure 4.4 Contribution of different carbon balance components with standard errors during the dry (2006) and the wet (2007) year

In our study, temperature was identified as a controlling parameter for ER which was consistent with other studies (Lafleur et al., 2005; Sottocornola and Kiely, 2010). However, despite evident temperature influence on ER in our study, inter-annual variations in both soil and air temperatures did not seem to be sufficient to be the main explanatory factor responsible for the strong inter-annual differences in NEE (Fig. 1a and 1d).

Besides a temperature effect, WT was identified as an important controlling factor for ER in our study. With lower WT level in 2006 compared to 2007, the aerobic peat layer was deeper which resulted in higher soil respiration and could decrease the net CO₂ uptake in 2006. On the other hand, higher and stable WT in 2007 could have limited soil respiration which resulted in higher net CO₂ uptake in this year. Effects of WT on NEE and ER reported previously in other studies are ambiguous. In a cool temperate bog, ER was shown to be correlated to air and soil temperatures, but was not strongly dependent on WT (Lafleur et al., 2005). However, WT was identified as the most important determinant of inter-annual differences in peatland growing season NEE and thus in the annual CO₂ balance as well when the extended dry conditions severely reduced the net sink strength of the peatland (Lafleur et al., 2003). Funk et al. (1994)

reported strong relationships of CO₂ fluxes in core microcosms with the position of the WT. In their experiment, lowering the WT to -15 cm tripled CO₂ emissions when compared with cores maintained with WT at the soil surface, and that respiration accounted for the differences since ecosystem photosynthesis was similar in the high and low WT cores (Funk et al., 1994). It seems that when temperature is not the limiting factor, WT plays an important role in our site in modifying the soil respiration flux and as a result, the overall NEE flux.

In other studies it was concluded that the leaf area index (LAI) influencing carbon assimilation potential correlates with soil respiration rates (Reichstein et al., 2003), and that large portions of soil respiration originate from recently assimilated C via root respiration (Kuzyakov and Cheng, 2001). Thus in our study, higher WT in the wet year might limit the soil respiration. This in turn could decrease ER fluxes leading to increased NEE, not caused by higher GPP, but by lower ER.

In our study, small NEE values in August and September in the dry year 2006, compared to 2007 (Fig. 4.2a), seem to be related to high ER during these months and might indicate the influence of increased soil respiration very likely due to lower WT in the dry year. It was previously shown that a dry year can represent a much smaller CO₂ sink due to large night time respiration values (Lafleur et al., 2003).

Indirect control of WT on GPP and ER was previously assigned to dry conditions, causing earlier senescence and thus a shorter growing season (Sonntag et al., 2010). Chivers et al. (2009) observed that lowering the WT position changed the fen ecosystem from a net sink to net source of atmospheric CO₂, although not by increasing the soil respiration, but primarily by reducing plant productivity. It is possible that low WT level in August in 2006 caused lower GPP in our study; however, during all other months, GPP was higher in the dry year, and thus the differences in annual NEE could not be attributed to reduced plant productivity during the dry year in our study.

The high differences in DOC export from the Salmisuo site were previously attributed to differences in discharge pattern influenced by precipitation translated into changes in WT level (Jager et al., 2009). Beside spring thaw known as the most important hydrological event of the year (Dyson et al., 2011), DOC concentrations in the summer months in soil water were particularly high (Jager et al., 2009). More runoff events in

this time of the year can markedly increase the annual DOC flux (Worrall et al., 2009), leading to the high DOC flux in the summer months of 2007 (Jager et al., 2009).

Differences in the seasonal CH₄ emissions between the dry and the wet year at the Salmisuo site were explained by differences in temperatures and WT position (Forbrich et al., 2011, submitted). Temperature is a factor regulating e.g. phenology and microbial activity, and a close relationship of CH₄ emissions and NEE was related to microbial substrate availability originating from plant root exudates (Whitting and Chanton, 1993; Segers, 1998; Lai, 2009). In our study, higher GPP in 2006 does not seem to be the main driver for CH₄ emissions, as CH₄ emissions in 2006 were always lower compared to 2007, although GPP was marginally higher in August 2007 compared to August 2006 and could amplify the difference in CH₄ emissions between the dry and the wet year in this month. Considering the complex effects of WT, temperature and GPP, it might be insightful to look at CH₄ emissions during May and June. In these months higher soil temperatures were recorded in 2006 (Fig. 4.1e) as well as higher GPP (Fig. 4.3). During May and June in 2006, WT levels were only marginally lower compared to 2007 (Fig. 4.1d). However, CH₄ emissions were lower in 2006 despite the favorable conditions (higher soil temperatures, higher GPP). We hypothesize, that higher CH₄ emissions in these months in 2007 are a result of the earlier onset of the growing season, and higher GPP in April in 2007 (Fig. 4.3).

Despite the absence of direct soil respiration measurements we suggest that differences between the wet and the dry year observed in our study were to a high extent influenced by WT effects mainly on ER. Higher spring T_{air} in 2007 were probably responsible for earlier onset of the growing season and resulted in a change of the peatland to a net CO₂ sink in 2007 ten days earlier than in 2006. Effects of WT during the growing season were responsible for higher ER in the dry year and thus lower net CO₂ uptake. On the contrary, high WT during 2007 decreased ER and favored CH₄ emission and DOC export. Higher CO₂ emissions in autumn/winter in 2006 contributed to lower annual C accumulation compared to 2007 as well.

Even after the higher DOC and CH₄ effluxes were included in the C balance, the net C accumulation was 51 g C m⁻² yr⁻¹ higher during the wet year 2007 compared to the dry year 2006.

4.5 Conclusions

Ecosystem CO₂, DOC and CH₄ fluxes in the Salmisuo boreal peatland site showed high inter-annual variability. In our study, WT was identified as the most important factor influencing NEE on the seasonal/inter-annual scale. Decrease in WT during the dry year resulted in increased ER very likely by increased soil respiration and lead to lower net CO₂ uptake of the peatland. On the contrary, with higher WT during the wet year the CO₂ flux from soil respiration was decreased which in turn decreased ER and caused higher overall net CO₂ uptake by the peatland. The higher CO₂ uptake in 2007 was partly compensated by higher DOC and CH₄ fluxes during the wet year; however, since NEE was by far the largest component of the C balance, the loss of C through CH₄ and DOC export did not compensate for effects of decreased ER. It seems that partitioning of soil C flux regulated by changes in WT had a decisive influence on the C balance of the peatland ecosystem in our study.

We observed a strong effect of spring temperatures regulating spring onset. In 2007, an earlier start of the growing season was most likely the cause for change of the peatland from a source to net CO₂ sink 10 days earlier compared to the year 2006 with low spring temperatures. Thus it seems that variations in growing season length due to changes in global climate might have additional influences on C balance at boreal peatland sites.

Acknowledgements

The study was conducted within the framework of the research project EURAPECC-“Eurasian peatlands in a changing climate”, and funds were provided by a Sofja Kovalevskaja Research Award and a German Research Foundation (DFG) grant # Wi 2680/2-I to M. Wilmking. M. Gažovič was supported by a Katholischer Akademischer Ausländer Dienst scholarship and a Slovak Gas Industry (SPP) travel grant. I. Forbrich was supported by a scholarship from Deutsche Bundesstiftung Umwelt during the field work. During the phase of data analysis and manuscript writing, L. Kutzbach and C. Wille were supported through the Cluster of Excellence “CliSAP” (EXC177), University of Hamburg, funded through the DFG. Infrastructure was partially

supported by the CarboNorth Project (6th FP of the EU, Contract # 036993). We would like to thank everyone involved in this study for their help and contribution.

Chapter 5

Boreal peatland net ecosystem CO₂ exchange – an integrative comparison between measured fluxes and LPJ-GUESS model output*

Abstract

Net ecosystem CO₂ exchange (NEE) was measured using closed chamber and eddy covariance (EC) techniques at a boreal peatland in Northwest Russia from April to November 2008. The in situ flux measurements on two different scales were compared, and the EC measurements were used to evaluate the CO₂ flux estimates of the mechanistic ecosystem model LPJ-GUESS. The peatland surface was composed of microforms which differed in water table level and vegetation composition. The distribution of microforms varied spatially within the peatland. Three different approaches were used to integrate the plot-scale chamber measurements with the larger-scale EC measurements: 1. upscaling based on the average microform distribution within the area of interest and the mean NEE flux for each microform type, 2. upscaling based on areal weighting which accounts for the microform distribution in the sector of the main wind direction and 3. upscaling based on footprint modeling which estimates the varying contribution of different land cover classes in the source area of the 30-minute EC CO₂ fluxes. Our results indicate a substantial discrepancy between the flux estimated from EC data and estimates obtained by upscaling of chamber measurements irrespective of the upscaling method. An intercomparison of

* This article was submitted to *Journal of Geophysical Research - Biogeosciences* as: J. Schneider, M. Gažovič, L. Kutzbach, I. Forbrich, J. Wu, R. Wania, P. A. Miller, S. Susiluoto, T. Virtanen, S. Zagirova and M. Wilmking, Boreal peatland net ecosystem CO₂ exchange – an integrative comparison between measured fluxes and LPJ-GUESS model output. (10/2010)

the CO₂ fluxes measured by EC and modeled LPJ-GUESS fluxes showed a pronounced disagreement in budgets and in seasonal cycles of measured and modeled CO₂ fluxes.

5.1 Introduction

In the last decade, the global carbon cycle received much attention as it was recognized that the human perturbation to the carbon cycle is one of the main factors driving the climate change over the last century [Intergovernmental Panel on Climate Change (IPCC) 2001, 2007]. The importance of terrestrial ecosystems in the global carbon cycle is underlined by the fact that about one third of the atmospheric carbon dioxide (CO₂) is exchanged annually with the terrestrial biosphere [Ciais et al., 1997]. Many studies have been conducted to quantify the exchange of CO₂ between the atmosphere and the biosphere and to analyze the underlying processes [e.g. Alm et al., 1997; Valentini et al., 2000; Bubier et al., 2003; Dore et al., 2003; Goulden et al., 2004; Coulter et al., 2006; Grant et al., 2009; Sierra et al., 2009; Gilmanov et al., 2010]. The closed chamber method and the eddy covariance (EC) technique are the two measurement techniques that are mainly used to determine the CO₂ fluxes. The two techniques are used at different spatial and temporal scales. The chamber measurements provide discontinuous data on the plot scale (10⁻²-10⁰ m²) while, under ideal conditions, the EC measurements provide continuous flux data on the ecosystem scale (10⁴-10⁶ m²). The comparability of the plot- and ecosystem-scale measurements of CO₂ flux has been mainly tested on areas with homogenous surfaces, e.g. Dore et al. [2003] in forests, Kabwe et al. [2005] on bare soils in a uranium mine. Some studies were conducted at more heterogeneous sites with one dominant surface type, e.g. Griffis et al. [2000] at a subarctic fen which was covered by *Carex* spp. hummocks up to 70 % or Heikkinen et al. [2002] at a patterned boreal mire with a 60 %-predominance of wet flarks and Laine et al. [2006] at an oceanic mire with a predominance of lawns. Comparisons at heterogeneous study sites are rare, e.g. Fox et al. [2008] at a tundra site covered by six different mosaic elements which occupied relatively even proportions. At the homogenous study sites and the subarctic fen studied by Griffis et al. [2000], the CO₂ flux measured by EC and the estimates obtained by areally weighted chamber measurements were within the maximum

probable error of each methodological approach. On the other hand, Heikkinen et al. [2002] and Fox et al. [2008] found a discrepancy between the fluxes obtained by the two different approaches. It is thus not easy to upscale chamber or downscale eddy covariance measurements [Forbrich et al., 2010] - the chamber method does not capture the full temporal variability and the EC technique can capture the small-scale spatial variability of the carbon fluxes only if the detailed information on the distribution of microforms or leaf area index (LAI) is available.

Simultaneously to the in situ CO₂ flux measurements, models of terrestrial biogeochemistry and biogeography have been developed and were used to evaluate potential effects of changing atmospheric CO₂ concentrations and climate on the global carbon cycle and to predict the future vegetation distribution. Recent developments on this subject are the fully integrated dynamic vegetation models [e.g. Cramer et al., 2001; Sitch et al., 2008]. LPJ-GUESS [Smith et al., 2001] is a process-based model of vegetation dynamics and land-atmosphere carbon and water exchanges. It incorporates the Lund-Potsdam-Jena Dynamic Global Vegetation Model (LPJ-DGVM) [Sitch et al., 2003] and the General Ecosystem Simulator (GUESS) [Smith et al., 2001] and is suitable for regional (10³-10⁵ km²) to continental (10⁶-10⁷ km²) simulations on time scales from days to millennia. Sitch et al. [2003] presented simulations on vegetation patterns and seasonal cycles of net ecosystem CO₂ exchange for ten plant functional types, of which eight were woody (two tropical, three temperate and three boreal) and two herbaceous. The simulations were made over the industrial period and agreed well with observations on vegetation structure and phenology and local measurements using EC. Recently, the LPJ-DGVM was enhanced by introducing processes which are necessary to simulate peatland vegetation and hydrology, and permafrost dynamics [Wania et al. 2009a, 2009b, 2010].

The objective of this study is to (1.) investigate the comparability of in situ CO₂ flux measurements conducted at different temporal and spatial scales by the chamber method and the EC technique at a patterned boreal peatland and (2.) to evaluate the CO₂ flux estimates of the LPJ-GUESS model using the flux data measured by EC technique.

5.2 Methods

5.2.1 Study site

The study site Ust-Pojeg is a boreal peatland located in east European Russia northwest of Syktyvkar, the capital of the Komi Republic, at 61°56'N, 50°13'E. Peatland and the study region were described intensively in Schneider et al. [2010], Gažovič et al. [2010] and Virtanen et al. [2010].

Within the peatland, we defined an area of interest, which is a circular area with a diameter of 600 m with a meteorological station and an eddy covariance tower placed in the center. Our intensive study site consists of a *Sphagnum angustifolium* pine bog in its northern part and a *Sphagnum jensenii* fen in its southern part. The ombrogenous bog part and the minerogenous fen part of the measurement site are composed of a mosaic of different microforms defined by their position within the microrelief. Hummocks which represent the driest conditions are elevated above the surrounding area and are covered by *Andromeda polifolia*, *Chamaedaphne calyculata*, *Betula nana* and partly by *Pinus sylvestris*. The hollows represent the wettest microforms and are occupied primarily by *Scheuchzeria palustris* and *Carex limosa*. The vegetation of lawns consists of a mixture of species growing at hummocks and hollows, respectively. The lawns are intermediate microforms with respect to water level. The transition zone between the fen and the bog part is dominated by *Carex rostrata* lawns.

5.2.2 Experimental setup and flux calculations

5.2.2.1 Chamber measurements – plot scale

CO₂ exchange was measured four times per week from 23 April to 20 October 2008 applying a closed chamber approach. To capture the variance of the CO₂ fluxes over the day, we conducted a series of measurements once per week during the morning (5 am to 11 am local time) and once per week during the evening (6 pm to 12 pm local time); two additional measurement series per week were conducted around midday from 11 am to 4 pm. The total number of measurements was 5517. A total of 18 measurement plots were established within the intensive study site in different microform types: 2 replicates each in ombrogenous hollows (OHO), lawns (OL) and hummocks (OH), and 3 replicates each in minerogenous hollows (MHO), lawns (ML)

and hummocks (MH), and *Carex rostrata* lawns (CL). The NEE was measured using a transparent chamber (60 cm x 60 cm x 32 cm) made of polycarbonate sheets with a thickness of 1.5 mm. The chamber was equipped with a fan, and the headspace air temperature was controlled to within approximately ± 1 °C of the ambient temperature by an automatic cooling system. A sensor of photosynthetically active radiation (SKP212, Skye Instruments Ltd., UK) was installed inside the chamber. During the flux measurements, the chamber was put on the preinstalled collars, which were equipped with a water-filled groove around the top to avoid air exchange between the headspace and the ambient air. The CO₂ concentrations were measured using a CO₂/H₂O infrared gas analyzer (LI-840, Licor, USA). CO₂ readings were taken at 1 second intervals over 180 seconds. The data was recorded using a data logger (CR850, Campbell Scientific, USA). The CO₂ flux was calculated from the change in CO₂ concentration in the chamber headspace over time by fitting an exponential model and determining the rate of the initial concentration change at the start of the closure period. More detailed information about the fitting method can be found in Kutzbach et al. [2007]. If the curvature of the nonlinear curves was not explainable by the theoretical model presented in Kutzbach et al. [2007], a linear function was fitted to the data, the slope of which was used for the flux calculation.

5.2.2.2 Eddy covariance flux measurements – ecosystem scale

The fluctuations of wind speed components were measured from April until December 2008 using a three-dimensional sonic anemometer (Solent R3, Gill Instruments Ltd., UK) installed 3 m above the ground level. From the sample intake 15 cm below the anemometer, a vacuum pump drew the sample air through a CO₂/H₂O infrared gas analyzer (LI-7000, LI-COR Inc., USA). All analogue signals were digitized at 20 Hz and stored on a PC running EcoFlux software (InsituFlux, AB, Sweden). The analyzer and the PC were housed in temperature regulated boxes (InsituFlux, AB, Sweden).

Raw data of the eddy covariance flux measurements were processed and turbulent fluxes calculated over 30 min intervals using the EdiRe software (R. Clement, University of Edinburgh, UK). Two coordinate rotations were applied to the wind components so that the mean transverse and the mean vertical wind components were reduced to zero. The time lag between wind and gas concentrations measurements was

determined and removed. Flux losses due to the limited frequency response of the eddy covariance system were corrected in the flux calculation process. The fluxes were corrected for the frequency attenuation due to tube attenuation, sensor path separation and spectral response of the instruments [Moore, 1986; Moncrieff et al., 1997]. Webb correction adapted for closed-path eddy covariance systems was applied [Ibrom et al., 2007]. Integral turbulence characteristics (ITC) were calculated and data were screened accordingly. Data were removed if the deviation of the measured ITC parameter from the modeled ITC parameter was greater than 30 %. Stationarity characteristics were calculated and used to discard the data obtained during non-stationary conditions [Foken and Wichura, 1996]. In total, the filtering methods removed 40 % of CO₂ data, and 8013 half-hour CO₂ flux values remained for further analysis. The data post-processing procedures are presented in more detail in Sachs et al. [2008] and Gažovič et al. [2010].

5.2.2.3 Ancillary measurements

Additional instruments installed near the eddy tower include sensors for air temperature and relative humidity (CS215, Campbell Scientific Ltd., UK), wind speed (M15103, R.M. Young, MI, USA), and photosynthetically active radiation (QS2 Delta-T Devices Ltd., UK). All signals from the ancillary sensors were automatically logged (CR-1000, Campbell Scientific Ltd., UK). At each measurement plot, soil temperature was measured at depths of 5 cm, 10 cm, 20 cm and 40 cm with a sampling frequency of 30 minutes (HOBO U12, HOBO, USA). The depth of ground water near the collars was measured manually each sampling date.

The green leaf area index (GAI) was determined to describe the vegetation development over the growing season and calculated as a sum of the green leaf area of vascular plants and of the green leaf area of mosses. The method was described thoroughly by Wilson et al. [2007]. The green leaf area index of vascular plants was calculated as a product of the leaf size and number of green leaves in 2-week intervals. The green leaf area of mosses was estimated as the projection coverage of living moss capitula. More detailed description on the green leaf area index determination can be found in Schneider et al. [2010]. The effective temperature sum index (ETI) was used to describe the thermal characteristics of the investigated area over the measurement

period. ETI was calculated by dividing the effective air temperature sum by day number, starting from 1st of April=day 1 [Alm et al., 1997; 1999].

5.2.3 Empirical time series modeling

5.2.3.1 Chamber measurements – plot scale

As the chamber measurements are discontinuous, we modeled the time series of net ecosystem CO₂ exchange fluxes (NEE, in $\mu\text{g CO}_2 \text{ m}^{-2}\text{s}^{-1}$) over the investigation period. Models based on photosynthetically active radiation (PAR, in $\mu\text{mol m}^{-2}\text{s}^{-1}$), air temperature (T_{air} , in °C), and GAI (in $\text{m}^2 \text{ m}^{-2}$) or ETI were used. Each measurement plot was modeled separately using the following nonlinear functions:

$$\text{NEE} = \frac{a_1 \times T_{\text{air}} \times \text{GAI} \times \text{PAR}}{\text{PAR} + k_1} + p_1 \times \exp(p_2 \times T_{\text{air}}) \quad (5.1)$$

or

$$\text{NEE} = \frac{a_1 \times T_{\text{air}} \times \text{ETI} \times \text{PAR}}{\text{PAR} + k_1} + p_1 \times \exp(p_2 \times T_{\text{air}}) \quad (5.2)$$

where a_1 , k_1 , p_1 and p_2 are fitting parameters. The first part of the equation including the parameters a_1 , k_1 represents the control of the microform photosynthesis, the second part with the parameters p_1 and p_2 represents the control of the microform respiration.

In this study, NEE is defined positive when carbon dioxide is released to the atmosphere and negative when it is taken up from the atmosphere.

Chamber walls reduce the radiation inside the chamber and result in lower photosynthetic rates inside the chamber as compared to outside. Thus, for the seasonal modeling of NEE not disturbed by a chamber, the NEE flux model derived from chamber PAR measurements was driven using the half-hourly mean PAR value measured at the weather station Schneider et al. [2010].

Empirical modeling was conducted by nonlinear least-squares fitting using the function *nlinfit* of the MATLAB® software package (version 7.1, The MathWorks Inc., Natick, USA).

5.2.3.2 Eddy covariance flux measurements – ecosystem scale

The NEE time series obtained by the EC approach was modeled in two periods: 4 May to 3 August using equation (5.3) and 4 August to 4 November using equation (5.4). Models were based on photosynthetically active radiation (PAR, in $\mu\text{mol m}^{-2}\text{s}^{-1}$), air temperature (T_{air} , in $^{\circ}\text{C}$), and soil temperature in 10 cm and 20 cm depth (T_{10} and T_{20} , respectively, in $^{\circ}\text{C}$). The modeled data was used for gapfilling.

$$\text{NEE} = \frac{a_1 \times T_{20} \times \text{PAR}}{\text{PAR} + k_1} + p_1 \times \exp(p_2 \times T_{\text{air}}) \quad (5.3)$$

$$\text{NEE} = \frac{a_1 \times T_{20} \times \text{PAR}}{\text{PAR} + k_1} + p_1 \times \exp(p_2 \times T_{10}) \quad (5.4)$$

5.2.4 Determination of the microform coverage and remote sensing

The relative coverage of the different microform types was determined at the beginning of August 2008 along eight 300 m long transects at the intensive study site. The transects started at the eddy covariance tower and headed towards the cardinal and inter-cardinal directions. The distribution of the microform types along transects were recorded, and the percentage contribution was assumed to be representative for the spatial coverage of the microform types in the 45° sectors around the transects (Fig. 5.1).

The main wind direction was SSE (Fig. 5.2), as there were no direct measurements along the SSE transect, we decided to use the microform distribution of the S transect for upscaling (Fig. 5.1).

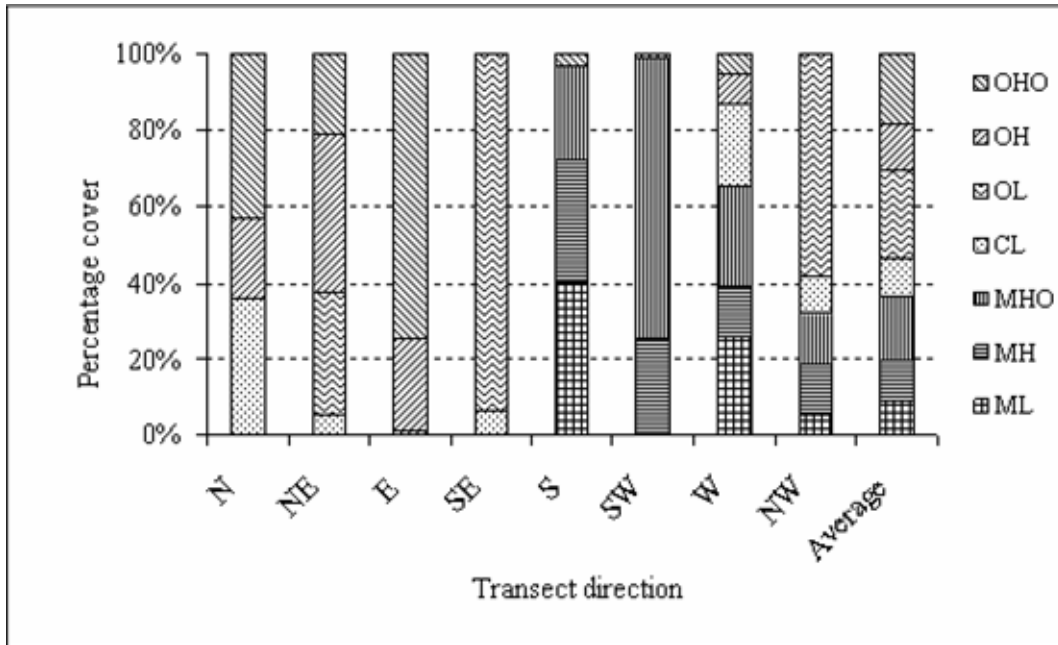


Figure 5.1 Percentage cover of microforms along the 8 transects at the intensive study site. The microforms are ombrogenous hollows (OHO), lawns (OL) and hummocks (OH), and minerogenous hollows (MHO), lawns (ML) and hummocks (MH), and *Carex rostrata* lawns (CL).

For land cover classification, a QuickBird satellite image acquired on 8 July 2008 and covering 70 km² was used in this study (QuickBird © 2007, DigitalGlobe; distributed by Eurimage/Pöyry). QuickBird image has five channels; four of them are multichromatic channels, with 2.4 m x 2.4 m pixel resolution, and one is a panchromatic channel with a 0.6 m x 0.6 m resolution. The four multichromatic channels were resampled to resolution of 0.6 m x 0.6 m pixel size using the panchromatic channel. The resampling was done using Erdas Imagine 8.6 software (Leica Geosystems, Germany) and a cubic convolution method. It was orthorectified and mapped to a cartographic projection, and radiometric, sensor and geometric corrections were applied. The image was georeferenced using field measured GPS points. The accuracy assessment was based on 79 points randomly defined along transects (see above).

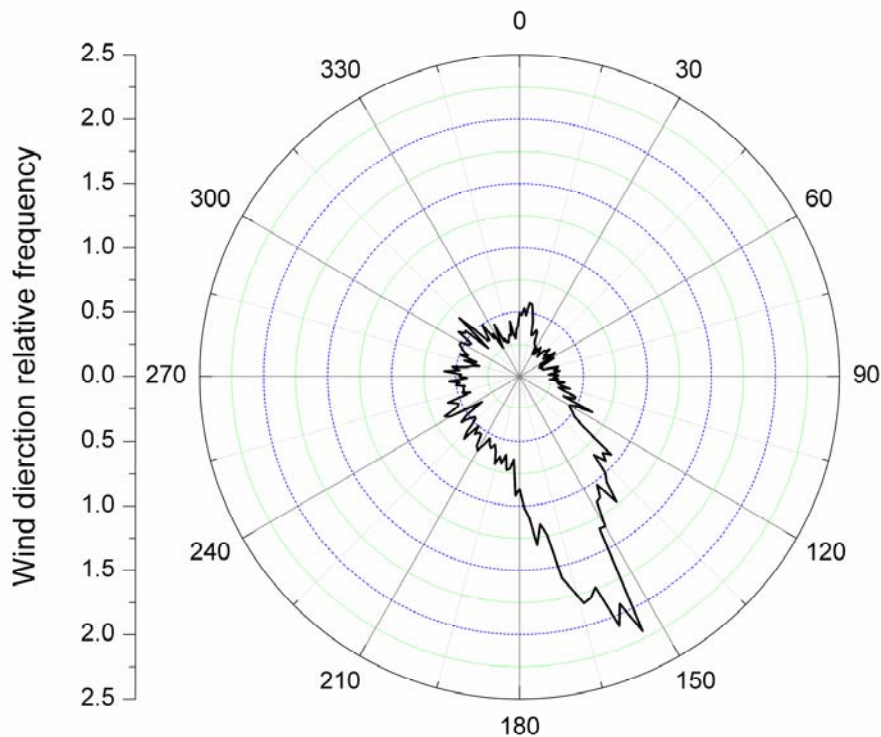


Figure 5.2 Frequency distribution of wind directions measured at the eddy covariance tower

Definiens Professional 5.0 program (Definiens AG, Germany) was applied for the land cover classification using the multiresolution segmentation method. The Kappa coefficient, which is a statistical measure of agreement – where a value of 1 means perfect agreement, was 0.94 for the classification in this study. The aim of the land cover classification by using the very high spatial resolution of the QuickBird image was to recognize the different microform types of the peatland. Regardless of this high spatial resolution, the size of some microforms e.g. minerogenous hollows was often smaller (0.25-0.5 m²) than the spatial resolution of the image. Technically pixel area of classified QuickBird image was 0.36 m², but as it was based on resampling technique described above, real precision for object separation was to some extent lower. Thus, we decided to group the microforms to classes based on the vegetation and water table depth characteristics. The following classes were therefore used for the footprint

analysis: ombrogenous part (OC), minerogenous part (MC) and transition zone (TC) (Fig. 5.3). For the use of the land cover classification in the footprint modeling, we created one image for each class covering the area of interest. These images were resampled to 1 m pixel resolution by nearest neighborhood method. The pixels incorporated the information about the presence of the respective land cover class (value 1 = land cover class present, value 0 = land cover class not present).

5.2.5 Footprint modeling

Footprint modeling was conducted to analyze how the source areas of the observed EC fluxes were characterized with respect to the coverage of land cover classes. The footprint model used in this study was the analytical model according to Kormann and Meixner [2001] which was developed for boundary layer conditions with non-neutral stratification. The two-dimensional footprint density function was determined based on the micrometeorological data from the EC measurements. To calculate the weighted fraction of each land cover class within each 30 min source area, the output of the footprint model was combined with the images of the land cover distribution. Therefore, a coordinate system with the tower in the origin was constructed, and the images were rotated into the main wind direction. Finally, the footprint density function was summed up for all pixels representing one land cover class. The contribution of each land cover class (j) is given as a weighted fraction (Ω_j) of the total source area of the 30 min EC flux.

As the footprint extension commonly exceeded the bounds of the area of interest, the sum of the source fractions of all land cover classes was usually less than 100 %. We assumed that the distribution of the land cover classes in the footprint area which lay outside of the area of interest was similar to the land cover class distribution in the footprint area which lay inside the area of interest. Thus, we scaled the source fraction of each land cover class so that the sum of them was 100 %. A check of the input parameters was then conducted and data characterized by low turbulence (friction velocity $u^* < 0.1 \text{ m s}^{-1}$), high crosswind fluctuations (standard deviation of the lateral wind $\sigma_v > 1$), and zero sensible heat flux were excluded from further calculations. The missing values were replaced by means of source area fractions calculated for one degree intervals of wind direction for both stable and unstable atmospheric conditions.

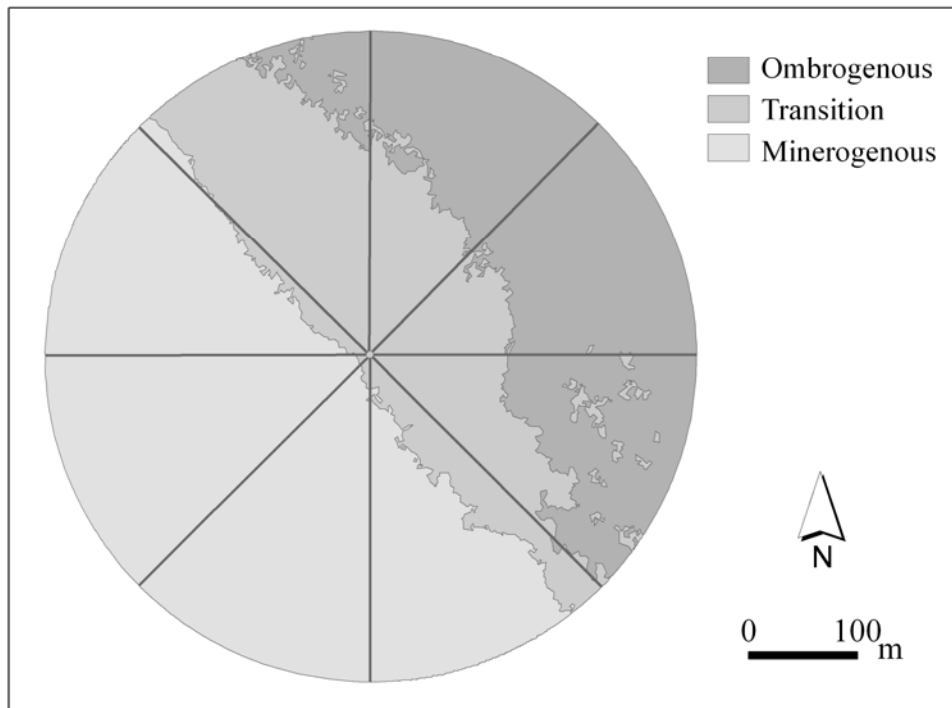


Figure 5.3 Land cover classification of the intensive study site. The lines indicate the transects

Fox et al. [2008] described a critical assumption for using this source area function modeling over a nonuniform surface: the CO₂ fluxes are influenced by spatial variation of the surface properties whereas the influence on the momentum flux is insignificant, and the mechanical setting of the exchange processes is thus approximately uniform throughout the entire potential source area for the instrument. For our study, this assumption seems to be reasonable, given that the vegetation of each land cover class was uniformly relative short and the topography of the site was relatively flat.

5.2.6 Upscaling of CO₂ fluxes from plot scale to ecosystem scale

Three different approaches were used to integrate the plot-scale chamber measurements of NEE with the larger-scale EC measurements of NEE: 1. upscaling based on the average microform distribution in the area of interest and the mean NEE flux for each microform type, 2. upscaling based on areal weighting which accounts for main wind direction and the mean NEE flux for each microform type, and 3. upscaling based on

the weighted fractions of the land cover classes within the source area of the 30 min EC source areas estimated by footprint modeling and the mean NEE flux for each microform type. To estimate the contributions of the different microforms to the EC source areas, the weighed fractions of land cover classes within the EC source areas were multiplied by the average relative microform coverage of the microforms within the respective land cover classes (Fig. 5.4). The following equations were used for different upscaling methods:

$$F_{AV} = \sum_{i=1}^N A_{AVi} \times F_i, \text{ for the upscaling method 1} \quad (5.5)$$

$$F_{WD} = \sum_{i=1}^N A_{WDi} \times F_i, \text{ for the upscaling method 2} \quad (5.6)$$

$$F_{FP} = \sum_{j=1}^N \Omega_j \sum_{i=1}^N A_{ji} \times F_i, \text{ for the upscaling method 3} \quad (5.7)$$

where F_i is the mean NEE flux of the different microform types which was calculated as the mean of the replicates for each half-hour. A_i is the mean relative coverage of the different microform types within the area of interest, which is different depending on the upscaling method and Ω_j the source area fraction for the different land cover classes.

5.2.7 LPJ-GUESS model

5.2.7.1 LPJ-GUESS model and changes made to the model for this study

LPJ-GUESS [Smith et al., 2001] is an ecosystem model that simulates the dynamics of plant populations in the manner of a forest gap model [e.g. Bugmann, 2001]. Biophysical and physiological processes are represented mechanistically, based on the same formulations as the Lund-Potsdam-Jena dynamic global vegetation model (LPJ-DGVM) [Sitch et al., 2003; Gerten et al., 2004]. Model output relevant to this study includes plant biomass and composition, as well as ecosystem carbon exchange

(including net and gross primary production and both autotrophic and heterotrophic respiration). LPJ-GUESS has been evaluated in numerous studies – see Smith et al. [2008] and references therein.

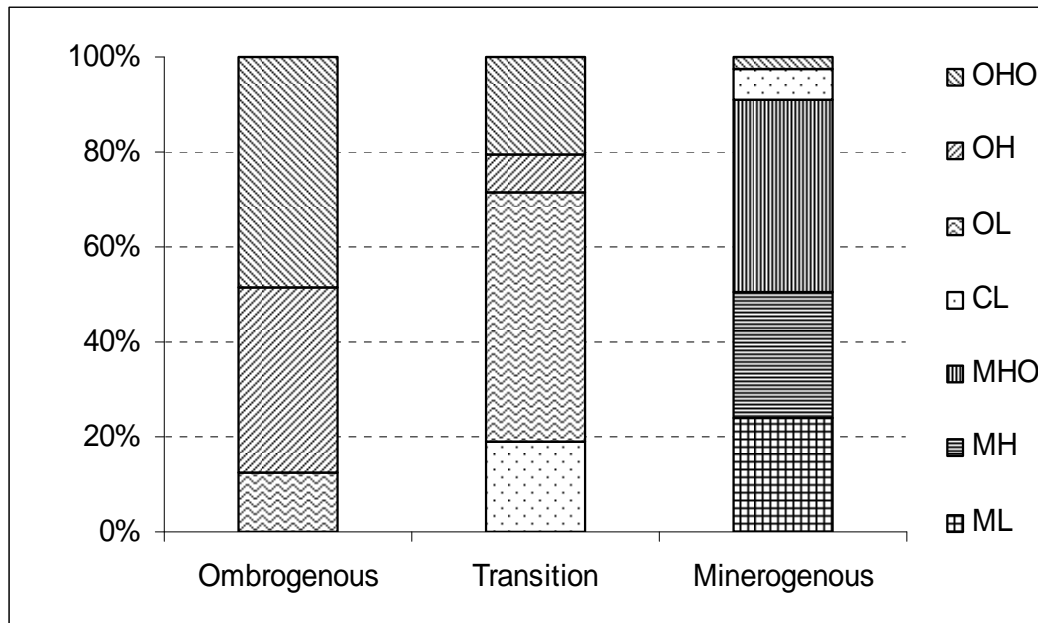


Figure 5.4 Percentage cover of microforms for the different land cover classes. The microforms are ombrogenous hollows (OHO), lawns (OL) and hummocks (OH), and minerogenous hollows (MHO), lawns (ML) and hummocks (MH), and *Carex rostrata* lawns (CL).

In order to apply the model to peatland ecosystems at high latitudes, we have incorporated the recent developments to LPJ-DGVM by Wania et al. [2009a, 2009b, 2010] into LPJ-GUESS. A brief overview of the developments relevant to peatland ecosystems is given here, but a more comprehensive description is given by Miller et al. [2010] (this issue), and in the papers by Wania et al.

Hydrology and Soil Temperature

Previously, LPJ-GUESS calculated soil temperature at 25 cm depth using an analytic solution to the heat diffusion equation, and neither the insulating effects of snow nor phase changes in the soil water were considered. Following the approach of Wania et al. [2009a, 2009b], we have therefore introduced a numerical solution of the heat diffusion equation to LPJ-GUESS. A major departure from the work of Wania et al.,

though, is the fact that LPJ-GUESS calculates the soil temperature in *each* of the replicate patches that together comprise the model's grid cells [Smith et al., 2001].

The model's soil column consists of four compartments: a snow layer of variable thickness, a litter layer of fixed thickness, a soil column of depth 2 m (with sublayers of thickness 0.1 m), and a final, "padding" column of depth 48 m (with thicker sublayers) which is present to aid in the accurate simulation of temperatures in the overlying compartments. Soil temperatures in each sublayer are updated daily, in response to changing surface air temperature forcing and precipitation input.

The peatland hydrology scheme of Wania et al. [2009a] and Granberg et al. [1999] is used to update the water table depth in response to daily precipitation, snowmelt, evapotranspiration and surface runoff. The 2 m soil column is subdivided into an upper 0.3 m-thick acrotelm within which the water table is allowed to fluctuate, and a lower, 1.7 m-deep, permanently saturated catotelm layer. The water table is also allowed to extend above the soil surface to a maximum depth of 0.1 m. Hence, the water table position in this version of the model can fluctuate between +0.1 m and -0.3 m.

Peatland Vegetation

In this study, the model allows the establishment of four plant functional types (PFT) on peatlands. Flood-tolerant graminoids (such as *Carex* spp.) and *Sphagnum* types follow the treatment of Wania et al. [2009b] and Yurova et al. [2007] with minor modifications [Miller et al., 2010]. We also include two shrub PFTs from the work of Wolf et al. [2008], specifically short (<0.5 m), evergreen and summergreen shrubs (e.g. *Andromeda polifolia*, *Chamaedaphne calyculata*). These PFTs differ in their tolerance of inundation, such that, for example, graminoids dominate at high water table levels, and shrubs only survive when the water table is low [Miller et al., 2010].

Carbon Exchange and Pools

Modeled net ecosystem exchange (NEE) used in the model-data comparisons is the difference between net carbon dioxide taken up by the four peatland PFTs (i.e. net primary production) and the CO₂ release due to soil carbon decomposition. Peatland fires are not treated in this version of LPJ-GUESS. The treatment of methane emission from peatlands follows Wania et al. [2010]. Mechanistic, process-based descriptions of

methane production, transport and oxidation are used to model daily methane emissions for the study site [Miller et al., 2010]. This is important since soil carbon emitted as methane does not contribute to NEE.

Two representations of soil carbon decomposition in peatlands are used. The decomposition 1 scenario follows Wania et al. [2009b], where decomposition rates for all modeled carbon pools increase exponentially with soil temperature at 25 cm depth and are then reduced uniformly by 65 % to account for reduced decomposition rates under inundated conditions. The decomposition 2 scenario used in this study is described by Miller et al. [2010] and takes into account the influence of the soil temperature and water content of each 10 cm layer in the model's soil column on the carbon decomposition rate.

5.2.7.2 Modeling protocol

Forcing and spin-up

To compare modeled NEE with observed carbon exchange, the model was run from 1901 to 2100 using monthly temperature and precipitation anomalies from Kuhry et al. [2010] applied to 1980-99 climatologies of these variables from HIRHAM-LSM [Matthes et al., 2010; Rinke et al., 2010]. Shortwave radiation forcing is used directly from HIRHAM-LSM. Yearly values of CO₂ concentration are taken from Matthes et al. [2010] and Rinke et al. [2010] and follow the A1B SRES scenario between 2001 and 2100.

To build up the modeled carbon pools, the model is spun up for 6,500 years using repeated 1901-1930 forcing prior to the transient 1901-2100 simulation. A period of 6,500 years was chosen since it is a typical basal peat age for the region (P. Kuhry, personal communication). Both soil carbon decomposition schemes are used in separate simulations.

Treatment of microforms

To simulate the vegetation and carbon dynamics in wetter regions of the studied peatland site, the water table position was artificially raised by imposing an additional water input of 2 mm d⁻¹. This value was chosen after comparisons of modeled and observed water table positions at the site. These simulations are denoted by “WET”.

Similarly, drier areas were simulated (“DRY” runs) by imposing an additional surface runoff of 5 mm d⁻¹, a value chosen to decrease the water table position to the lowest possible value of -0.3 m after spring snow melt.

5.2.8 Uncertainty analysis

The error of the area estimates for the different microforms cannot be considered as random error. Thus, the error propagation routine for random errors is not suitable for the uncertainty analysis of the upscaled CO₂ fluxes, and we used the method of maximum error estimation.

In order to estimate the uncertainty of the upscaled fluxes (δF), we used the formula:

$$\delta_{F_{AV}} = \sum_{i=1}^N A_{AVi} \times \delta F_i + |F_i| \times \delta A_{AVi}, \text{ for the upscaling method 1} \quad (5.8)$$

$$\delta_{F_{WD}} = \sum_{i=1}^N A_{WDi} \times \delta F_i + |F_i| \times \delta A_{WDi}, \text{ for the upscaling method 2} \quad (5.9)$$

and for the upscaling method 3:

$$\delta_{F_{FP}} = \sum_{j=1}^N (\Omega_j \times (\sum_{i=1}^N A_{ji} \times \delta F_i + |F_i| \times \delta A_{ji})) + (\sum_{i=1}^N A_{ji} \times F_i) \times \delta \Omega_j, \quad (5.10)$$

where F_i is the mean NEE flux of the different microform types and δF_i is the uncertainty of the mean NEE flux. A_i is the mean relative coverage of the different microform types within the area of interest and δA_i is the uncertainty of the coverage estimation, both are different depending on the upscaling method. Ω_j is the source area fraction for the different land cover classes (j) and $\delta \Omega_j$ is the uncertainty of the source area fraction estimation.

For CO₂ estimates by EC technique, we calculated the random error from the difference between the observed and modeled half-hourly fluxes following Aurela et al. [2002]. Systematic errors in EC measurements have their origin in the limited frequency

response of the EC system. An uncertainty of 30 % was assumed for the frequency and Webb correction procedures itself [Aurela et al., 2002].

5.2.9 Evaluation of the model performance

To compare the results of modeled and upscaled chamber measurements to measurements observed by the EC technique, the Willmott index of agreement, d [Willmott, 1982; Yurova et al., 2007] was calculated using daily sums values. To evaluate the model performance of the LPJ-GUESS model, the modeled NEE fluxes were compared to values observed by EC technique on the basis monthly sums.

$$d = 1 - \left[\frac{\sum_{i=1}^N (M_i - O_i)^2}{\sum_{i=1}^N (|M_i'| + |O_i'|)^2} \right], \quad (5.11)$$

where $M_i' = M_i - \bar{O}$, $O_i' = O_i - \bar{O}$, M – modeled values (modeled and upscaled chamber measurements or results of LPJ-GUESS model) and O – observed values (EC technique). \bar{O} is the mean of observed values. The Willmott index varies between 0 and 1, with $d = 1$ indicating a perfect match.

We did not compare the modeled and upscaled chamber measurements to the results of the LPJ-GUESS model as such a comparison of results of a deterministic model to those of a mechanistic model has only a low informative value when the uncertainty analysis is missing.

5.3 Results

5.3.1 Variability of NEE fluxes at plot and ecosystem scales

The NEE fluxes measured by the closed chamber technique varied strongly on spatial and temporal scales (Fig. 5.5). The main difference between the microforms regarding the seasonal variations of the CO₂ fluxes was the date when the daily sum of NEE fluxes became negative (CO₂ sink) in spring or again positive (CO₂ source) in autumn. The MHO sites, for example, changed from being a daily CO₂ source to a daily CO₂ sink at the end of June while this change from source to sink occurred at the ML sites

about three weeks earlier. Also, the ML sites became CO₂ sources in autumn about three weeks later than MHO sites, resulting in a much longer net CO₂ uptake period. The OH sites were CO₂ sources over the complete investigation period and OL as well as one of the CL sites became a CO₂ source already in July after a very short period being CO₂ sink. The seasonal cycle of NEE at two of the MH sites was exceptional. They were CO₂ sources in spring, during summer and in autumn and changed in between to CO₂ sinks in early summer and in early autumn.

On the spatial scale, the NEE fluxes varied not only between the minerogenous and ombrogenous parts of the peatland but also between different microforms and between replicate plots of the same microform. The net CO₂ uptake as a result of photosynthesis and respiration was usually higher in the minerogenous part of the peatland compared to ombrogenous part. NEE fluxes ranged from strong CO₂ sinks (ML) to strong CO₂ sources (OL, OH) over the investigated period. The biggest differences between the replicates of one microform type were determined at ML, OL and CL sites. At *Carex* lawn sites, for example, one plot was a strong CO₂ source; one plot a weak CO₂ source and one plot a CO₂ sink over the investigated period apparently related to their leaf area.

Daily NEE fluxes detected by EC showed a similar seasonal pattern as fluxes detected by chamber measurements: NEE fluxes were highest during the summer and on a shorter time scale similar day-to-day variability could be observed (Fig. 5.5). The daily net ecosystem uptake varied from 0 to -12 g CO₂ m⁻² d⁻¹ during the period from the end of May to the end of September. During the other months, the CO₂ flux was characterized by a relatively steady CO₂ loss of 0 to 2 g CO₂ m⁻² d⁻¹. More detailed information on the results of the EC flux measurements can be found in Gažovič et al. [2010].

The empirical regression models of microform NEE which were used to integrate the chamber fluxes over the investigated period explained 24-94 % of the variation in NEE. 70 % of the regression models had an R²_{adj} (coefficient of determination adjusted for the number of independent variables and the number of measurements) between 0.64 and 0.94. There were differences in model performance between different seasons. A general trend could not be observed, but the trends within the microform type were consistent; for example at minerogenous hollows, the model performance during the

summer was weakest. We found contrary results for the minerogenous lawns; here the model performance was best in summer. The empirical model output for the data measured by the EC system agreed reasonably well with measured data (R^2_{adj} of 0.88 and 0.92, for the 4 May to 3 August and 4 August to 4 November model periods, respectively).

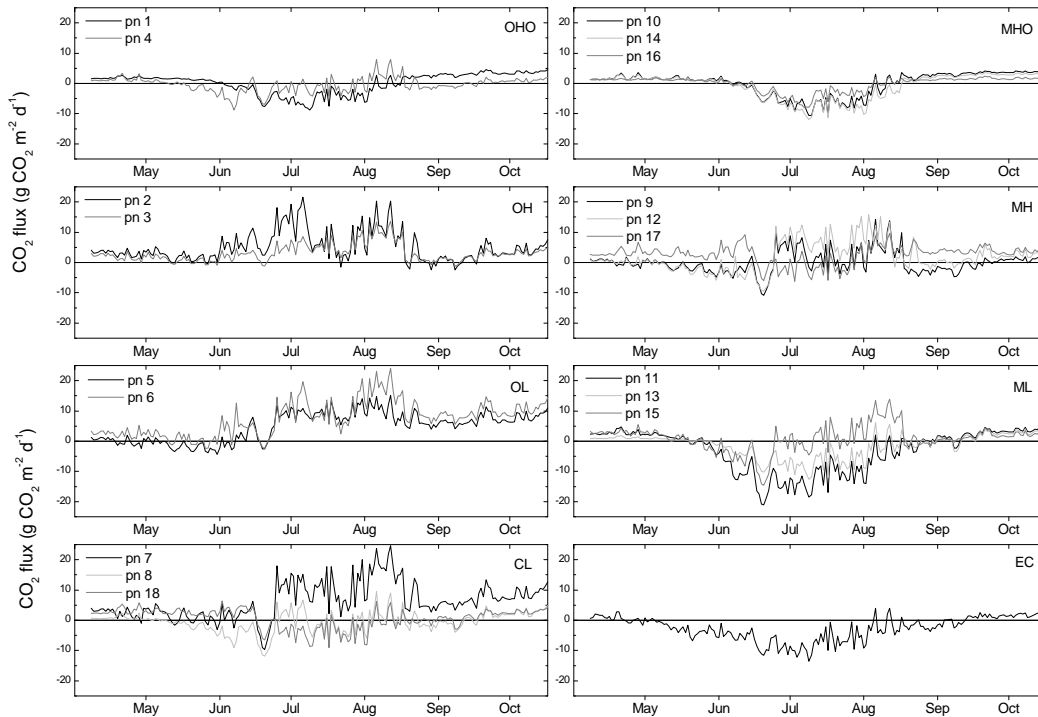


Figure. 5.5 Daily sums of NEE measured by chamber measurements and the eddy covariance technique. The chamber measurements are grouped by microform type. The microforms are ombrogenous hollows (OHO), lawns (OL) and hummocks (OH), and minerogenous hollows (MHO), lawns (ML) and hummocks (MH), and *Carex rostrata* lawns (CL)

5.3.2 Microform distribution at the intensive study site

The average microform distribution in the area of interest were estimated as 18.4 %, 11.8 %, 23.0 %, 10.1 %, 17.3 %, 10.5 % and 8.9 % for OHO, OH, OL, CL, MHO, MH and ML, respectively (Fig. 5.1). OL was the most common and ML the least common of all microform types. The microform distribution along the transects reflected the

clear boundary between the bog in the northern part and the fen in the southern part of the intensive study site. Along the E, SE, SW and NW transects a dominance of one microform type could be observed. If we consider the average microform distribution, no such dominance could be detected. The transect of the main wind direction (S) was composed of the microform types ML (40.4 %), MH (31.7 %), MHO (25%) and OHO (2.9 %) (Fig. 5.1). In the ombrogenous as well as in the minerogenous parts of the peatland, a frequent change of microforms could be observed along the transects. The extension of the microforms varied from 0.5 m to 30 m. The transitional zone was characterized by CL and OL, which occurred in stripes of 50 m to 150 m. The microform distribution varies strongly between the land cover classes (Fig. 5.4). The ombrogenous class is characterized by OHO (48.4 %), OH (38.9 %) and OL (12.7 %), the minerogenous class by OHO (2.3 %), MHO (40.5 %), MH (26.6 %), ML (24 %) and CL (6.5 %) and the transition class by OHO (20.3 %), OH (8.3 %), OL (52.6 %) and CL (18.3 %).

5.3.3 Footprint analysis

The footprint analysis indicated that for 3998 half-hour flux values 80 % of the EC flux source area lay within 300 m of the measurement tower, and the most sensitive distance was at 18 m. The relative frequency of the source area fraction for each of the land cover class is illustrated in Fig. 5.6. The source area fractions of the minerogenous and the transition class were very high, and they were sampled evenly, whereas the ombrogenous class never exceeded 30 % of the source area and for much of the study period (60 %) was zero. The footprint analysis showed that the ombrogenous class was under-sampled by the EC measurement set-up and the EC measurements were representative only for the minerogenous and transition part of the investigated peatland.

5.3.4 Comparison of CO₂ fluxes observed from chamber and eddy covariance measurements

The chamber method and the eddy covariance technique were compared using three different upscaling approaches (Fig. 5.7). Independently of the upscaling or measurement method, the CO₂ fluxes showed similar seasonal trends - they were

highest during the summer and lowest during spring - but the date when the daily sum of NEE fluxes measured by the EC technique became negative was earlier than for the upscaled fluxes and became again positive later in autumn. In addition, shorter scale variations such as the first strong uptake peak in the middle of June were also captured by both methods. However, the magnitude of the modeled fluxes varied between the methods used.

The NEE estimates from chamber measurements upscaled based on the average microform distribution in the area of interest (NEE_{AV}) were positive most time of the investigated period and showed higher net CO_2 release than estimates by EC. The NEE estimates from chamber measurements based on areal weighting which accounts for the microsite distribution in the sector of the main wind direction (NEE_{WD}) were lower than NEE_{AV} estimates but still higher than EC estimates. Best agreement could be observed during some periods in summer. The comparison of the NEE estimates from chamber measurements upscaled using the simulated source area fraction (NEE_{FP}) and the EC CO_2 flux estimates showed high discrepancies between the two methods: the EC measurements showed a much higher uptake of the CO_2 fluxes. The Willmott index for the comparison of modeled and upscaled chamber measurements to measurements observed by EC technique is 0.59 (NEE_{AV} to NEE_{EC}), 0.85 (NEE_{WD} to NEE_{EC}) and 0.57 (NEE_{FP} to NEE_{EC}).

The results of continuous eddy covariance observations were also compared with modeling results based on chamber measurements at different plots. The best agreement was observed for plot number 13 which was a ML site and represented the intermediate minerogenous lawns with respect to the water level and CO_2 fluxes. Even higher uptake of CO_2 was observed at plot number 15 which was a ML site with higher water table level than plot number 13. MH microsities (plot 9 and 12) showed the early change (around 21 May) of daily NEE budget from source to sink of CO_2 in spring as it was measured by EC (Fig. 5.5). These were the same microforms that showed CO_2 uptake in early autumn (September).

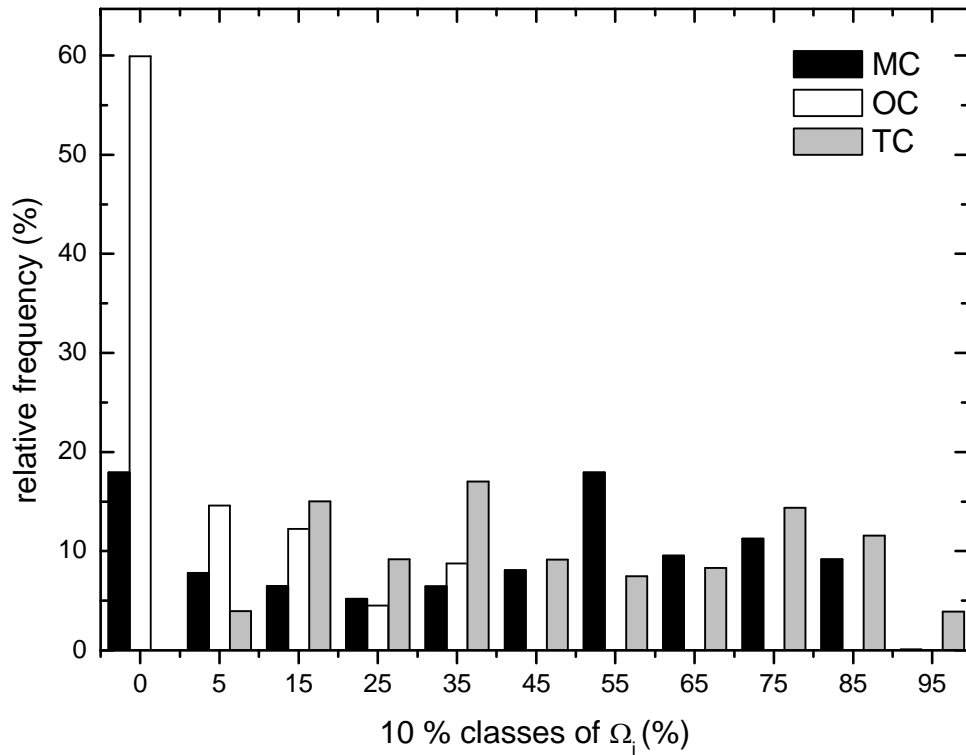


Figure 5.6 Relative frequency of the weighed source area fractions for each land cover class (ombrogenous (OC), minerogenous (MC) and transition (TC)) during the study period. The contribution of each land cover class (j) is given as a weighted fraction (Ω_j) of the total source area of the 30 min EC flux. On the X-axis the class mean is shown.

The comparison of the half-hourly NEE fluxes measured by the EC method (NEE_{EC}) and NEE_{FP} showed that the two methods agreed better during nighttime ($PAR < 10 \mu\text{mol m}^{-2} \text{s}^{-1}$) than during the daytime ($PAR > 10 \mu\text{mol m}^{-2} \text{s}^{-1}$). The EC method showed much higher daytime uptake of CO_2 than the upscaled chamber fluxes.

The cumulative sum of the CO_2 fluxes over the investigation period showed the differences in CO_2 fluxes measured by the EC technique and upscaled using the chamber measurements even more clearly (Fig. 5.8). The cumulative flux of $-533 \pm 6 \text{ g CO}_2 \text{ m}^{-2}$, $344 \pm 533 \text{ g CO}_2 \text{ m}^{-2}$, $-68 \pm 591 \text{ g CO}_2 \text{ m}^{-2}$, and $367 \pm 593 \text{ g CO}_2 \text{ m}^{-2}$ were estimated for the NEE_{EC} , NEE_{AV} , NEE_{WD} and NEE_{FP} , respectively (Tab. 5.1).

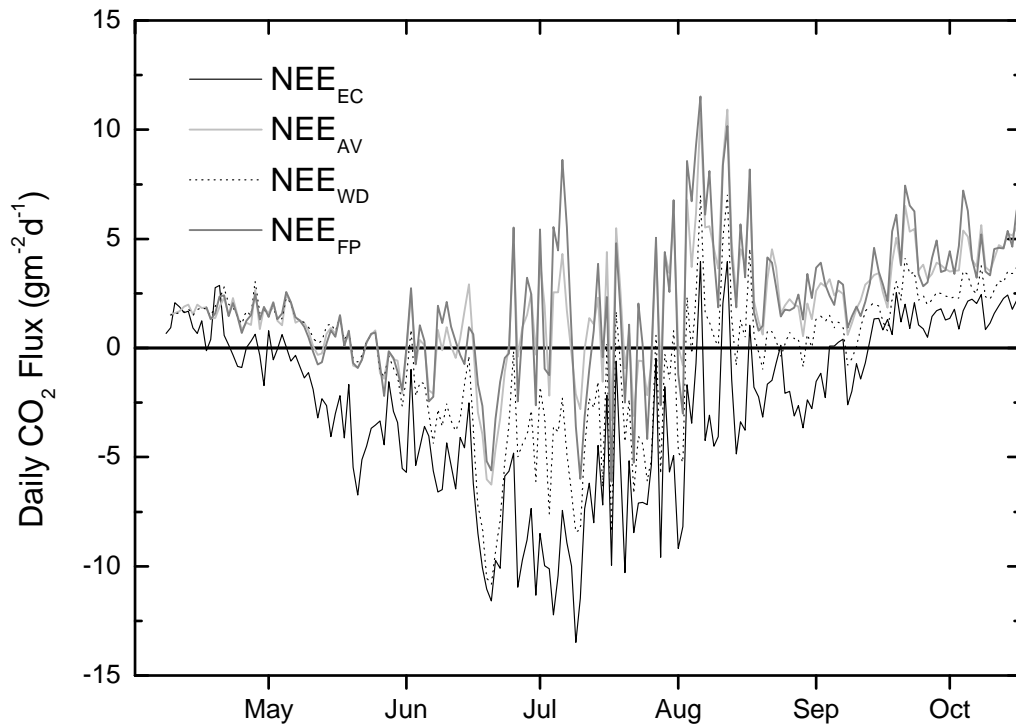


Figure 5.7 Daily sums of NEE calculated from eddy covariance measurements (NEE_{EC}) and upscaled chamber measurements based on average microform distribution (NEE_{AV}), on areal weighting which accounts for the main wind direction (NEE_{WD}), and on simulated source area fraction (NEE_{FP}).

Although the error of the upscaling methods is high, the estimates of the NEE by the EC method are not within the range of the uncertainty of the NEE_{AV} and NEE_{FP} fluxes. Interestingly, the CO₂ flux estimates based on the upscaling method using the average microform distribution and CO₂ flux estimates using the simulated source fraction do not differ by much. They show similar seasonal pattern and budgets over the investigated period. The estimates based on the simulated source fraction are characterized by higher uncertainty as this upscaling method included more calculation steps, all of which contained errors.

Table 5.1 Cumulative NEE flux (in g CO₂ m⁻²) for the investigation period May to October 2008 estimated from eddy covariance measurements (NEE_{EC}) and upscaled chamber measurements based on average microform distribution (NEE_{AV}), on areal weighting which accounts for the main wind direction (NEE_{WD}), and on simulated source area fraction (NEE_{FP}), and modeled by LPJ-GUESS, where D1 is the decomposition 1 and D2 – decomposition 2 scenario

	NEE _{EC}	NEE _{AV}	NEE _{WD}	NEE _{FP}
	-533 ± 6 g CO ₂ m ⁻²	344 ± 533 g CO ₂ m ⁻²	-68 ± 591 g CO ₂ m ⁻²	367 ± 593 g CO ₂ m ⁻²
D1	Standard 15 g CO ₂ m ⁻²	Wet -370 g CO ₂ m ⁻²	Dry -125 g CO ₂ m ⁻²	
D2	Standard -77 g CO ₂ m ⁻²	Wet -800 g CO ₂ m ⁻²	Dry -106 g CO ₂ m ⁻²	

5.3.5 Evaluation of LPJ-GUESS model output

This is a site level model-data comparison as the model was driven by site meteorology. High discrepancies were observed between monthly NEE simulated by the model and observed from the EC measurements (Fig. 5.9). The CO₂ fluxes modeled by the different decomposition scenarios differed mainly in spring and autumn when the NEE fluxes modeled based on the decomposition scenario 1 showed higher CO₂ release than based on the decomposition scenario 2. When comparing the measured EC data to the output of the model, we have to consider that the EC measurements are representative only for the minerogenous and transition part of the investigated peatland. A general trend in agreement between the simulated results and EC observations could not be observed.

Compared to the EC measurements, the seasonal dynamics were generally successfully reproduced by the standard run of the model although the model estimated the onset of daily net CO₂ uptake to occur later in spring and the onset of daily net CO₂ release to occur earlier in autumn (Fig. 5.9). The model performance is summarized in Table 5.2. The wet and dry runs showed the maximum uptake in summer about one month earlier than measured by EC method. The modeling results and EC estimates differed not only

in seasonal dynamics but also in the CO₂ budgets which were calculated for the period from May to October 2008.

All LPJ-GUESS models showed negative budgets (CO₂ uptake) and one slightly positive budget (standard run, decomposition 1). The NEE flux modeled based on the decomposition 1 scenario was 15 g CO₂ m⁻², -370 g CO₂ m⁻² and -125 g CO₂ m⁻² for standard, wet and dry runs, respectively and -77 g CO₂ m⁻², -800 g CO₂ m⁻² and -106 g CO₂ m⁻² for the decomposition scenario 2 (Tab. 5.1).

The highest CO₂ uptake was modeled by the wet runs of the LPJ-GUESS model. The growing season NEE measured by EC showed a much higher uptake of CO₂ than in the standard model run and lower than in the wet model run; it was between the cumulative NEE values estimated by the two wet runs of LPJ-GUESS.

We tested if the vegetation phenology, water table level (WTL), soil temperature as well as the CO₂ fluxes of the different model runs were representative for the fen or bog part of the peatland or for specific microforms. In the real world, the vegetation composition of a bog or a fen reflects the vegetation of the different microforms. In a model, different runs usually represent different microforms, e.g. the vegetation composition of the standard run is representative for the vegetation of hummocks, the wet run for the vegetation of hollows and the dry run either for the vegetation of hummocks or lawns (Tab. 5.3). The WTL of the standard run is not in agreement to the mean WTL of all microforms but to the mean of MHO microforms (Fig. 5.10). Also the WTL of the wet and dry runs differ strongly from the means of the WTL of the fen and bog part and have highest agreement to the MHO and OH microforms, respectively. The soil temperatures differed strongly between the measured and the modeled data in May, June and July, the difference was up to 10 °C.

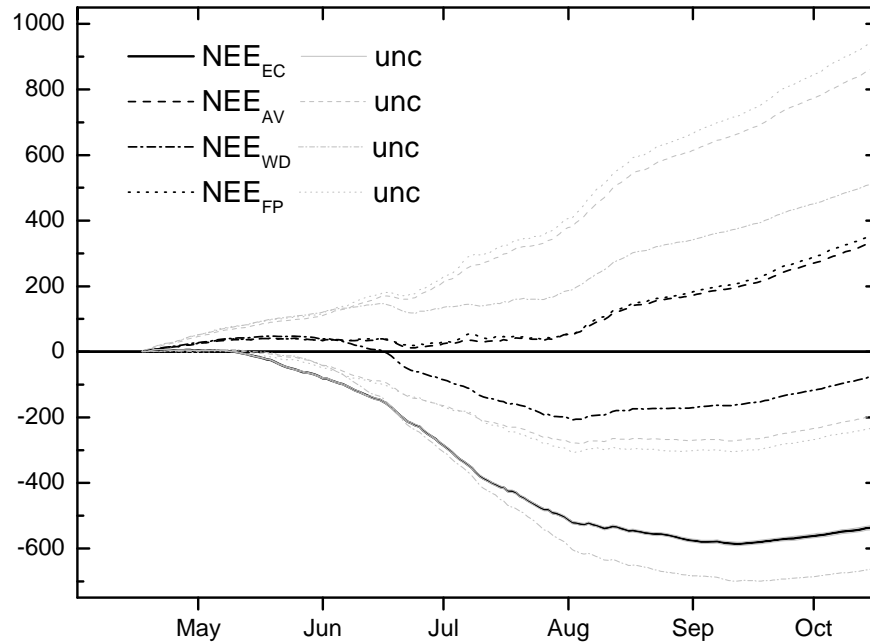


Figure 5.8 Cumulative sum of the CO₂ fluxes over the investigation period measured by the EC technique (NEE_{EC}) and upscaled chamber measurements based on average microform distribution (NEE_{AV}), on areal weighting which accounts for the main wind direction (NEE_{WD}), and on the simulated source area fraction (NEE_{FP}) and uncertainty estimates (unc) for all methods.

Table 5.2 Quantitative measure of model performance based on the Willmott index of agreement ($d=0$, no agreement, $d=1$, perfect match) for different model runs and flux estimations by eddy covariance measurements (NEE_{EC})

	decomposition 1			decomposition 2		
	Standard	Wet	Dry	Standard	Wet	Dry
NEE_{EC}	0.80	0.59	0.60	0.80	0.67	0.57

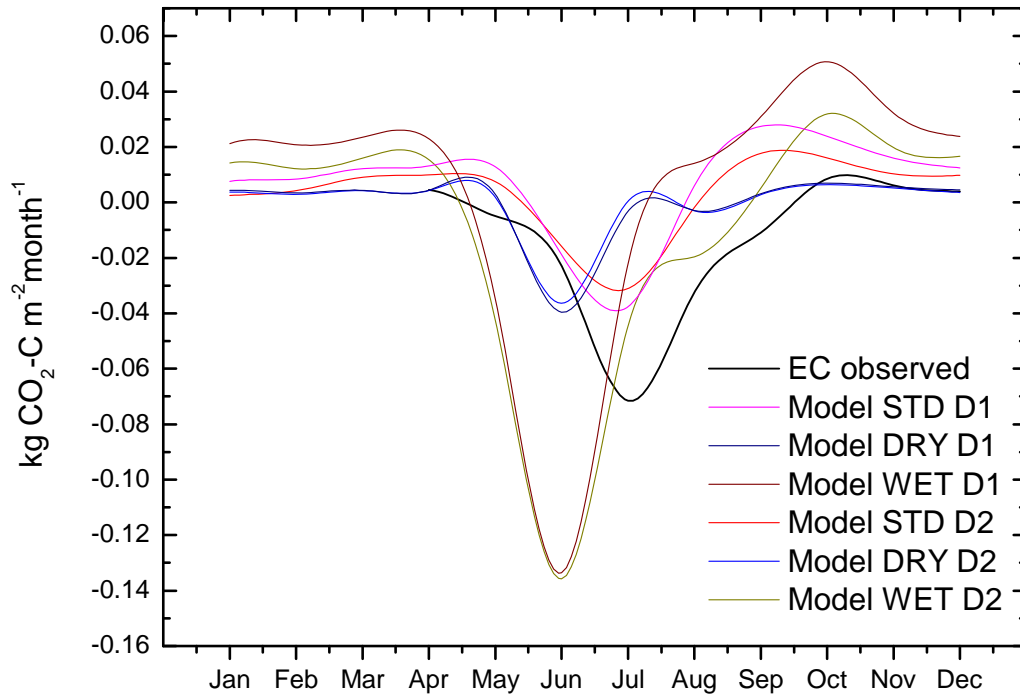


Figure 5.9 Observed and simulated monthly NEE at Ust-Pojeg peatland. The abbreviation for model runs mean STD - standard run, D1 – decomposition 1 and D2 – decomposition 2 scenario.

Table. 5.3 The vegetation composition, water table level and CO₂ fluxes of different model runs are representative for different microforms of the investigated peatland: ombrogenous hollows (OHO), lawns (OL) and hummocks (OH), and minerogenous hollows (MHO), lawns (ML) and hummocks (MH).

Model run	CO ₂ flux	Vegetation composition	Water table level
Standard	OHO	MH/OH	MHO
Wet	ML	MHO/OHO	MHO
Dry	OHO	MH/OH or ML/OL	OH

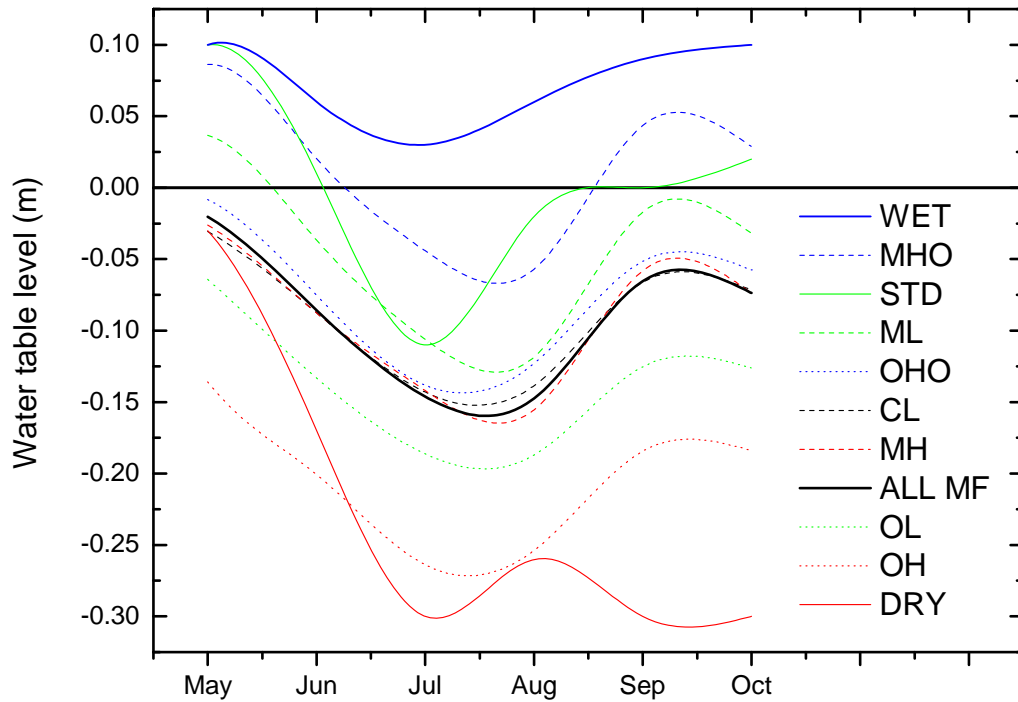


Figure 5.10 Observed and simulated mean monthly water table level (WTL) at Ust-Pojeg peatland. The observed WTL is for the microforms ombrogenous hollows (OHO), lawns (OL) and hummocks (OH), and minerogenous hollows (MHO), lawns (ML) and hummocks (MH), and *Carex rostrata* lawns (CL), ALL MF is the mean of all microforms. The simulated WTL is for the wet, dry and standard (STD) runs of the model. The WTL does not differ between the different decomposition scenarios

5.4. Discussion

5.4.1 Mismatch between NEE fluxes upscaled from chamber and observed from eddy covariance measurements

The observed strong difference between the CO₂ budgets derived from the closed chamber method and the eddy covariance approach calls for intensified search for biases in both measurement approaches. Estimates based on chamber measurements are subject to systematic and sampling errors. Many of the systematic errors are known and can be prevented or corrected for, for example (1) the increase in temperature and

humidity beneath the chamber [Wagner and Reicosky, 1992; Welles et al., 2001], (2) length of the sampling interval [Griffis et al., 2000], (3) inaccurate determination of chamber headspace volume [Livingston and Hutchinson, 1995], (4) leakage at chamber components or via the underlying soil pore space [Hutchinson and Livingston, 2001], (5) elimination of turbulence within the chamber [Reicosky, 2003], (6) gradient problems – build-up or reduction of CO₂ concentration within the chamber which alters the underlying concentration gradients and results in modified CO₂ fluxes [Hutchinson et al., 2000; Livingston et al., 2006; Kutzbach et al., 2007], (7) lack of temporal representation with limited number of sampling points during early morning and late afternoon hours [Griffis et al., 2000]. In this study all of the errors described above were considered and minimized by careful experiment planning, chamber design and data analysis, as described in sections 5.2.2 and 5.2.3. But some errors, such as limited area and measurement intervals, are inherent to the method and can not be prevented, only be reduced by, for example, using bigger measurement plots (in this study 0.36 m²) and increasing the number of measurements (in this study 5517).

A substantial error occurs if the sampling routine does not account for the spatial heterogeneity in NEE fluxes [Janssens et al., 2001; Drewitt et al., 2002]. In a peatland ecosystem, the pronounced heterogeneity can be caused by differences in vegetation type and coverage, water table depth and nutrient supply. In this study the sampling design was adjusted to the heterogeneity of the investigated site by increasing the number of measurement plots. However, an increased number of replicates would have enhanced the accuracy of the mean of the replicate measurements.

The choice of the modeling and reconstruction method influences the CO₂ flux estimates for a peatland investigation site [Laine et al., 2009]. The models can be parameterized by individual sample plots, plant communities or the entire investigation site. According to the findings of Laine et al. [2009], the spatial variation is best captured by the plot method, and the reliability of estimates is also improved. Fluxes were modeled on plot level in this study.

The EC technique has well-known limitations, for example, stable atmospheric conditions lead to a systematic underestimation of CO₂ fluxes if not properly accounted for [Goulden et al., 1996]. Therefore, the obtained data was carefully checked and gap-

filled. A prerequisite is that the method should be applied over flat terrain. This is fulfilled at the Ust-Pojeg study site.

Both closed chamber and eddy covariance methods were carried out simultaneously to allow for comparison by empirical modeling of the flux time series and a footprint model to integrate the point based chamber measurements with the larger scale eddy covariance measurements.

Strikingly, the measurements by the EC approach showed much higher uptake of CO₂ during the daytime compared to the upscaled chamber measurements, whereas during the nighttime the difference in CO₂ flux estimates of the two approaches was minor. The photosynthetic action spectrum of plants is not restricted to the wavelength of photosynthetically active radiation (PAR). Leaves are also effective in ultraviolet (UV) absorption. Mantha et al. [2001] described in their study that the photosynthetic rates at UV-A radiation were up to 10 % higher than at PAR. For the construction of transparent chambers two materials are mainly used: polycarbonate and polyacrylics (mainly Plexiglas®). Polycarbonate, which was also used in this study, has very low or no UV-A-transmission whereas polyacrylics are usually more transparent for these wavelengths. The low UV-A-transmission of the polycarbonate chambers might suppress the photosynthetic activity of plants within the chamber and might be a source of error (underestimation of CO₂ uptake during photosynthesis) in NEE chamber measurements. As this potential error only influences the CO₂ uptake, there is a high potential for a serious bias in the carbon balance which might explain some of the differences in our (higher) NEE flux estimates by the EC approach compared to the upscaled fluxes based on the polycarbonate chambers. Griffis et al. [2000] observed a difference in net photosynthesis between measurements by a gradient technique and upscaled chamber measurements of about 21 %.

5.4.2 Biases in land cover classification and upscaling

The NEE measurements were conducted at different spatial scales. The environmental variables which influence the CO₂ exchange, e.g. peat physical and chemical properties, vegetation or water flow, showed also variability on the different spatial scales. The exchange of CO₂ between the peatland and atmosphere is characterized by a nonlinear response to spatial variations in the driving variables [Baird et al., 2009].

The upscaling methods used in this study do not account for this nonlinear response which might lead to the observed discrepancies between the NEE fluxes upscaled chamber measurements and those measured by eddy covariance measurements.

Due to the small size of some microforms, it was not possible to classify the land cover on the microform level of detail even with our extreme high resolution QuickBird image (0.6 m pixel in panchromatic channel, 2.4 m in multispectral channels). In autumn 2008, GeoEye-1 images (0.41 m pixel in panchromatic channel, 1.65 m in multispectral channels) became available. This increased resolution might already allow a detailed microform classification. An alternative strategy still would be the use of aerial images. Due to failure in microform classification, we used the microform distribution within the land cover class for upscaling. We had to assume that the microforms were evenly distributed within the class. This assumption might be an important source of error in upscaling of the CO₂ fluxes. Due to high spatial heterogeneity of the vegetation and water table levels in a peatland and thus of the CO₂ fluxes, the upscaling of the fluxes from plot to ecosystem level is characterized by higher potential errors than upscaling at homogenous study sites as presented in studies by Dore et al. [2003], Kabwe et al. [2005], Laine et al. [2006] and Yurova et al. [2007]. Fox et al. [2008] described pronounced discrepancies in CO₂ flux estimates between the closed chamber and EC approaches when used at heterogeneous tundra study sites.

Due to the similar mean microform distribution of the upscaling methods based on the average microform distribution and based on footprint modeling, there was no significant difference in seasonal trends and in budgets over the investigation period between NEE_{AV} and NEE_{FP}. The explanation for the substantial difference in the results NEE_{AV} and NEE_{FP} compared to NEE_{WD} might be the large difference in the percentage cover of the different microforms along the south transect compared to the mean percentage cover in the area of interest.

The microform OL had the strongest control on the upscaled fluxes. This is due to their relatively large surface coverage and, more importantly, the large flux values observed for respiration. Although there were microforms which show the early uptake of CO₂ in spring, the upscaling methods integrated all microforms in an ecosystem flux, and this showed the change in daily CO₂ flux from release to uptake much later compared to the flux measurements by the EC technique.

A study by Soegaard et al. [2000] using a footprint model in an arctic valley showed that for the interpretation of the CO₂ fluxes measured by EC the LAI was more important than the vegetation type. It might be more suitable to base the upscaling methods not on the microform distribution but on the leaf area index classes or on a combination of both.

5.4.3 Sources of uncertainty in the model simulations

Model errors are usually caused by an incomplete understanding of biospheric responses to climate forcing across time scales [Mahecha et al., 2010]. The version of LPJ-GUESS used in this study shows reasonable agreement with observations of soil temperature, water table depth, NEE and methane fluxes for both upland and wetland sites across the Arctic [Miller et al., 2010; Wania et al. 2009a, 2009b, 2010]. Having access to a longer time series of NEE values would have allowed a site-specific adjustment of parameters to give a better match to the observations than the results shown here [e.g. Braswell et al. 2005]. We implemented two different soil carbon decomposition schemes to account for uncertainty due to the incompletely unknown influence of soil temperature and moisture on soil carbon decomposition [Davidson and Janssens, 2006].

Nonetheless, there remain a number of other sources of model uncertainty and error that could also have contributed to the large discrepancies between model output and observed NEE seen in this study (Tab. 5.2 and Fig. 5.9). First, model forcing comprised monthly average temperature and precipitation gathered at the site (and subsequently linearly interpolated to give quasi-daily forcing), and this may have led to errors in the timing of the onset and the end of the growing season. Although modeled vegetation may reflect the observed vegetation in some of the microforms (Tab. 5.3), the version of LPJ-GUESS used in this study does not distinguish between the observed nutrient supply and pH differences between ombrogenous and minerogenous areas of the study area, and thus the influence of these variables on primary production, soil carbon decomposition and methane production. Furthermore, soil carbon quality variations (such as age and lability) within and between microsites will influence soil carbon decomposition, but such information was not available for use in the model initialization.

5.4.4 Comparison to other peatland studies and forest flux estimates

Although peatlands cover vast areas of boreal Russia, there are not many boreal peatland carbon flux study sites established. Arneth et al. [2002] and Friborg et al. [2003] published NEE values measured by the EC technique for peatlands in European Russia, Central Siberia and West Siberia, respectively. The CO₂ uptake measured by the EC technique at the Ust-Pojeg site was representative for the minerogenous part of the peatland and was much higher than reported by Arneth et al. [2002], possibly because the study sites of Arneth et al. [2002] were bogs. In contrast, the range and the seasonal dynamics of the CO₂ fluxes at the Ust-Pojeg site and the fen studied by Friborg et al. [2003] were in good agreement.

There are more studies on CO₂ exchange between peatlands and atmosphere in Russia and at other boreal peatlands measured by the closed chamber technique [e.g. Golovatskaya and Dyukarev, 2009; Alm et al., 1997, 1999; Griffis et al., 2000; Riutta et al., 2007a, 2007b]. A detailed comparison of the CO₂ fluxes at the Ust-Pojeg site and other boreal peatland study sites was given in Schneider et al. [2010].

Another important ecosystem of the boreal zone in Russia is the spruce forest. CO₂ flux measurements were conducted in the spruce forests close to the Ust-Pojeg peatland in the year 2007, which was climatically very similar to 2008 (for the investigation period May to October precipitation sums were 354 mm and 348 mm, and the mean air temperatures were 11.6 °C and 11.0 °C for the years 2007 and 2008, respectively). The cumulative sum of forest NEE fluxes for the period from May to October showed only a small sink of CO₂ of -5 g CO₂ m⁻², for the whole year 2007 the estimate is -32 g CO₂ m⁻². This value lay within the range of the annual NEE measured for different spruce forests at the southern boundary of the boreal forest zone in European Russia by closed chamber and EC techniques, which varied from -609 to 1015 g CO₂ m⁻² a⁻¹ [Vygodskaya and Milynkova, 1995; Olychev et al., 2009].

5.5 Summary and conclusions

In this study, we compared NEE of a boreal peatland site measured by closed chambers, EC and modeled by LPJ-GUESS. While the general trend and even shorter scale variations of NEE were similar between chambers and EC, the summed seasonal

NEE showed strong disagreement between the methods. Based on the EC technique measurements, the peatland was a sink of $-533 \pm 6 \text{ g CO}_2 \text{ m}^{-2}$ over the investigation period May - October 2008 whereas the upscaled chamber measurements showed a release of $344 \pm 533 \text{ g CO}_2 \text{ m}^{-2}$, $367 \pm 593 \text{ g CO}_2 \text{ m}^{-2}$ or a small uptake of $-68 \pm 591 \text{ g CO}_2 \text{ m}^{-2}$ for the upscaling methods based on the average microform distribution, the results of the footprint modeling or the microform distribution of the main wind direction, respectively. The upscaled cumulative NEE fluxes are characterized by high uncertainty and can vary from CO_2 sink to source.

To simulate the vegetation and carbon dynamics of the peatland, different runs and soil organic matter decomposition scenarios were used in the LPJ-GUESS model, altogether 6 combinations. The cumulative NEE varied from 15 to $-800 \text{ g CO}_2 \text{ m}^{-2}$ for the investigation period between the different model runs. The wet runs showed highest uptake of CO_2 by the peatland, followed by dry and standard runs.

The main error sources in the upscaling of the fluxes probably were the calculation of the area occupied by the different microform types and the high variability of the CO_2 fluxes within one microform type. As the individual microforms were smaller than the resolution of the QuickBird image, we used the vegetation description along eight transects within the investigated site for the upscaling of the CO_2 fluxes. This method is characterized by higher uncertainty than using the land cover classification provided that the classification resolves the land forms of interest. The variability in CO_2 fluxes within one microform type could be mainly explained by differences in LAI. We recommend basing future upscaling methods not only on microform distribution but also on the spatial distribution of LAI or biomass. These values can be evaluated from high resolution satellite images.

It might happen that even the next generation ecosystem models will not be able to reproduce the heterogeneity in vegetation, hydrology and nutrient supply of a peatland, but it will be possible to model the properties and hence the carbon fluxes of different microform types. So if we would like to model the recent and future carbon budgets of a peatland it might be an alternative to couple these microform models with the microform distribution of the peatland of interest to obtain more realistic results.

Acknowledgements

We gratefully acknowledge the contribution of J. Ibendorf, O. Michajlov, M. Miglovec, P. Schreiber, C. Wille and U. Wolf for assisting us in carrying out the CO₂ flux chamber measurements and of N. Kuusinen and M. Ek (University of Helsinki) for the help in the field and in processing the land cover data. Martin T. Sykes provided valuable feedback on LPJ-GUESS model development. The main funding for the project was provided by the EU Project "CarboNorth" (036993), the German Science Foundation (WI -2680 1/1 and 2/1) and a Sofja Kovalevskaja Research Award to M. Wilmking. During the period of data analysis and manuscript preparation, L. Kutzbach was supported through the Cluster of Excellence "CliSAP" (EXC177), University of Hamburg, funded through the German Research Foundation (DFG).

Chapter 6

General discussion and conclusions

In this dissertation the challenge of quantification of the various components of the C balance of boreal peatlands was demonstrated. The results of the previous chapters showed that besides well established controlling factors, generally associated with effects of temperature, radiation and water table, the evidence that their influence can change sometimes over very short time periods is of great importance. During the few days of the spring thaw, multiple controlling factors were responsible for the patterns of methane emissions and often their influence can be observed following certain phases. Although the spring thaw period is very short, characteristic of changing parameters were further extended into the growing season, when on sub-seasonal scales the controlling parameters did not always follow the empirical model describing the seasonal changes. In our study at Ust-Pojeg peatland, by using moving window regression, we could characterize the times when the typical relationship of night time ecosystem respiration and temperature was changing throughout the season. While temperature was exponentially related to ER in the beginning and at the end of the growing season, the contrary was true for late spring and peak summer period. Such changes in relationship between temperature and ER are not new per-se and are in agreement with other studies (e.g. Atkin and Tjoelker, 2003; Reichstein et al., 2003; Davidson et. al. 2006), but we could show the mechanism of such changes and use the moving parameters for more precise modeling. With rapid increase in air and soil temperatures in the spring, followed by rapid vascular plant development, the exponential relationship between ER and temperature was very weak. Such a rapid temperature increase caused the temperatures to be in the relatively narrow range, which caused changes of the parameter p_2 describing the curvature of the exponential function. The extension of a weak exponential relationship into the growing season was later similarly caused by the range of the temperatures which were in the seasonal maximum with small fluctuations. Although when environmental parameters are not optimal, short time changes in the flux strength might occur. This was the case of

decreased day-time photosynthesis and night-time ER at Ust Pojeg site in the middle of the growing season (beginning of August) with highest LAI, very likely associated with low air temperatures reaching $-0.5\text{ }^{\circ}\text{C}$ at night.

Variability in NEE and primarily in GPP was related to changes in temperature and PAR at both sites. Inter-annual comparison at Salmisuo site showed that in the dry year, with higher PAR sums in nearly all months, higher GPP compared to the wet year was observed. However, high difference in NEE between the two years seems to be related mostly to ER patterns. In the dry year with lower WT, ER was always higher, and we hypothesized that the differences in NEE were caused mainly by the effects of WT on soil respiration, which was higher during the dry year and contrary during the wet one. Higher NEE (higher CO_2 uptake) during the wet year was thus not caused by higher primary production but indirectly by lower ecosystem respiration. High NEE values from Ust-Pojeg peatland compared to values reported in other studies might be expected to be a result of low soil respiration and thus lower ER caused by high and stable WT level during the year. Although the eddy covariance measurements from Ust Pojeg peatland are representative only for more productive and nutrient rich minerogenic and transition parts, while the nutrient poor ombrogenic bog part with lower WT level and more hummocks characterized by higher ER was under-sampled due to prevailing wind directions during the study. Such restrictions have to be taken into consideration when interpreting the results of different measurement methods (see chapter 5). It is evident how important it is to refer to the underlying surface when making such comparisons.

Comparing single year measurements from Ust-Pojeg and the two year measurements from Salmisuo site, the interesting questions about parameters controlling CH_4 emissions appeared. At both sites, CH_4 emissions were related to effects of temperature as higher temperatures coincide with the highest emissions. Comparison of two year measurements at Salmisuo site showed that temperature differences alone were not able to explain inter-annual variations in CH_4 emissions and water table was identified as an important controlling parameter at this site. It was observed that higher CH_4 emissions appeared in the year with higher WT levels which was consistent with other studies (e.g. Moore and Roulet, 1993, Hargreaves et al., 2001). However, in both years the

highest rates of methane emissions appeared during the lowest WT in the middle of the growing season with peaks in the temperature and the primary production.

At the Ust-Pojeg site, high WT levels and little fluctuations throughout the year showed that there was no statistically significant relationship between the CH₄ flux and WT, and again highest CH₄ emissions appeared with the lowest WT levels, highest temperatures and peak in NEE. A rapid increase in CH₄ fluxes in the spring was observed after a rapid increase in air and soil temperatures, triggering rapid growth of the vascular plants. It is likely that besides the influence of temperature and plant substrate supply for methane production, the increase in CH₄ flux was partly influenced by plant mediated transport. The decline in LAI and temperature started moderately in the beginning of August with a following decline in CH₄ fluxes which was compared to the spring time increase more moderate. At the Ust-Pojeg site, an increase in WT after a rainy period in August did not cause drastically increased methane emissions probably because both ecosystem productivity and soil temperatures were on decline.

On the contrary, in 2007 at the Salmisuo site we assume that after high precipitation events in July maintaining a high WT, the following month August experienced an increase in CH₄ emissions as a combination of high WT, high soil temperatures and high primary production, while in the same month in 2006 a decline in emissions in the annual course was recorded associated with the dry conditions. Highest methane emissions coincide with highest NEE and highest temperatures. It seems that a peak in the primary production and substrate availability in the soil influenced by temperature have the primary effects on CH₄ emission magnitude and WT is a controlling parameter responsible for partitioning of the soil carbon flux into soil respiration or methane production. Considering the high CH₄ emissions from Ust-Pojeg site, it might be expected that they are caused namely by a high WT level throughout the year and high NEE, with limited soil respiration.

Rocha and Goulden (2008) reported that the inter-annual cycle of NEE was closely correlated with latent heat flux with high NEE observed during the years with high evapotranspiration (ET), highlighting the importance of canopy development in controlling both fluxes. The importance of plants in controlling ET through transpiration of large amounts of water was stressed previously. It was indicated that transpiration accounted for 80% of the total ET (Goulden et al., 2007).

ET dynamics from Salmisuo site during the dry and the wet years 2006 and 2007 were described by Wu et al. (2010). ET rates were higher in the dry year 2006 compared to the wet year 2007. Considering the results of ET dynamics and the results from our study, we can say that higher GPP was observed during the year with higher ET in the dry year, and vice versa. However, the contrary is true for NEE, where the dry year with higher ET and GPP showed lower NEE (smaller negative number). On the other hand, the wet year 2007 despite smaller GPP and smaller ET resulted in a stronger CO₂ sink. This further supports our hypothesis that soil respiration was in our study a determining parameter influencing NEE.

Chivers et al. (2009) observed in an experiment with manipulating water table position and surface temperature that experimental drought changed the ecosystem from a net sink to a net source of atmospheric CO₂, primarily by reducing plant productivity and experimental flooding caused the ecosystem to serve as a stronger net CO₂ sink, which they attributed to greater plant productivity, lower maximum respiration rates and reduced sensitivity of the soil to temperature. Although in our study higher GPP was observed in the dry year, it is still unclear how low the WT level has to decrease to cause a decrease in the primary production. At Salmisuo site, the roots of vascular plants go deeper than 50 cm under the peat surface (Dorodnikov et al., 2011) which is deeper than was the deepest WT position during the dry year in 2006. Despite the assumption that the roots could supply the water for the plants, we have observed asymmetrical NEE curves (not shown) in the late afternoon associated with effects of high VPD. This indicates a stomata closure of the vascular plants preventing the full potential for assimilation and also reduced plant respiration during early afternoon. It is thus possible that more frequent occurrence of high VPD during the dry year might partly decrease the primary production. Photosynthesis by bryophytes as *Sphagnum* moss is not influenced by stomata closure as bryophytes do not possess stomata, but drought and decreased leaf water content in *Sphagnum* moss can reduce the net photosynthesis (Murray et al., 1989).

WT depth can also influence the positive relationship between GPP and CH₄ which might not be true at the drier sites, although the threshold at which plant production can enhance peatland CH₄ fluxes was not determined yet (Lai, 2009).

It is not easy to evaluate the influence of the length of the growing season on C fluxes. In the year 2007 we have observed earlier snow thaw and earlier start of the growing season, probably induced by warm air temperatures at the Salmisuo site. The DOC export started nearly one month earlier in 2007, and we observed the switch to net daily CO₂ sink 10 days earlier in 2007. While an earlier start of the growing season caused a smoother transition to net CO₂ sink in 2007, a steeper transition was observed in May 2006 with more negative NEE in the dry year. The WT levels were very similar until June, thus it seems that higher CO₂ uptake was related to an earlier start of the growing season rather than to differences in soil respiration. There is an indication that the earlier start of the growing season influenced the CH₄ emissions in the beginning of the season. We hypothesized that this was induced by substrate supply for methanogenesis to the soil. It was observed that despite higher soil temperatures and higher GPP, CH₄ emissions in May and June in 2006 were lower at comparable WT levels, thus we assume that higher CH₄ emissions in 2007 could be caused by higher primary production starting earlier in the season and thus higher substrate content for methanogenesis.

It became evident how complex the question of controlling parameters is and how closely all parts of the C cycle are interrelated, making the answer not less complex than the question itself. It seems that there is a delicate relationship between plant photosynthesis (GPP) as the single most important C balance component and other C flux components. Plant activity stimulates substrate availability in the soil, which, depending on the environmental conditions, is then partitioned into soil respiration flux, CH₄ flux and DOC flux. However, in 2007 higher primary production at Salmisuo site compared to Ust-Pojeg site in 2008 was observed, although the annual CH₄ emissions of 6.6 g C-CH₄ m⁻² at Salmisuo were much lower than the annual CH₄ emissions of 22.5 g C-CH₄ m⁻² at Ust-Pojeg site. This was probably caused by lower air and soil temperatures at Salmisuo site. Thus, besides primary production and WT, temperature still seems to be an important parameter controlling the CH₄ emissions.

Further research relying on eddy covariance technique has a great potential for answering interesting research questions as parallel measurements of energy and mass

fluxes (e.g. water, CO₂ and CH₄) are available in matching temporal and spatial resolution. This might bring deeper understanding of the relationship between all major C components. We suggest that the relationships between energy and mass fluxes should be studied simultaneously. There is an indication that phenological plant development has a strong influence on all C balance components, related to water and energy balance and might be a link for understanding the C cycle. Furthermore, based on our study it seems necessary to extend the measurement periods beyond single year measurements to be able to properly address complicated relationships between ecosystem responses and environmental parameters. It was shown how relative a statement about significance of some parameters might be when only single year measurements are taken into account. For example during single year measurements, a stable and high water table might not be significantly related to CH₄ emissions due to e.g. low WT fluctuations, but on the other hand, it might be responsible for the quantity of the emissions which might be high namely depending on high WT levels. On the other hand, stable WT can significantly reduce the soil respiration component of the ER. Only by comparing multiple year measurements, a correct understanding might be obtained. Strong attention should be paid to phenological changes of vascular plants as a major controller of above and below ground processes.

Bibliography

- Alm, J., Schulman, L. , Walden, J., Nykänen, H., Martikainen, P. J. and Silvola, J. 1999. Carbon balance of a boreal bog during a year with an exceptionally dry summer. *Ecology*. **80** (1), 161-174.
- Alm, J., Shurpali, N.J., Tuittila, E.S., Laurila, T., Malajanen, M., Saarnio, S. and Minkkinen, K. 2007. Methods for determining emission factors for the use of peat and peatlands - flux measurements and modelling. *Boreal Env.Res.* **12**, 85-100.
- Alm, J., Talanov, A., Saarnio, S., Silvola, J., Ikkonen, E., Aaltonen, H., Nykänen, H. and Martikainen, P. J. 1997. Reconstruction of the carbon balance for microsites in a boreal oligotrophic pine fen, Finland. *Oecologia*. **110**, 423-431.
- Arneth, A., Kurbatova, J., Kolle, O., Shibistova, O. B., Lloyd, J., Vygodskaya, N. N. and Schulze, E. D. 2002. Comparative ecosystem-atmosphere exchange of energy and mass in a European Russian and a central Siberian bog. II. Interseasonal and interannual variability of CO₂ fluxes. *Tellus* **54B**, 514-530.
- Atkin, O. K. and Tjoelker, M. G. 2003. Thermal acclimation and the dynamic response of plant respiration to temperature. *Trends Plant Sci.* **8**, 343-351.
- Aurela, M., Laurila, T. and Tuovinen, J. P. 2002. Annual CO₂ balance of a subarctic fen in northern Europe: Importance of the wintertime efflux. *J. Geophys. Res.-Atmos.* **107**(D21), 4607.
- Badeck, F. W., Bondeau, A., Bottcher, K., Doktor, D., Lucht, W., Schaber, J. and Sitch, S. 2004. Responses of spring phenology to climate change. *New Phytol.* **162**(2), 295-309.
- Baldocchi, D. D. 2003. Assessing the eddy covariance technique for evaluating carbon dioxide exchange rates of ecosystems: past, present and future. *Glob. Change Biol.* **9**(4), 479-492.
- Baird, A. J., Belyea, L. R. and Morris, P. J. 2009. Upscaling of peatland-atmosphere fluxes of methane: small-scale heterogeneity in process rates and the pitfalls of “bucket-and-slab” models, in: *Carbon Cycling in Northern Peatlands*, edited by A. J. Baird, L. R. Belyea, X. Comas, A. S. Reeve, and L. D. Slater, pp. 37-54, American Geophysical Union, Washington D. C. USA.
- Becker, T., Kutzbach, L., Forbrich, I., Schneider, J., Jager, D., Thees, B. and Wilmking, M. 2008. Do we miss the hot spots? - The use of very high resolution aerial photographs to quantify carbon fluxes in peatlands. *Biogeosciences*, **5**, 1387–1393.
- Bellisario, L. M., Bubier, J. L., Moore T. R. and Chanton, J. P. 1999. Controls on CH₄ emissions from a northern peatland. *Global Biogeochem. Cycles* **13**(1), 81-91.
- Biondi, F. 1997. Evolutionary and moving response functions in dendroclimatology. *Dendrochronologia* **15**,139-150.
- Braswell, B. H., Sacks, W. J., Linder, E. and Schimel, D. S. 2005. Estimating diurnal to annual ecosystem parameters by synthesis of a carbon flux model with eddy covariance net ecosystem exchange observations. *Global Change Biol.* **11**, 335-355.

- Bubier, J., Costello, A., Moore, T. R., Roulet, N. T. and Savage, K. 1993. Microtopography and methane flux in boreal peatlands, northern Ontario, Canada. *Can. J. Bot.* **71**(8), 1056-1063.
- Bubier, J. L., Crill, P. M., Mosedale, A., Frohking, S. and Linder, E. 2003. Peatland responses to varying interannual moisture conditions as measured by automatic CO₂ chambers. *Global Biogeochem. Cycles.* **17** (2), doi: 10.1029/2002GB001946.
- Bugmann, H. (2001), A review of forest gap models. *Climatic Change.* **51**, 259–305.
- Ciais, P., Denning, A. S., Tans, P. P., Berry, J. A., Randall, D. A., Collatz, G. J., Sellers, P. J., White, J. W. C., Troler, M., Meijer, H. A. J., Francey, R. J., Monfray, P. and Heimann, M. 1997. A three-dimensional synthesis study of $\delta^{18}\text{O}$ in atmospheric CO₂ 1. Surface fluxes. *J. Geophys. Res.* **102**(D5), 5857–5872.
- Chivers, M. R., Turetsky, M. R., Waddington, J. M., Harden, J. W. and McGuire, A. D. 2009. Effects of experimental water table and temperature manipulations on ecosystem CO₂ fluxes in an Alaskan rich fen. *Ecosystems*, **12**(8), 1329-1342.
- Christensen, T. R., Ekberg, A., Strom, L., Mastepanov, M., Panikov, N., Mats, O., Svensson, B. H., Nykanen, H., Martikainen, P. J. and Oskarsson, H. 2003. Factors controlling large scale variations in methane emissions from wetlands. *Geophys. Res. Lett.* **30**, 67-1 - 67-4.
- Clymo, R. S. and Pearce, D. M. E. 1995. Methane and carbon-dioxide production in, transport through, and efflux from a peatland. *Philos. Trans. R. Soc. Lond.* **351**, 249-259.
- Comas, X., Slater, L. and Reeve, A. 2008. Seasonal geophysical monitoring of biogenic gases in a northern peatland: Implications for temporal and spatial variability in free phase gas production rates. *J. Geophys. Res.-Biogeosci.* **113**, G01012, doi:10.1029/2007JG000575.
- Coulter, R. L., Pekour, M. S., Cook, D. R., Klazura, G. E., Martin, T. J. and Lucas, J. D. 2006. Surface energy and carbon dioxide fluxes above different vegetation types within ABLE. *Agric. For. Meteorol.* **136**, 147-158.
- Cramer, W., Bondeau, A., Woodward, I., Prentice, I. C., Betts, R. A., Brovkin, V., Cox, P. M., Fisher, V., Foley, J. A., Friend, A. D., Kucharik, C., Lomas, M. R., Ramankutty, N., Sitch, S., Smith, B., White, A. and Young-Molling, C. 2001. Global response of terrestrial ecosystem structure and function to CO₂ and climate change: results from six dynamic global vegetation models. *Global Change Biol.* **7**(4), 357-373.
- Davidson, E. A. and Janssens, I. A. 2006a. Temperature sensitivity of soil carbon decomposition and feedbacks to climate change. *Nature.* **440**(7081), 165-173.
- Davidson, E. A., Janssens, I. A. and Luo, Y. Q. 2006b. On the variability of respiration in terrestrial ecosystems: moving beyond Q₁₀. *Glob. Change Biol.* **12**. 154-164.
- Denman, K.L., Brasseur, G., Chidthaisong, A., Ciais, P., Cox, P.M., Dickinson, R.E., Hauglustaine, D., Heinze, C., Holland, E., Jacob, D., Lohmann, U., Ramachandran, S., Silva Dias, P.L., Wofsy, S.C. and Zhang, X. 2007. Couplings between changes in the climate system and biogeochemistry. In: *Climate Change 2007: The physical science basis. Contribution of working group I to the fourth assessment report of the Intergovernmental Panel on Climate Change.* (eds. Solomon, S., Qin, D., Manning, M., Chen, Z., Marquis, M., Averyt, K.B., Tignorand, M. and Miller, H.L.). Cambridge University Press, Cambridge, United Kingdom and New York, NY, USA.

- Dise, N. B. 1992. Winter Fluxes of Methane from Minnesota Peatlands. *Biogeochemistry* **17**(2): 71-83.
- Dore, S., Hymus, G. J., Johnson, D. P., Hinkle, C. R., Valentini, R. and Drake, B.G. 2003. Cross validation of open-top chamber and eddy covariance measurements of ecosystem CO₂ exchange in a Florida scrub-oak ecosystem. *Global Change Biol.* **9**, 84-95.
- Drewitt, G. B., Black, T. A., Nestic, Z., Humphreys, E. R., Jork, E. M., Swanson, R., Ethier, G. J., Griffis, T. and Morgenstern, K. 2002. Measuring forest floor CO₂ fluxes in a Douglas-fir forest. *Agric. For. Meteorol.* **101**, 299–317.
- Dyson, K. E., Billett, M. F., Dinsmore, K. J., Harvey, F., Thomson, A. M., Piirainen, S. and Kortelainen, P. 2011. Release of aquatic carbon from two peatland catchments in E. Finland during the spring snowmelt period. *Biogeochemistry* **103**(1-3), 125-142.
- Edwards, G., Neumann, H., den Hartog, G., Thurtell, G., Kidd, G., 1994. Eddy correlation measurements of methane fluxes using a tunable diode laser at the Kinosheo Lake Tower Site during the Northern Wetlands Study (NOWES). *J. Geophys. Res.-Atmos.* **99** (D1), 1511–1517.
- Fan, S., Wofsy, S., Bakwin, P., Jacob, D., Anderson, S., Keabian, J., McManus and J., Kolb, C., 1992. Micrometeorological measurements of CH₄ and CO₂ exchange between the atmosphere and subarctic tundra *J. Geophys. Res.-Atmos.* **97** (D15), 16627–16643.
- Fischlin, A., G.F. Midgley, J.T. Price, R. Leemans, B. Gopal, C. Turley, M.D.A. Rounsevell, O.P. Dube, J. Tarazona, A.A. Velichko, 2007. Ecosystems, their properties, goods, and services. *Climate Change 2007: Impacts, adaptation and vulnerability. Contribution of working group II to the fourth assessment report of the Intergovernmental Panel on Climate Change.* (eds. Parry, M.L. , Canziani, O.F., Palutikof, J.P., Linden van der, P.J. and Hanson, C.E.) Cambridge University Press, Cambridge, 211-272.
- Foken, T. and Wichura, B. 1996. Tools for quality assessment of surface-based flux measurements. *Agric. For. Meteorol.* **78**: 83-105.
- Forbrich, I., Kutzbach, L., Wille, C., Becker, T., Wu, J., Wilmking. 2011. M. Cross-evaluation of measurements of peatland methane emissions on microform and ecosystem scales using high-resolution landcover classification and source weight modeling. *Agric. For. Meteorol.*
- Forbrich, Wania, Kutzbach, Saarnio, Schäfer, and Wilmking, submitted, Evaluation of methane flux dynamics in peatlands as simulated by LPJ-WHyMe using microform and ecosystem scale observations.
- Fox, A. M., B. Huntley, C. R. Lloyd, M. Williams, and R. Baxter (2008), Net ecosystem exchange over heterogeneous Arctic tundra: Scaling between chamber and eddy covariance measurements. *Global Biogeochem. Cycles.* **22**, GB2027, doi:10.1029/2007GB003027.
- Friberg, T., Soegaard, H., Christensen, T. R., Lloyd, C. R. and Panikov, N. S. 2003. Siberian wetlands: Where a sink is a source. *Geophys. Res. Lett.* **30**(21): 4.
- Fritz, Ch., Pancotto, V. A., Elzenga, J. T. M., Visser, E. J., Grootjans Ab. P., Pol, A., Iturraspe, R., Roelofs, J. G.M. and Smolders A. J. P. 2011. Zero methane emission bogs: extreme rhizosphere oxygenation by cushion plants in Patagonia. *New Phytol.* doi:10.1111/j.1469-8137.2010.03604.

- Funk, D. W., Pullman E. R., Peterson, K. M., Crill, P. M. and Billings, W. D. 1994. Influence of water table on carbon dioxide, carbon monoxide, and methane fluxes from Taiga Bog microcosms. *Global Biogeochem. Cycles*, **8**(3), 271–278, doi:10.1029/94GB01229.
- Gažovič, M., Kutzbach, L. Forbrich, I., Schneider, J., Wille, C. and Wilmking, M. Temperature and plant phenology control the seasonal variability of CO₂ and CH₄ fluxes from a boreal peatland in North-West Russia, manuscript, 2010.
- Gerten, D., Schabhoff, S., Haberlandt, U., Lucht, W. and Sitch, S. 2004. Terrestrial vegetation and water balance – hydrological evaluation of a dynamic global vegetation model. *J. Hydrol.* **286**, 249-270.
- Gilmanov T.G., Aires, L., Barcza, Z., Baron, V. S., Belelli, L., Beringer, J., Billesbach, D., Bonal, D., Bradford, J., Ceschia, E., Cook, D., Corradi, C., Frank, A., Gianelle, D., Gimeno, C., Gruenwald, T., Guo, H., Hanan, N., Haszpra, L., Heilman, J., Jacobs, A., Jones, M. B., Johnson, D.A., Kiely, G., Li, S., Magliulo, V., Moors, E., Nagy, Z., Nasyrov, M., Owensby, C., Pinter, K., Pio, C., Reichstein, M., Sanz, M. J., Scott, R., Soussana, J. F., Stoy, P. C., Svejcar, T., Tuba, Z., and Zhou, G. 2010. Productivity, respiration, and light-response parameters of world grassland and agroecosystems derived from flux-tower measurements. *Rangeland Ecol. Manage.* **63**, 16-39.
- Golovatskaya, E. A. and Dyukarev E.A. 2009. Carbon budget of oligotrophic mire sites in the Southern Taiga of Western Siberia. *Plant Soil* **315**(1-2): 19-34.
- Gorham, E. 1991. Northern Peatlands - Role in the carbon-cycle and probable responses to climatic warming. *Ecol. Appl.* **1**(2): 182-195.
- Goulden, M. L., Litvak, M. and Miller, S. D. 2007. Factors that control Typha marsh evapotranspiration. *Aquat. Bot.* **86**(2), 97-106.
- Goulden, M. L., Munger, J. W., Fan, S.-M., Daube, B. C. and Wolfsy, S. C. 1996. Measurements of carbon sequestration by long-term eddy covariance: Methods and critical evaluation of accuracy. *Global Change Biol.* **2**, 169-182.
- Goulden, M. L., Miller, S. D., da Rocha, H. R., Menton, M. C., de Freitas, H. C., e Silva Figueira A. M. and de Sousa, C. A. D. 2004. Diel and seasonal patterns of tropical forest CO₂ exchange. *Ecol. Appl.* **14**, 42-54.
- Granberg, G., Grip, H., Loefvenius, M. O., Sundh, I., Svensson, B. H. and Nilsson, M. 1999. A simple model for simulation of water content, soil frost, and soil temperatures in boreal mixed mires. *Water Resour. Res.* **35**(12), 3771-3782.
- Grant R.F., Barr, A. G., Black, T. A., Margolis, H. A., Dunn, A. L., Metsaranta, J., Wang, S., McCaughey, J. H. and Bourque, C.A. 2009. Interannual variation in net ecosystem productivity of Canadian forests as affected by regional weather patterns - A Fluxnet-Canada synthesis. *Agric. For. Meteorol.* **149**, 2022-2039.
- Griffis, T.J., Rouse, W. R. and Waddington, J.M. 2000. Scaling net ecosystem CO₂ exchange from the community to landscape-level at a subarctic fen. *Global Change Biol.* **6**, 459-473.
- Hargreaves, K. J., Fowler, D., Pitcairn, C. E. R. and Aurela, M. 2001. Annual methane emission from Finnish mires estimated from eddy covariance campaign measurements. *Theor. Appl. Climatol.* **70**, 203-213.
- Heikkinen, J. E. P., Maljanen, M., Aurela, M., Hargreaves, K. J. and Martikainen, P. J. 2002. Carbon dioxide and methane dynamics in a sub-Arctic peatland in northern Finland. *Polar Res.* **21**(1), 49–62.

- Heikkinen, J. E. P., Virtanen, T., Huttunen, J. T., Elsakov, V. and Martikainen, P. J. 2004. Carbon balance in East European tundra. *Global Biogeochem. Cycles* **18**(1): 14.
- Hendriks, D., van Huissteden, J., Dolman, A., 2010. Multi-technique assessment of spatial and temporal variability of methane fluxes in a peat meadow. *Agricultural and Forest Meteorology* **150** (6), 757–774.
- Heyer, J., Berger, U., Kuzin, I. L. and Yakovlev, O. N. 2002. Methane emissions from different ecosystem structures of the subarctic tundra in Western Siberia during midsummer and during the thawing period. *Tellus* **54B**, 231-249.
- Houghton, R. A, Davidson, E. A and Woodwell, G. M. 1998. Missing sinks, feedbacks, and understanding the role of terrestrial ecosystems in the global carbon balance. *Glob. Biogeochem. Cycles* **12**(1), 25-34.
- Hutchinson, G. L., and Livingston, G. P. 2001. Vents and seals in non-steady state chambers used for measuring gas exchange between soil and the atmosphere. *Eur. J. Soil Sci.* **52**, 675-682.
- Hutchinson, G. L., Livingston, G. P., Healy, R. W. and Striegl, R. G. 2000. Chamber measurement of surface-atmosphere trace gas exchange: numerical evaluation of dependence on soil, interfacial layer, and source/sink properties. *J. Geophys. Res.* **105**, (D7), 8865-8875.
- Huttunen, J. T., H. Nykanen, Turunen, J. and Martikainen, P. J. 2003. Methane emissions from natural peatlands in the northern boreal zone in Finland, Fennoscandia. *Atmos. Environ.* **37**(1): 147-151.
- Ibrom, A., Dellwik, E., Flyvbjerg, H., Jensen, N. O. and Pilegaard, K. 2007. Strong low-pass filtering effects on water vapour flux measurements with closed-path eddy correlation systems. *Agric. For. Meteorol.* **147**, 140-156.
- Ibrom, A., Dellwik, E., Larsen, S. E. and Pilegaard, K. 2007. On the use of the Webb-Pearman-Leuning theory for closed-path eddy correlation measurements. *Tellus B.* **59**(5), 937-946.
- Intergovernmental Panel on Climate Change (IPCC) (2001), *Climate Change 2001: Synthesis Report. A Contribution of Working Groups I, II, and III to the Third Assessment Report of the IPCC*, edited by Watson, R.T. and the Core Writing Team, Cambridge University Press, Cambridge, United Kingdom, and New York, USA, 398 pp.
- Intergovernmental Panel on Climate Change (IPCC) (2007), Summary for policymakers, in *Climate Change 2007: The Physical Science Basis: Working Group I Contribution to the Fourth Assessment Report of the IPCC*, edited by S. Solomon, D. Qin, and M. Manning, pp. 1–18, Cambridge University Press, New York, USA.
- Jager, D. F., Wilmking, M. and Kukkonen, J. V. K. 2009. The influence of summer seasonal extremes on dissolved organic carbon export from a boreal peatland catchment: Evidence from one dry and one wet growing season. *Sci. Total Environ.* **407**(4): 1373-1382.
- Janssens, I. A., Kowalski, A. S. and Ceulemans, R. 2001. Forest floor CO₂ fluxes estimated by eddy covariance and chamber-based model. *Agric. For. Meteorol.* **102**, 61– 69.
- Jonasson, S., Michelsen, A., Schmidt, I. K., Nielsen, E. V. and Callaghan, T. V. 1996. Microbial biomass C, N and P in two arctic soils and responses to addition of

- NPK fertilizer and sugar: Implications for plant nutrient uptake. *Oecologia* **106**(4): 507-515.
- Kabwe, L. K., Farrell, R. E., Carey, S. K., Hendry, M. J. and Wilson, G.W. 2005. Characterizing spatial and temporal variations in CO₂ fluxes from ground surface using three complementary measurement techniques. *J. Hydrol.* **311**, 80-90.
- Kettunen, A. 2000. Short-term carbon dioxide exchange and environmental factors in a boreal fen. *Verh. Internat. Verein. Limnol.* **27**: 1446-1450.
- Kettunen, A. 2002. Modeling of microscale variations in methane fluxes. In: *Systems Analysis Laboratory Research Reports*. Helsinki University of Technology. **A83**.
- Kim, J., Verma, S., Billesbach, D., Clement, R., 1998. Diel variation in methane emissions from a midlatitude prairie wetland: Significance of convective throughflow in *Phragmites australis*. *Journal of Geophysical Research* 103 (D21), 28029–28039.
- Koch, O., Tschirko, D. and Kandeler, E. 2007. Seasonal and diurnal net methane emissions from organic soils of the Eastern Alps, Austria: Effects of soil temperature, water balance, and plant biomass. *Arct. Antarct. Alp. Res.* **39**, 438-448.
- Kormann, R., and Meixner, F. 2001. An analytical footprint model for non-neutral stratification. *Boundary Layer Meteorol.* **99** (2), 207-224.
- Kuhry, P. et al., Carbon Balance of NEE Russia: past, present and future. manuscript in preparation, 2010.
- Kunkel, K. E., Easterling, D. R., Hubbard, K. and Redmond, K. 2004. Temporal variations in frost-free season in the United States: 1895-2000. *Geophys. Res. Lett.* **31**(3), doi:10.1029/2003GL018624, 2004.
- Kutzbach L., Schneider J., Sachs T., Giebels M., Nykänen H., Shurpali N. J., Martikainen P. J., Alm J. and Wilmking M., 2007a. CO₂ flux determination by closed-chamber methods can be seriously biased by inappropriate application of linear regression, *Biogeosciences*, **4**(6), 1005-1025.
- Kutzbach, L., Wille, C., Pfeiffer, E. M. 2007. The exchange of carbon dioxide between wet arctic tundra and the atmosphere at the Lena River Delta, Northern Siberia. *Biogeosciences* **4**(5), 869-890.
- Kuzyakov, Y. and Cheng, W. 2001. Photosynthesis controls of rhizosphere respiration and organic matter decomposition. *Soil Biol. Biochem.* **33**(14), 1915-1925.
- Laine, A., Sottocornola, M., Kiely, G., Byrne, K. A., Wilson, D. and Tuittila, E.-S. 2006. Estimating net ecosystem exchange in a patterned ecosystem: Example from blanket bog. *Agric. For. Meteorol.* **138**, 231-243, doi: 10.1016/j.agrformet.2006.05.005.
- Laine, A., Riutta, T., Juutunen, S., Väiranta, M. and Tuittila, E.-S. 2009. Acknowledging the spatial heterogeneity in modeling/reconstructing carbon dioxide exchange in a northern aapa mire. *Ecol. Modell.* **220**, 2646-2655, doi:10.1016/j.ecolmodel.2009.06.047
- Lafleur, P. M., Moore, T. R., Roulet, N. T. and Frohking, S. 2005. Ecosystem respiration in a cool temperate bog depends on peat temperature but not water table. *Ecosystems* **8**(6), 619-629.
- Lafleur, P.M., Roulet, N.T., Bubier, J.L., Frohking, S. and Moore, T.R. 2003. Interannual variability in the peatland-atmosphere carbon dioxide exchange at and ombrotrophic bog. *Global Biochem. Cycles*, **17**(2), 1036, doi:10.1029/2002GB001983.

- Lai, D. Y. F. 2009. Methane Dynamics in Northern Peatlands: A Review. *Pedosphere* **19**(4), 409-421.
- Lasslop, G., Reichstein, M., Papale, D., Richardson, A. D., Arneeth, A., Barr, A., Stoy, P. and Wohlfahrt, G. 2010. Separation of net ecosystem exchange into assimilation and respiration using a light response curve approach: critical issues and global evaluation. *Glob. Change Biol.* **16**(1), 187-208.
- Lindroth, A., Lund, M., Nilsson, M., Aurela, M., Christensen, T. R., Laurila, T., Rinne, J., Riutta, T., Sagerfors, J., Strom, L., Tuovinen, J. P. and Vesala, T. 2007. Environmental controls on the CO₂ exchange in north European mires. *Tellus* **59B**, 812-825.
- Livingston G. P. and Hutchinson, G. L. 1995. Enclosure-based measurement of trace gas exchange: Applications and sources of error, in: *Biogenic Trace Gases: Measuring Emissions from Soil and Water*, edited by P. A. Matson and R. C. Harriss, pp. 15-51, Blackwell Science Ltd, Oxford, UK.
- Livingston, G. P., Hutchinson, G. L. and Spartalian, K. 2006. Trace gas emission in chambers a non-steady-state diffusion model. *Soil Sci. Soc. Am. J.* **70**, 1459-1469.
- Lloyd, J. and Taylor, J. A. 1994. On the temperature-dependence of soil respiration. *Funct. Ecol.* **8**(3), 315-323.
- Long, K., L.B., F. and Cai, T., 2009. Diurnal and seasonal variation in methane emissions in a northern Canadian peatland measured by eddy covariance. *Global Change Biology Early* **16** (9), 2420–2435.
- Lund, M. 2009. Peatlands at a threshold: Greenhouse gas dynamis in a changing climate. Faculty of science, Lund University. ISBN: 978-91-95793-08-2.
- Mahecha, M. D., Fürst, L. M., Gobron, N. and Lange, H. 2010. Identifying multiple spatiotemporal patterns: A refined view on terrestrial photosynthetic activity. *Pattern Recogn.Lett.* **31**(14), 2309-2317.
- Mahecha, M. D., Reichstein, M., Jung, M., Seneviratne, S. I., Zaehle, S., Beer, C., Braakhekke, M. C., Carvalhais, N., Lange, H., Le Maire, G. and Moors, E. 2010. Comparing observations and process-based simulations of biosphere-atmosphere exchanges on multiple timescales. *J. Geophys. Res.* **115**, G02003, doi:10.1029/2009JG001016.
- Mantha, S. V., Johnson, G. A. and Day, T. A. 2001. Evidence from action and fluorescence spectra that UV-induced violet-blue-green fluorescence enhances leaf photosynthesis. *Photochem. Photobiol.* **73**, 249-256.
- Mastepanov, M., Sigsgaard, C., Dlugokencky, E. J., Houweling, S., Strom, L., Tamstorf, M. P. and Christensen, T. R. 2008. Large tundra methane burst during onset of freezing. *Nature* **456**, 628–630.
- Matthes, H., Rinke, A. and Dethloff, K. 2010. Variability of extreme temperature in the Arctic – Observation and RCM. *Open Atmos. Sci. J.* **4**, 126-136, doi: 10.2174/1874282301004010126
- Melloh, R. A. and Crill, P. M. 1995. Winter methane dynamics beneath ice and in snow in a temperate poor fen. *Hydrol. Proc.* **9**, 947-956.
- Menzel, A. 2002. Phenology: Its importance to the global change community - An editorial comment. *Clim. Change* **54**(4)379-385.
- Mikkela, C., Sundh, I, Svensson, B. H. and Nilsson, M. 1995. Diurnal variation in methane emission in relation to the water-table, soil-temperature, climate and vegetation cover in a Swedish acid mire. *Biogeochemistry.* **28**, 93-114.

- Miller, P. A. et al., Present-day and future carbon fluxes from Northwestern Russian tundra – an integrative approach. manuscript in preparation, 2010.
- Moncrieff, J. B., Malhi Y. and Leuning, R. 1996. The propagation of errors in long-term measurements of land-atmosphere fluxes of carbon and water. *Glob. Change Biol.* **2**(3): 231-240.
- Moncrieff, J., Valentini, R., Greco, S., Seufert, G. and Ciccioli, P. 1997. Trace gas exchange over terrestrial ecosystems: Methods and perspectives in micrometeorology. *J. Exp. Bot.* **48**, 1133-1142.
- Moore, C. J. (1986) Frequency response corrections for eddy correlation systems. *Bound.-Layer Meteor.* **37**, 17–35.
- Moore, T. R. and Roulet, N. T. 1993. Methane flux - water-table relations in northern wetlands. *Geophys. Res. Lett.* **20**(7), 587-590.
- Morrissey, L. A. and Livingston, G. P. 1992. Methane emissions from Alaska arctic tundra - an assessment of local spatial variability. *J. Geophys. Res.-Atmos.* **97**(D15), 16661-16670.
- Olychev, A. V., Kurbatova, Yu. A., Tatarinov, F. A., Molchanov, A. G., Varlagin, A. V., Gorshkova, I. I. and Vygodskaya, N. N. 2009. Оценка первичной валовой и чистой продуктивности еловых лесов Центрально-европейской части России с помощью полевых измерений и математической модели. *Успехи современной биологии.* **129** (6), 565-578.
- Panikov, N. S. and Dedysh, S. N. 2000. Cold season CH₄ and CO₂ emission from boreal peat bogs (West Siberia): Winter fluxes and thaw activation dynamics. *Global Biogeochem. Cycles.* **14**, 1071-1080.
- Pastor, J., Solin, J., Bridgham, S. D., Updegraff, K., Harth, C., Weishampel, P. and Dewey, B. 2003. Global warming and the export of dissolved organic carbon from boreal peatlands. *Oikos* **100**(2), 380-386.
- Raich, J. W. and Tufekcioglu, A. 2000. Vegetation and soil respiration: Correlations and controls. *Biogeochemistry* **48**(1), 71-90.
- Rastetter, E. B. Williams, M. Griffin, K. L. Kwiatkowski, B. L. Tomasky, G. Potosnak, M. J. Stoy, P. C. Shaver, G. R. Stieglitz, M. Hobbie, J. E. and Kling, G. W. 2010. Processing arctic eddy-flux data using a simple carbon-exchange model embedded in the ensemble Kalman filter. *Ecol. Appl.* **20** (5): 1285-1301.
- Reichstein, M., Falge, E., Baldocchi, D., Papale, D., Aubinet, M., Berbigier, P., Bernhofer, C., Buchmann, N., Gilmanov, T., Granier, A., Grunwald, T., Havrankova, K., Ilvesniemi, H., Janous, D., Knohl, A., Laurila, T., Lohila, A., Loustau, D., Matteucci, G., Meyers, T., Miglietta, F., Ourcival, J. M., Pumpanen, J., Rambal, S., Rotenberg, E., Sanz, M., Tenhunen, J., Seufert, G., Vaccari, F., Vesala, T., Yakir, D. and Valentini, R. 2005. On the separation of net ecosystem exchange into assimilation and ecosystem respiration: review and improved algorithm. *Glob. Change Biol.* **11**, 1424-1439
- Reichstein, M., Rey, A., Freibauer, A., Tenhunen, J., Valentini, R., Banza, J., Casals, P., Cheng, Y. F., Grunzweig, J. M., Irvine, J., Joffre, R., Law, B. E., Loustau, D., Miglietta, F., Oechel, W., Ourcival, J. M., Pereira, J. S., Peressotti, A., Ponti, F., Qi, Y., Rambal, S., Rayment, M., Romanya, J., Rossi, F., Tedeschi, V., Tirone, G., Xu, M. and Yakir, D. 2003. Modeling temporal and large-scale spatial variability of soil respiration from soil water availability, temperature and vegetation productivity indices. *Glob. Biogeochem. Cycles.* **17**. 1104, doi:10.1029/2003gb002035

- Reicosky, D. C. 2003. Tillage-induced soil properties and chamber mixing effects on gas exchange, Proceedings of the 16th Triennial Conference of International Soil Tillage Research Organizations, 13-18 July 2003, Brisbane, Australia.
- Rinke, A., Matthes, H. and Dethloff, K. 2010. Regional characteristics of Arctic temperature variability: Comparison of regional climate simulations with observations. *Climate Res.* **41**, 177-192, doi: 10.3354/cr00854.
- Rinne, J., Riutta, T., Pihlatie, M., Aurela, M., Haapanala, S., Tuovinen, J. P., Tuittila E. S. and Vesala, T. 2007. Annual cycle of methane emission from a boreal fen measured by the eddy covariance technique. *Tellus* **59B**(3), 449-457.
- Riutta, T., Laine, J., Aurela, M., Rinne, J., Vesala, T., Laurila, T., Haapanala, S., Pihlatie, M. and Tuittila, E.-S. 2007a. Spatial variation in plant community functions regulates carbon gas dynamics in a boreal fen ecosystem, *Tellus B*, **59**, 838-852.
- Riutta, T., Laine, J. and Tuittila, E.-S. 2007b. Sensitivity of CO₂ exchange of fen ecosystem components to water level variation. *Ecosystems*, **10**, 718-733.
- Rocha, A. V. and Goulden, M. L. 2008. Large interannual CO₂ and energy exchange variability in a freshwater marsh under consistent environmental conditions. *J. Geophys. Res.-Biogeosci.* **113**(G4), doi: 10.1029/2008jg000712.
- Sachs, T., Wille, C., Boike, J. and Kutzbach, L. 2008. Environmental controls on ecosystem-scale CH₄ emission from polygonal tundra in the Lena River Delta, Siberia. *J. Geophys. Res.-Biogeosci.* **113**, 12.
- Saarnio, S., Alm, J., Silvola, J., Lohila, A., Nykanen, H. and Martikainen, P. J. 1997. Seasonal variation in CH₄ emissions and production and oxidation potentials at microsites on an oligotrophic pine fen. *Oecologia* **110**(3), 414-422.
- Schneider, J., Kutzbach, L. and Wilmking, M. Carbon dioxide dynamics of a boreal peatland over a complete growing season, Komi Republic, NW Russia. submitted to *Biogeochemistry*, 2010.
- Segers, R. 1998. Methane production and methane consumption: a review of processes underlying wetland methane fluxes. *Biogeochemistry*. **41**(1), 23-51.
- Shurpali, N. J., Verma, S. B., Kim, J and Arkebauer, T. J. 1995. Carbon-dioxide exchange in a peatland ecosystem. *J. Geophys. Res.-Atmos.* **100**(D7): 14319-14326.
- Sierra C. A., Loescher, H. W., Harmon, M.E., Richardson, A. D., Hollinger, D. Y. and Perakis, S. S. 2009. Inter-annual variation of carbon fluxes from three contrasting evergreen forests: the role of forest dynamics and climate. *Ecology*. **90**, 2711-2723.
- Sitch, S., Smith, B., Prentice, I. C., Arneth, A., Bondeau, A., Cramer, W., Kaplan, J., Levis, S., Lucht, W., Sykes, M., Thonicke, K. and Venevsky, S. 2003. Evaluation of ecosystem dynamics, plant geography and terrestrial carbon cycling in the LPJ Dynamic Global Vegetation Model. *Global Change Biol.* **9**, 161–185.
- Sitch, S., Huntingford, C., Gedney, N., Levy, P. E., Lomas, M., Piao, S., Betts, R., Ciais, P., Cox, P. M., Friedlingstein, P., Jones, C. D., Prentice, I. C. and Woodward, F. I. 2008. Evaluation of the terrestrial carbon cycle, future plant geography and climate-carbon cycle feedbacks using 5 Dynamic Global Vegetation Models (DGVMs). *Global Change Biol.* doi: 10.1111/j.1365-2486.2008.01626.x.

- Smith, B., Prentice, I. C., and Sykes, M. T. 2001. Representation of vegetation dynamics in modeling of terrestrial ecosystems: comparing two contrasting approaches within European climate space. *Global Ecol. Biogeogr.* **10**, 621–637.
- Smith, B., Knorr, W., Widlowski, J.-L., Pinty, B. and Gobron, N. 2008. Combining remote sensing data with process modelling to monitor boreal conifer forest carbon balances. *For. Ecol. Managem.* **255**, 3985-3994.
- Soegaard, H., Nordstroem, K., Friborg, T., Hansen, B. U., Christensen, T. and Bay, C. 2000. Trace gas exchange in a high-arctic valley 3. Integrating and scaling CO₂ fluxes from canopy to landscape using flux data, footprint modelling, and remote sensing. *Global Biogeochem. Cycles*. **14** (3), 725-744.
- Sonnentag, O., van der Kamp, G., Barr, A. G. and Chen, J. M. 2010. On the relationship between water table depth and water vapor and carbon dioxide fluxes in a minerotrophic fen. *Glob. Change Biol.* **16**(6), 1762-1776.
- Sottocornola, M. and Kiely, G. 2010. Hydro-meteorological controls on the CO₂ exchange variation in an Irish blanket bog. *Agric. For. Meteorol.* **150**(2), 287-297.
- Suyker, A. E., Verma, S. B., Clement, R. J. and Billesbach, D. P. 1996. Methane flux in a boreal fen: Season-long measurement by eddy correlation. *J. Geophys. Res.-Atmos.* **101**(D22): 28637-28647.
- Sutton-Grier, A. E. and Megonigal, J. P. 2011. Plant species traits regulate methane production in freshwater wetland soils. *Soil Biology and Biochemistry* **43**(2), 413-420.
- Thomas, K. L., Benstead, J., Davies, K. L., Lloyd, D. 1996. Role of wetland plants in the diurnal control of CH₄ and CO₂ fluxes in peat. *Soil Biol. Biochem.* **28**, 17-23.
- Tokida, T., Mizoguchi, M., Miyazaki, T. Kagemoto, A., Nagata, O. and Hatano, R. 2007. Episodic release of methane bubbles from peatland during spring thaw. *Chemosphere.* **70**, 165-171.
- Valentini, R., Dore, S., Marchi, G., Mollicone, D., Panfyorov, M., Rebmann, C., Kolle, O. and Schulze, E.-D. 2000. Carbon and water exchanges of two contrasting Central Siberia landscape types: regenerating forest and bog. *Funct. Ecol.* **14**, 87-96.
- Virtanen, T., Kuusinen, N. and Lopatin, E. Vegetation biomass and carbon storage in forest ecosystems in Komi, Russia: how accurate are the regional estimates? submitted to *Eur. J. For. Res.* 2010.
- Visser, H. 1986. Analysis of Tree-Ring Data Using the Kalman Filter Technique. *Iawa Bulletin* **7**(4): 289-297.
- Vygodskaya, N. N., and Milynkova, I. M. 1995. CO₂-ассимиляция хвойных лесов как компонент газообмена углекислым газом подстилающей поверхности с атмосферой. *Вестник МГУ.* **5** (1), 36-42.
- Waddington, J. M. and Roulet, N. T. 1996. Atmosphere-wetland carbon exchanges: Scale dependency of CO₂ and CH₄ exchange on the developmental topography of a peatland. *Glob. Biogeochem. Cycles* **10**(2), 233-245.
- Wagner, S. W., and Reicosky, D. C. 1992. Closed-chamber effects on leaf temperature, canopy photosynthesis, and evapotranspiration. *Agron. J.* **84** (4), 731-738.
- Walther, G. R., Post, E., Convey, P., Menzel, A. Parmesan, C. Beebee, T. J. C., Fromentin, J. M., Hoegh-Guldberg, O. and Bairlein, F. 2002. Ecological responses to recent climate change. *Nature* **416**(6879), 389-395.
- Wania, R., I. Ross, and I. C. Prentice (2009a), Integrating peatlands and permafrost into a dynamic global vegetation model: I. Evaluation and sensitivity of physical

- land surface processes. *Global Biogeochem. Cycles*. **23**, GB3014, doi:10.1029/2008GB003412.
- Wania, R., Ross, I. and Prentice, I. C. 2009b. Integrating peatlands and permafrost into a dynamic global vegetation model: II. Evaluation and sensitivity of vegetation and carbon cycle processes. *Global Biogeochem. Cycles*. **23**, GB015, doi:10.1029/2008GB003413.
- Wania, R., Ross, I. and Prentice, I. C. (2010, *in revision*), Implementation and evaluation of a new methane model within a dynamic global vegetation model: LPJ-WhyMe v1.3. *Geosci. Model Dev. Discuss.* **3**, 1-59.
- Whiting, G. J. and Chanton, J. P. 1993. Primary production control of methane emission from wetlands. *Nature*. **364**(6440), 794-795.
- Williams, R. T. and Crawford, R. L. 1984. Methane production in Minnesota peatlands. *Appl. Environ. Microbiol.* **47**(6), 1266-1271.
- Willmott, C. J. 1982. Some comments on the evaluation of model performance. *Bull. Am. Meteorol. Soc.* **63**, 1309-1913.
- Wilson, D., Alm, J., Riutta, T., Laine, J., Byrne, K. A., Farrell, E.P., and Tuittila, E.-S. 2007. A high resolution green area index for modelling the seasonal dynamics of CO₂ exchange in peatland vascular plant communities. *Plant Ecol.* **190**, 37-51.
- Wolf, A., Callaghan, T. V. and Larson, K. 2008. Future changes in vegetation and ecosystem function of the Barents Region. *Climatic Change*. **87**, 51-73, doi:10.1007/s10584-007-9342-4.
- Welles, J. M., Demetriades-Shah, T. H. and McDermitt, D. K. 2001. Considerations for measuring ground CO₂ effluxes with chambers. *Chem. Geol.* **177**, 3-13.
- Worrall, F., Burt, T. P., Rowson, J. G., Warburton, J. and Adamson, J. K. 2009. The multi-annual carbon budget of a peat-covered catchment. *Sci. Total Environ.* **407**(13), 4084-4094.
- Wille, C., Kutzbach, L., Sachs, T., Wagner, D. and Pfeiffer, E. M. 2008. Methane emission from Siberian arctic polygonal tundra: eddy covariance measurements and modeling. *Glob. Change Biol.* **14**(6): 1395-1408.
- Williams, R. T. and Crawford, R. L. 1984. Methane production in Minnesota peatlands. *Appl. Environ. Microbiol.* **47**(6), 1266-1271.
- Wu, J. B., Kutzbach, L., Jager, D., Wille, C. and Wilmking, M. 2010. Evapotranspiration dynamics in a boreal peatland and its impact on the water and energy balance. *J. Geophys. Res.-Biogeosci.* **115**, doi: 10.1029/2009JG001075.
- Yurova, A., Wolf, A., Sagerfors, J. and Nilsson, M. 2007. Variations in net ecosystem exchange of carbon dioxide in a boreal mire: Modeling mechanisms linked to water table position. *J. Geophys. Res.* **112**, G02025, doi:10.1029/2006JG000342.
- Zimov, S. A., Schuur, E. A. G. and Chapin, F. S. 2006. Permafrost and the global carbon budget. *Science*. **312**(5780), 1612-1613.

Eidesstattliche Erklärung

Hiermit erkläre ich, dass diese Arbeit bisher von mir weder an der Mathematisch-Naturwissenschaftliche Fakultät der Ernst-Moritz-Arndt Universität Greifswald noch einer anderen wissenschaftlichen Einrichtung zum Zwecke der Promotion eingereicht wurde.

Ferner erkläre ich, dass ich diese Arbeit selbstständig verfasst und keine anderen als die darin angegebenen Hilfsmittel benutzt habe.

Curriculum vitae

Personal information

Name and surname: Ing. Michal Gažovič
Date of birth: 28.01.1983
Place of birth: Poprad
Nationality: Slovak
Present position: Inetgrated flood prevention program; project coordinator,
Slovakia

Education

02/2007-... PhD student at University of Greifswald, Germany
2001-2006 Faculty of Forestry, Technical University of Zvolen, Slovakia, diploma
with distinction
1994-2001 School leaving exam, Secondary grammar school Kežmarok, Slovakia

Previous positions

02/2007-03/2008 Postgraduate scholarship, University of Greifswald, Institute of
Botany and Landscape Ecology
04/2008-03/2009 Fellow of Katholischer Akademischer Ausländer Dienst
(KAAD), University of Greifswald, Institute of Botany and
Landscape Ecology
02/2007-03/2008 Postgraduate scholarship, University of Greifswald, Institute of
Botany and Landscape Ecology
09/2006-12/2006 Research associate at Czech Agricultural University, Prague,
Faculty of Forestry and Environment

Awards

KAAD scholarship - Katholischer Akademischer Ausländer Dienst
SPP –Slovak Gas Industry foundation- study and travel grant
Volksbank award for excellent study results
Price of the Rector of the Technical University of Zvolen

Publications

Submitted

Gažovič, M., Forbrich, I; Jager, D, Kutzbach, L, Wille, C and Wilmking, M. Hydrology driven ecosystem respiration determines the carbon balance of a boreal peatland. Submitted to *Oecologia* (05/2011).

Schneider J., **Gažovič M.**, Kutzbach L., Forbrich I., Wu J., Wania R., Miller P.A., Susiluoto S., Virtanen T., Zagirova S. and M. Wilmking (2010): Boreal peatland net ecosystem CO₂ exchange- an integrative comparison between measured fluxes and LPJ-GUESS model output. Submitted to *Journal of Geophysical Research* (10/2010).

Published

Gažovič, M., Schreiber, P, Kutzbach, L, Wille, C and Wilmking, M. (2010) Diurnal dynamics of CH₄ from a boreal peatland during snowmelt, *Tellus B*, 62, 133-139.

Abstracts

Gažovič, M., Kutzbach, L, Schneider, J, Wille, C and Wilmking, M. (2010) Ecological analysis of a boreal peatland CO₂ flux based on eddy covariance data set from Ust Pojega, Russia. 02-07. May, EGU, Vienna, Austria

Schneider, J., **Gažovič, M.**, Kutzbach, L, Miller, P., Susiluoto, S., Virtanen, T., Wilmking, M and Wu, J. (2010) Integrative comparison of CO₂ flux measurements at a boreal peatland by chamber and eddy covariance methods with LPJ-GUESS model output. 02-07 May, EGU, Vienna, Austria.

Schneider J., Kutzbach, L., **Gažovič, M.**, Wolf, U., Miglovec, M., Michajlov, O., Wille, C., Schreiber, P., Ibendorf, J., Wilmking, M. 2009. Carbon dioxide dynamics of a boreal peatland over a complete growing season, Komi Republic, NW Russia. EGU general assembly, 19-24 April, Vienna, Austria.

Schneider J., **Gažovič, M.**, Kutzbach L., Wolf U., Miglovec M., Michajlov O., Wille C., Schreiber P., Ibendorf J., Wilmking M. (2009) Environmental controls on carbon dioxide fluxes of a boreal peatland, Komi Republic, NW Russia. 2nd Symposium "Peatlands in the Global Carbon Cycle" of the Peatland Ecosystem Analysis and Training NETWORK (PEATNET), 25- 30. September, Prague, Czech Republic.

Gažovič, M., L. Kutzbach, C. Wille and M. Wilmking, 2009. Year-round measurements of CO₂ and CH₄ exchange from a boreal peatland in north-west Russia. 2nd International Symposium: Peatlands in the Global Carbon Cycle, Prague, Czech Republic.

Gažovič, M., L. Kutzbach, P. Schreiber, C. Wille and M. Wilmking, 2009. Pronounced short-term temporal dynamics of methane fluxes during the snowmelt period at a boreal peatland in NW Russia. Poster at: EGU General Assembly, Vienna, Austria.

P. Schreiber, **Gažovič, M.**, J. Ibendorf, C. Wille, M. Wilming, L. Kutzbach 2008. Cool, But Highly Dynamic - Spring CH₄ emissions in a boreal peatland, Komi Republic, NW Russia. Poster at the Conference: Global Change and Landscape Response, Bonn, Germany.

Ťupek, B., Minkkinen K, **Gažovič, M.**, Slížiková, M., Alm, J., Laine, J, 2006. Methane dynamics along hydrological gradient from upland forest to lowland mire. Poster at conference, NECC workshop, 6-8.3.2006, Umea, Sweden.

Monograph

Gažovič, M., CO₂, CH₄ production and consumption along hydrological gradient from upland forest to lowland mire in central Finland; Technical University in Zvolen. Department of natural environment. Zvolen: Faculty of Forestry TU, 2006. 66 p. (diploma thesis in Slovak language)

Acknowledgements

“...but I force a smile, knowing that my ambition far exceeded my talent...”

In the beginning there was an ambition and wish to go to Russia. Then a project came across, which could make it come true. Then I met the people involved and they were great. And so it all started.

The biggest thank goes to my supervisor Prof. Martin Wilmking, PhD, for putting trust and patience in me, for great time and friendship during the last four years.

To Jun. Prof. Dr. Lars Kutzbach, for his supervision and nice talks, not only about science. Daniel Jager, for nice walks in Finland and inspiring conversations. Julia Schneider, for being a nice companion on our Russian mission. Inke Forbrich, for her patience with all my questions and for her help. Christian Wille, for his help and support whether it was in the office or in the field.

To Oleg Michailov and Misha Miglovec, for friendship during long months in Russia and for showing me some important things I was missing.

And to all the great people whom I met on my way, but listing them all at this place would make this part extremely boring for others. Thank you very much, you know whom I mean!

To my friends, for “long” distance support over the years. To my family for constant support and being here.

Special thank goes to my friends and flat mates here in Greifswald: Chiara Piazzesi for listening when I was low, Amro Daboul, Ghalib Qadry and Hamzeh Mazahery for lot of fun and great time.